

Theoretical Studies on Redox Potential of Molecules by Molecular Dynamics simulation

メタデータ	言語: eng 出版者: 公開日: 2017-10-05 キーワード (Ja): キーワード (En): 作成者: メールアドレス: 所属:
URL	http://hdl.handle.net/2297/42337

This work is licensed under a Creative Commons Attribution-NonCommercial-ShareAlike 3.0 International License.



**THEORETICAL STUDIES
ON REDOX POTENTIAL OF MOLECULES
BY MOLECULAR DYNAMICS SIMULATION**

Ph.D Thesis

MASASHI IWAYAMA

*Division of Mathematical and Physical Sciences,
Graduate School of Natural Science and Technology,
Kanazawa University*

2015

博士論文

THEORETICAL STUDIES ON REDOX POTENTIAL OF MOLECULES BY MOLECULAR DYNAMICS SIMULATION

金沢大学大学院自然科学研究科

数物科学専攻

計算科学講座

学籍番号 1123102001

氏名 岩山 将士

主任指導教員氏名 長尾 秀実

ACKNOWLEDGEMENT

This doctoral thesis is a summary of the author's study from April 2011 to January 2015 at the Division of Mathematical and Physical Sciences, Graduate School of Natural Science and Technology of Kanazawa University.

Firstly, the author would like to express my gratitude to Prof. Hidemi Nagao for many valuable discussions, suggestions, encouragements and supports through this study. He also would like to acknowledge Dr. Kazutomo Kawaguchi and Dr. Hiroaki Saito for their helpful discussions, suggestions, encouragements and helps me not only in study and research but also in my life of doctoral course.

He is deeply grateful to Emeritus Prof. Kiyoshi Nishikawa, Emeritus Prof. Yasuaki Hiwatari, Prof. Shinichi Miura, Prof. Mineo Saito, Prof. Tatsuki Oda, Prof. Masahide Sato, Dr. Fumiya Ishii, Dr. Kimikazu Sugimori, Dr. Ayumu Sugiyama at Yamanashi Ewa College, Prof. Hiroyuki Kawabe at Kinjo University, Dr. Acep Purqon at Institut Teknologi Bandung in Indonesia, Dr. Phung Thi Viet Bac at University of Fukui, Dr. Shuhei Kawamoto at Nagoya University and Dr. Takeshi Miyakawa at Tokyo University of Pharmacy and Life Sciences for their advices and their supports. Without their helps, this work would not be produced.

Special thanks are given to Prof. Masako Takasu at Tokyo University of Pharmacy and Life Sciences, Prof. Yasuteru Shigeta at University of Tsukuba for helpful discussions and suggestions.

The author also would like to thank to Prof. Muhamad Abdulkadir Martoprawiro and Prof. Rukman Hertadi for the discussions in this study during a short period of study abroad at Institut Teknologi Bandung in Indonesia.

Many thanks are given to all the members of the computational biophysics laboratory, Graduate School of Natural Science and Technology of Kanazawa University, especially to Dr. Micke Rusmerryani, Dr. Muhamad Koyimatu, Ms. Gia Septiana Wulandari, Ms. Yuriko Omae, Ms. Megumi Nishimura, Mr. Hiroyuki Takagi, Mr. Tetsuya Sugimori, Mr. Masato Teragishi, Mr. Takuhito Shiogama, Mr. Tsuhito Yoshida, Mr. Isman Kurniawan, Ms. Meidy Triana Pakpahan, Mr. Kazuma Tamura, Mr. Shogo Horiguchi, Mr. Takahiro Matsui, Mr. Yuma Tanaka, Mr. Seiichiro Ito and Ms. Saori Nakano for useful discussions and many helps.

He would like to give his thanks to the staff of program of Young Researchers Training Program for Promoting Innovation of Kanazawa University; in particular, he thanks Prof. Akiharu Morimoto, Specially-Appointed Prof. Shigeru Mori, Prof. Shigeyoshi Kanoh, and all the members adopted in this program in 2014. Thanks are due to Director Yoshimi Ogawa, Dr. Kazuyoshi Baba, Dr. Naoto Okuyama at Daicel Corporation for giving him a chance to training and study of the process simulation and the molecular dynamics simulation of polymer in Himeji.

The author is helped by lots of people, indeed, it is not easy to write and describe all kindness of their here. He really apologize he can not write all the names one by one.

Finally, the author would like to express grateful acknowledgement to his parents, Yukio Iwayama and Nobuko Iwayama, and his brothers, Satoshi Iwayama and Tomonori Iwayama, for their continuous supports and encouragements.

Masashi Iwayama

Kanazawa

January 2015

LIST OF PUBLICATIONS

- [1] **M. Iwayama**, K. Kazutomo, H. Saito, H. Nagao, "Structure and hydration free energy of ketone compound in neutral and cationic state by molecular dynamics simulation", *Recent Development in Computational Science*, **4**, 59-69 (2013).
- [2] **M. Iwayama**, I. Kurniawan, K. Kawaguchi, H. Saito, H. Nagao, "A hybrid type approach with MD and DFT calculations for estimation of redox potential of molecules", *Mol. Simul.*, submitted.

Papers not included in this thesis

- [3] T. Mizukami, H. Saito, S. Kawamoto, T. Miyakawa, **M. Iwayama**, M. Takasu, H. Nagao, "Solvation Effect on the Structural Change of a Globular Protein: A Molecular Dynamics Study", *Int. J. Quantum Chem.*, **112**, 344-350 (2012).
- [4] H. Saito, T. Mizukami, S. Kawamoto, T. Miyakawa, **M. Iwayama**, M. Takasu, H. Nagao, "Molecular Dynamics Studies of Lipid Bilayer With

- Gramicidin A: Effects of Gramicidin A on Membrane Structure and Hydrophobic Match”, *Int. J. Quantum Chem.*, **112**, 161-170 (2012).
- [5] Y. Omae, H. Saito, H. Takagi, M. Nishimura, **M. Iwayama**, K. Kawaguchi, H. Nagao, ”Molecular Dynamics Study of Glutathione S-transferase: Structure and Binding Character of Glutathione”, *Progress in Theoretical Chemistry and Physics*, **26**, 545-553 (2012).
- [6] H. Saito, **M. Iwayama**, H. Takagi, M. Nishimura, T. Miyakawa, K. Kawaguchi, M. Takasu, T. Mizukami, H. Nagao, ”Molecular Dynamics Study of Gramicidin A in Lipid Bilayer: Structure and Lateral Pressure Profile”, *Int. J. Quantum Chem.*, **112**, 3834-3839 (2012).
- [7] K. Kawaguchi, H. Takagi, **M. Iwayama**, M. Nishimura, T. Miyakawa, H. Saito, M. Takasu, H. Nagao, ”Molecular Dynamics Analyses of the Dissociation Process of ADP from Hsp90”, *Int. J. Quantum Chem.*, **112**, 3791-3795 (2012).
- [8] H. Saito, **M. Iwayama**, T. Mizukami, K. Jiyoung, T. Masaru, H. Nagao, ”Molecular dynamics study on binding free energy of Azurin-Cytochrome c551 Complex”, *Chem. Phys. Lett.*, **556**, 297-302 (2013).
- [9] M. Koyimatu, H. Shimahara, **M. Iwayama**, K. Sugimori, K. Kawaguchi, H. Saito, H. Nagao, ”Theoretical model for assessing properties of local structures in metalloprotein”, *AIP Conf. Proc.*, **1518**, 626-629 (2013).
- [10] H. Saito, **M. Iwayama**, K. Kawaguchi, T. Mizukami, T. Miyakawa, M. Takasu, H. Nagao, ”Molecular Dynamics Study of Gramicidin A in Lipid Bi-

layer: Electrostatic Map and Ion Conduction”, *JPS Conf. Proc.*, **1**, 012053
1-4 (2014).

CONTENTS

ACKNOWLEDGEMENT	i
LIST OF PUBLICATIONS	iv
CONTENTS	xii
LIST OF TABLES	xv
LIST OF FIGURES	xx
1 GENERAL INTRODUCTION	1
1.1 Redox Reaction in Biological Systems	1
1.2 Theoretical Studies on Estimation of Redox Potential	2
1.3 Thesis Overview	4
2 DEVELOPMENT OF FORCE FIELD PARAMETERS FOR REDUCED AND OXIDIZED MOLECULES	7
2.1 Introduction	7
2.2 Optimization	9
2.2.1 Computational details	9

2.2.2	Optimized structure	11
2.2.3	Ionization potential	13
2.3	Force Field Parameters of Intermolecular Interaction	14
2.3.1	Partial charge	15
2.4	Force Field Parameters of Intramolecular Interaction	16
2.4.1	Computational details	17
2.4.2	Bond stretching	18
2.4.3	Angle bending	21
2.5	Concluding Remarks	24

3 STRUCTURE AND HYDRATION PROPERTIES OF ORGANIC COMPOUNDS IN NEUTRAL AND RADICAL CATIONIC STATES 25

3.1	Introduction	25
3.2	Computational Procedure	26
3.2.1	Chemical potential	26
3.2.2	Energy representation method	29
3.3	Computational Details	30
3.3.1	Molecular dynamics simulation	30
3.3.2	Root mean square deviation	34
3.3.3	Radial distribution function	35
3.3.4	Energy distribution function	36
3.4	Results and Discussion	37
3.4.1	Conformation and fluctuation in solution	37
3.4.2	Solvent structure	45
3.4.3	Excess chemical potential	45

<i>CONTENTS</i>	xi
3.5 Concluding Remarks	52
4 A HYBRID TYPE APPROACH WITH MD AND DFT CALCULATIONS: EVALUATION OF REDOX POTENTIAL OF ORGANIC COMPOUNDS	55
4.1 Introduction	55
4.2 Computational Procedure	56
4.2.1 Redox potential	56
4.2.2 Gibbs free energy of redox reaction	57
4.3 Results and Discussion	58
4.3.1 Ionization free energy	59
4.3.2 Standard redox potential	62
4.3.3 Relative value of redox potentials	63
4.4 Concluding Remarks	64
5 GENERAL CONCLUSION	65
A A HYBRID TYPE APPROACH WITH MD AND QM/MM CALCULATIONS: EVALUATION OF REDOX POTENTIAL OF METALLOPROTEIN	69
A.1 Introduction	69
A.2 Materials	70
A.3 Computational Procedure	70
A.4 Computational Details	72
A.4.1 Molecular dynamic simulation	72

A.4.2	Hybrid QM/MM calculation	73
A.4.3	Energy distribution function	74
A.5	Results and Discussion	74
A.6	Summary	77
B	EFFECT OF COUNTER-ION ON EVALUATION OF REDOX POTENTIAL	79
B.1	Introduction	79
B.2	Computational Details	81
B.3	Results and Discussion	82
B.3.1	Dependence of redox potential from the number of water molecules	82
B.4	Summary	88
C	COMPUTATION OF REDOX POTENTIAL OF MOLECULES BY MD SIMULATION OF WATER DROPLET MODEL	91
C.1	Introduction	91
C.2	Computational Procedure	92
C.2.1	Solvation free energy	92
C.2.2	Gibbs free energy of redox reaction	95
C.3	Computational Details	96
C.3.1	MD simulation of water droplet model	96
C.4	Results and Discussion	97
	REFERENCES	101

LIST OF TABLES

2.1	The dependence of the quantum chemical calculation method and the basis set on the investigation of total energy of the acetone in the neutral and radical cationic states. Units are hartree.	10
2.2	RESP charges of the acetone and 3-pentanone in the neutral (N) and radical cationic ($N + 1$) states by DFT-B3LYP-6-31+G(d,p) calculations. Units are elementary charge.	16
2.3	The spring constants, K_r , and equilibrium lengths, r_{eq} , for the intramolecular bond stretching of acetone in the neutral (N) and radical cationic ($N + 1$) states with parm99 force field parameter. Units of K_r and r_{eq} are kcal/mol/Å ² and Å.	19
2.4	The force constants, K_r , and equilibrium lengths, r_{eq} , for the intramolecular bond stretching of 3-pentanone in the neutral (N) and radical cationic ($N+1$) states with parm99 force field parameter. Units of K_r and r_{eq} are kcal/mol/Å ² and Å.	20
2.5	The spring constants, K_θ , and equilibrium angles, θ_{eq} , for the intramolecular angle bending of acetone in the neutral and radical cationic states with parm99 force field parameter. Units of K_θ and θ_{eq} are kcal/mol/deg ² and deg.	22

2.6	The spring constants, K_θ , and equilibrium angles, θ_{eq} , for the intramolecular angle bending of 3-pentanone in the neutral and radical cationic states with parm99 force field parameter. Units of K_θ and θ_{eq} are kcal/mol/deg ² and deg.	23
3.1	Spring constant and equilibrium torsion angle for the harmonic potential, K_ϕ and ϕ_{eq} used to the MD simulation of acetone. The number behind the atomic symbol is compatible with the number showed in Figure 2.1. Units of K_ϕ and ϕ_{eq} are kcal/mol/deg. ² and deg..	32
3.2	Spring constant and equilibrium torsion angle for the harmonic potential, K_ϕ and ϕ_{eq} used to the MD simulation of 3-pentanone. The number behind the atomic symbol is compatible with the number showed in Figure 2.1. Units of K_ϕ and ϕ_{eq} are kcal/mol/deg. ² and deg..	33
3.3	The average value and standard deviation of intramolecular bond length and angle for the acetone and 3-pentanone in the neutral and radical cationic states (showed by using valence of molecule, N and $N + 1$) in solution. These intramolecular conformation of optimized structure are shown to compare in liquid phase with in gas phase. Units of bond length and angle are Å and deg.. . . .	41
3.4	Excess chemical potentials, $\Delta\mu^{ex}$, of acetone and 3-pentanone in the neutral and radical cationic states. The units are in kcal/mol. The values in parentheses show the standard deviation.	48

- 4.1 The average of ionization free energies, ΔE , the average of excess chemical potentials of molecule in the neutral and the radical cationic states, $\Delta\mu_{(N)}^{ex}$ and $\Delta\mu_{(N-1)}^{ex}$, and the standard Gibbs free energies ΔG of redox reaction, for the acetone and 3-pentanone. The units are in kcal/mol. The values in parentheses show the standard deviation. 62
- B.1 Dependence of the excess chemical potential in the neutral and radical cationic states, $\mu_{(N)}^{ex}$ and $\mu_{(N+1)}^{ex}$, the free energy change in oxidation reaction, ΔG , redox potential, E° from the number of water molecules. Units of the $\mu_{(N)}^{ex}$, $\mu_{(N+1)}^{ex}$, ΔG and the E° are the kcal/mol and the V. 82
- C.1 The ionization potentials in gas phase, ΔE^{gas} , the solvation free energies of molecule in the neutral and the radical cationic states, $\Delta G_{(N)}^{sol}$ and $\Delta G_{(N-1)}^{sol}$, and the standard Gibbs free energies ΔG of redox reaction, for the acetone and 3-pentanone. The units are in kcal/mol. The values for 3-pentanone are in estimation. 98

LIST OF FIGURES

2.1	The optimized structures of the acetone and 3-pentanone in the neutral and radical cationic states obtained by the DFT-B3LYP/6-31+G(d,p) calculations.	12
3.1	Initial solution system for acetone in neutral state.	34
3.2	Initial solution system for 3-pentanone in neutral state.	34
3.3	The RMSD of acetone in the neutral and radical cationic states as a function of MD time steps.	38
3.4	The RMSD of 3-pentanone in the neutral and radical cationic states as a function of MD time steps.	39
3.5	RDF between the COM of acetone and the oxygen atom of the water molecules is shown in the neutral and radical cationic states, the $g_{(N)}(r)$ and $g_{(N-1)}(r)$. The number of oxygen atoms of the water molecule are shown as a function of distance from the COM of acetone in the neutral and radical cationic states, the $N_{(N)}(r)$ and $N_{(N-1)}(r)$	43

- 3.6 RDF between the COM of 3-pentanone and the oxygen atom of the water molecules is shown in the neutral and radical cationic states, the $g_{(N)}(r)$ and $g_{(N-1)}(r)$. The number of oxygen atoms of the water molecule are shown as a function of distance from the COM of 3-pentanone in the neutral and radical cationic states, the $N_{(N)}(r)$ and $N_{(N-1)}(r)$ 44
- 3.7 The energy distribution function $\rho^e(\varepsilon)$ and $\rho_0^e(\varepsilon)$, which are averaged on the 400 configurations, for acetone in the neutral (N) and radical cationic ($N + 1$) states. 46
- 3.8 The energy distribution function $\rho^e(\varepsilon)$ and $\rho_0^e(\varepsilon)$, which are averaged on the 400 configurations, for 3-pentanone in the neutral (N) and radical cationic ($N + 1$) states. 47
- 3.9 The average value of the excess chemical potential for acetone in the neutral and radical cationic states, the $\Delta\mu_{(N)}^{ex}$ and $\Delta\mu_{(N-1)}^{ex}$, as a function of the number of configurations. 49
- 3.10 The average value of the excess chemical potential for 3-pentanone in the neutral and radical cationic states, the $\Delta\mu_{(N)}^{ex}$ and $\Delta\mu_{(N-1)}^{ex}$, as a function of the number of configurations. 50
- 4.1 Thermodynamic cycle model used in calculation of free energy change in oxidation reaction. "Red (gas)" and "Ox (gas)" indicates the reduced and the oxidized molecules in gas phase, and "Red (solv)" and "Ox (solv)" indicates the reduced and the oxidized molecules in salvation. The free energy change is evaluated without computing excess chemical potential of an excess electron. 58

4.2	The average of the total energies for acetone in the neutral and radical cationic states, $E_{(N)}$ and $E_{(N-1)}$, as a function of the number of configurations.	60
4.3	The average of the total energies for 3-pentanone in the neutral and radical cationic states, $E_{(N)}$ and $E_{(N-1)}$, as a function of the number of configurations.	61
A.1	The X-ray structure of Azurin in the reduced and oxidized states. This Figure is done RMS fit between the reduced and oxidized states.	71
A.2	The RMSD of azurin in the reduced and oxidized states as a function of MD time steps.	75
B.1	The average of excess chemical potential of acetone in the radical cationic state, $\mu_{(N-1)}^{ex}$, using a configuration of 10 ns as a function of the number of samples for solution system.	84
B.2	Change of distance between the COM of acetone and the counter-ion as a function of the number of samples for solution system. . .	85
B.3	State probability distribution of distance between the COM of acetone and the counter-ion.	86
B.4	The average of the difference of excess chemical potential, $\Delta(\Delta\mu_{(N-1)}^{ex})$, of acetone between the 1,425 and 2,850 solvent systems (dark) and between the 1,425 and 4,250 solvent systems (thin). Points indicate the each value. Curve lines indicate the fitting curves each point.	87

C.1 Thermodynamic cycle model used in calculation of free energy change in oxidation reaction.	95
---	----

CHAPTER 1

General Introduction

1.1 Redox Reaction in Biological Systems

Redox (redouction and oxidation) reactions in biological systems have much interest in their biological functions, mechanisms of the redox reactions and their applications in relation to the electron transfer [1, 3, 4], metabolism [5], intracellular signal transduction [6] and so on [7, 41]. Many research groups have investigated a lot of kind of redox reactions in biological systems such as the oxidation reactions of waters associated with higher plant systems [8], the redox reactions between metalloproteins in vivo [9], the electron transfer reactions between enzymes and organic compounds to materialize bio-fuel cells [10, 11] and so on [12].

In these investigations related to the electron transfer with the redox reactions, the redox potential is a powerful tool in the case of analysis of the mechanism of the redox reactions in the biological reactions with the electron transfer. One of research topics on the redox reactions is to find mechanism of the high ox-

oxidation potential of water molecule in biological system reviewed in Ref. [13]. Research into the photosynthesis of the water oxidation has recently intensified, because it can serve as an important inspiration for the development of artificial water-oxidation catalysts. Zouni and co-workers have presented the first crystallographic model of a photosystem (PS) II complex in which the position of the catalytic site, the Mn₄Ca complex, is uniquely determined [14]. Recently, Umena and co-workers have discovered to determine the crystal structure of PS II including the manganese cluster at high resolution of 1.9 Å [15]. In the water oxidation, four stable or semistable states intermediated the reaction cycle of the photosynthetic manganese complex can be observed by saturating laser flashes of light [16]. Dau and co-workers have presented a thermodynamic cycle of the oxidation of manganese complex and have discussed the deprotonation and successive oxidation steps for a hypothetical manganese complex by using the redox potential and pK_a values for each state to explain the possibility of the mechanism of the water oxidation [13].

1.2 Theoretical Studies on Estimation of Redox Potential

In theoretical investigations of redox reactions, many models and methods to estimate the value of redox potential have been presented to discuss the mechanism of redox reactions. One of popular methods is a calculation of the standard Gibbs free energy of redox reaction with the thermodynamic cycle model [17]. In the procedure of the method, the redox potential can be calculated by the estimation

of the free energy change with ionization free energy in gas phase and the excess chemical potentials of the oxidized and reduced molecules. Many groups have presented and have reproduced the reduction potential of organic molecules by using the several computational methods such as the molecular orbital (MO) calculations or the density functional theory (DFT) calculations for the estimation of the ionization free energy in gas phase and the quantum chemical calculations with polarizable continuum model (PCM) [18] for the estimation of excess chemical potential [20, 21, 22, 23, 24, 25, 26]. The PCM is the most frequently used method to consider the solvent effects and shows a reasonable results for the calculation of excess chemical potential of the simple small molecules, however, it is not easy to apply to estimate the redox potential of the complex systems. This is because the excess chemical potential has known to strongly depend on the solvated structure of the solute molecule [42], and the PCM does not reflect solvent dynamics and not describe the effect of hydrogen bonds between the solute and the solvent molecules. To avoid such issues, the computational method involving solute and solvent dynamics is required to estimate the redox potential of large molecules including proteins.

On the other hand, instead of using the PCM to calculate the excess chemical potential, one of other popular methods is based on the molecular dynamics (MD) simulation using the explicit solvent model. The excess chemical potential can be calculated by using the thermodynamic integration (TI) method [27, 28] and the energy representation (ER) method [29, 30, 31, 32] and so on [33, 34]. Some hybrid type calculations such as combined method with quantum-mechanics/molecular-mechanics (QM/MM) calculation [19] and the MD simulation etc. have been

presented by many groups [35, 36, 37, 38]. In those computational methods to calculate redox potential, it is not easy to get the accurate value comparing with experimental results for the large molecules including proteins and to simulate for the huge systems involving solvent molecules due to a problem of computational costs. Thus, development of theoretical methods for biomolecular systems is still challenging topics to get accurate values of the redox potential.

The goal of this study is to estimate the redox potential of molecules including proteins and to elucidate the mechanism of the electron transfer reaction between the molecules. The purpose of this study is to present a simple calculation method to evaluate the redox potential of molecules including proteins by sampled configurations obtained from the molecular dynamics (MD) simulation in order to estimate the redox potential including the fluctuation of conformation in long time order and to discuss the estimated redox potential in relation to the difference of the redox potentials of the molecules with the experimental data. This thesis calculates the redox potential of the mainly simple organic molecules, acetone and 3-pentanone, by using the conventional approach, and also estimates the redox potential of blue copper protein, azurin, in appendix.

1.3 Thesis Overview

This thesis is organized as the following 5 chapters and 3 appendices. As already mentioned, chapter 1 has provided the introduction relevant to the redox reaction in biological systems and the theoretical studies on the estimation of redox potential of the molecules so far. The motivation and purpose of this study and thesis are also given in this Chapter. Chapter 2 has presented the developed force field

parameters of acetone and 3-pentanone in the reduced and oxidized states to carry out the MD simulation. In this study, force field parameters of the stretching vibration and angle bending as intramolecular potential and the partial charge as intermolecular potential are estimated by the DFT calculations. The optimized structures in the reduced and oxidized states and the ionization potential of these molecules are compared with the experimental data and the AMBER force field parameters. Chapter 3 has performed the MD simulation of the small organic molecules, acetone and 3-pentanone, using the force field parameters developed in Chapter 3. From the MD simulations and the free energy calculation by the ER method, the structure and hydration properties of these organic molecules in the neutral and radical cationic states are investigated. Chapter 4 has presented a simple calculation method to compute the redox potential of the molecules by using a hybrid type calculation with the MD and DFT calculations with discussions of the difference of the redox potential. Chapter 5 has presented the conclusion of this thesis and the future work. These contents from chapter 1 to chapter 5 are based on the publication papers, as showed in List of Publications.

Moreover, Appendix A has presented a hybrid type method with MD and QM/MM calculations for evaluation of redox potential of the proteins. The evaluated redox potential of the protein is also compared with the experimental data and discussed the redox potential of the proteins with computation of the difference of redox potential between the protein and the organic molecules, acetone and 3-pentanone, evaluated in Chapter 4. In this study, there are still some tasks we have to settle, where the computation of the absolute redox potential of the molecules with presented computational method to estimate the redox potential.

Thereupon, appendix B has discussed the effect of the number of water molecules in simulation cell and the behavior of counter-ion in solution on the estimation of redox potential of molecules or the excess chemical potential in the oxidized state. Lastly, appendix C has presented the more development of the computational method to estimate the redox potential using the MD simulation with spherical boundary condition. All of the references for this thesis have listed at the end of this thesis.

CHAPTER 2

Development of Force Field Parameters for Reduced and Oxidized Molecules

2.1 Introduction

The molecular dynamics (MD) simulations have been used to take the snapshot structures of solute molecule with the structural fluctuation by solvent in solution. In order to perform the MD simulations of biological molecules such as organic compounds and proteins, several types of potential function on the based of empirical force field such as the CHARMM (Chemistry at HARvard Molecular Mechanics) [43] developed by Martin Karplus's group at the Harvard University, AMBER (Assisted Model Building with Energy Refinement) developed by Peter Kollman's group at the University of California [64, 44] etc. and the program packages developed and maintained their groups have been used so far.

The potential energy function for the biological systems commonly consists of the bond stretching, angle bending, torsional energetics for the intramolecular potential and the coulomb and van der Waals (vdW) interactions for the intermolecular potential [45, 46, 47, 48, 49]. The force field parameters such as OPLS (Optimized Potential for Liquid Simulations) [50] and the CHARMM and AMBER force fields have been used so far. In the case of AMBER force field, the partial charges of the molecule are mainly calculated by the empirical scheme called AM1-BCC (Bond Charge Correction) [52, 53]. However, the restrained electrostatic potential (RESP) charge calculated by a larger basis set should be adopted for more accurate electrostatic property of the molecules. While, The parm99 force field [63, 51], which is a representative in the recent AMBER force field, have been presented for the force field parameters of intramolecular potential. The torsional energetics parameters have presented using the results of investigation using small 82 organic molecules with the RESP charges by the density functional theory (DFT) calculations with B3LYP method and cc-PVDZ basis set. These parameters are determined to represent the smallest root mean square deviation (RMSD) compared with the experimental data, however, the torsion parameters for 11 hydrocarbons and 7 chlorides are evaluated with absolute errors in 0.1 kcal/mol relative to the experimental values. These intramolecular parameters are evaluated for the molecules in neutral state, however, that of ionized molecules have not been presented yet. The force field parameters for the MD simulations of biological molecules should be improved and developed for the sampling of the organic solute conformation in reduced and oxidized states.

The purpose of this chapter is to develop the force field parameters of the small

organic molecules, acetone and 3-pentanone, in the neutral and radical cationic states. In order to obtain these parameters, this chapter performs the density functional theory (DFT) calculations with high-level basis set to obtain the optimized structures of organic molecules in the neutral and radical cationic states. The force field parameters of equilibrium stretching vibration and angle bending for the intramolecular potential are obtained from the optimized structures, and partial charge for the intermolecular potential is estimated by the single point calculation with the DFT calculation. The force field parameters of force constant of the stretching vibration and angle bending are estimated from the dependence of the total energy of the molecule on the distance and angle in the structure of molecules by the DFT calculation. From these results, the ionization potential of the molecules are estimated, and compared with the experimental data. The force field parameters of the equilibrium stretching vibration and angle are also compared with the experimental data, and the estimated force field parameters of force constant are compared with the AMBER force field parameters.

2.2 Optimization

2.2.1 Computational details

Geometry optimization of the organic molecules, acetone and 3-pentanone, in the neutral and radical cationic states in gas phase is performed by DFT-B3LYP [59, 59] method with 6-31+G(d,p) basis set [59, 61, 55]. The diffuse function is adopted for the ionized molecule to estimate the influence of extent of charge distribution [62]. In this study, the dependence of the method and basis set on

Table 2.1: The dependence of the quantum chemical calculation method and the basis set on the investigation of total energy of the acetone in the neutral and radical cationic states. Units are hartree.

Basis set	Neutral state		Radical cationic state	
	B3LYP	MP2	B3LYP	MP2
3-21G	-192.093	-190.884	-191.751	-190.587
6-31G(d)	-193.156	-191.960	-192.810	-191.659
6-31G(d,p)	-193.164	-191.970	-192.820	-191.670
6-31+G(d)	-193.166	-191.965	-192.814	-191.661
6-31+G(d,p)	-193.175	-191.975	-192.822	-191.672
CC-PVTZ	-193.164	-191.976	-192.820	-191.677
6-311G(d,p)	-193.213	-192.011	-192.864	-191.710
6-311+G(d,p)	-193.218	-192.015	-192.865	-191.712

the total energy of the optimized structure of acetone in the neutral and radical cationic states is examined by using the two method, MP2 and B3LYP, and the various basis sets of 3-21G, 6-31G(d), 6-31G(d,p), 6-31+G(d), 6-31+G(d,p), 6-311G(d,p), and 6-311+G(d,p), for the quantum chemical calculation, as shown in Table 2.1. The calculations of the 6-31G including the extended basis set such as the polarization function and the diffuse function showed lower energy than that with 3-21G basis set. The triple split valence basis sets showed even lower values. The differences of the minimum energies between in the neutral and radical cationic states are similar with that of the 6-31G in the each molecule. These calculations are done by Gaussian 03 [68].

2.2.2 Optimized structure

The optimized structures of the acetone and 3-pentanone in the neutral and radical cationic states in gas phase are shown in Figure 2.1. The detailed values of the bond length and angle of intramolecule are listed in the Table 2.3, Table 2.4, Table 2.5 and Table 2.6. The optimized structure of the acetone in neutral state can be compared with the experimental data in gas phase. The bond lengths, $O=C_{sp2}$, $C_{sp2}-C_{sp3}$ and $C_{sp3}-H$, has known to be the 1.213 Å, 1.520 Å and 1.103 Å, respectively. The angle, $C_{sp3}-C_{sp2}-C_{sp3}$ has known to be 116.0 deg., respectively. These values are measured by the microwave spectroscopy [57]. The differences of the predicted bond length and angle with the experimental data are 0.012 Å and 0.8 degree, respectively at most, showing an excellent agreement the computation with the experimental data. On the other hand, the equilibrium bond lengths of both molecules in the neutral state are in good agreement with those of the parm99 force field parameters. The differences of bond lengths between the computations and the parm99 force field parameters are in 0.01 Å, as shown in Table 2.3 and Table 2.4. While, the differences of angles are shown to be 3.1 deg. in the 3-pentanone. However, because the estimated angles in this study are obtained by large level basis set (6-31+G(d,p)) in comparison with that used in the development of the parm99 force field parameters, the predicted structures in this study should be more accurate.

In the case of comparison with those in cationic state, the differences of the bond length and angle between in the neutral and radical cationic states are 0.48 Å and 6.4 deg., respectively at most. This large angle change in the cationic state should be due to the change of molecular orbital by ionization of the molecule;

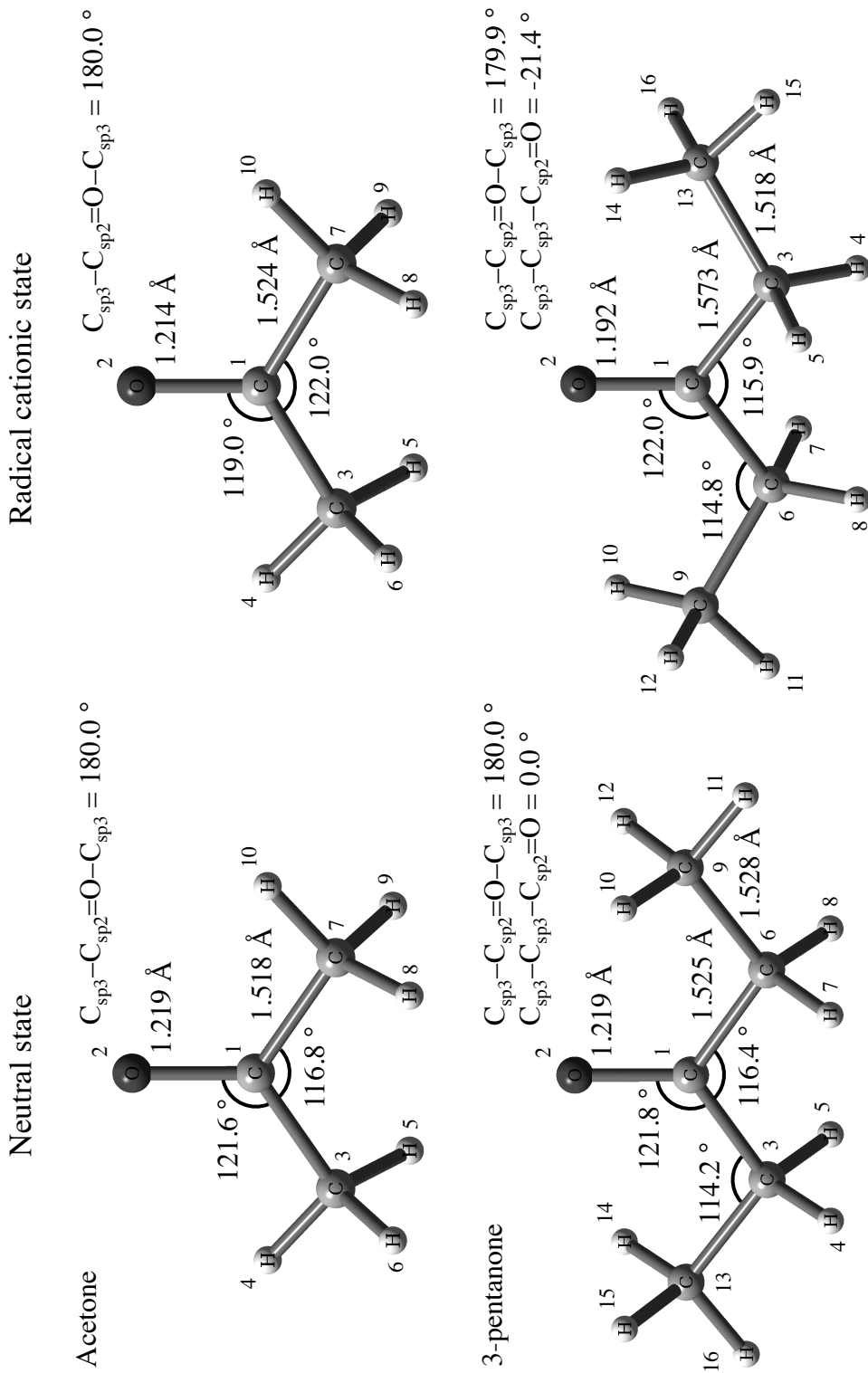


Figure 2.1: The optimized structures of the acetone and 3-pentanone in the neutral and radical cationic states obtained by the DFT-B3LYP/6-31+G(d,p) calculations.

the change of molecular polarization should influence the intramolecular interaction between the atoms in the molecule, resulting in the change of molecular structure.

2.2.3 Ionization potential

The total energies of the optimized structures for the acetone in the neutral state and radical cationic states obtained by the DFT calculations are -121,218.8 kcal/mol and -120,997.9 kcal/mol in gas phase, respectively. While, the total energies of that for the 3-pentanone are -170,563.2 kcal/mol and -170,351.2 kcal/mol, respectively.

The ionization potential is estimated the difference of total energy of the molecules between in the neutral and radical cationic states. From above results, The values of ionization potential of the acetone and 3-pentanone are 220.9 kcal/mol and 212.0 kcal/mol, respectively. By way of comparison, the experimental data of the first adiabatic ionization potential in gas phase are 223.0 kcal/mol for the acetone and 215.0 kcal/mol for the 3-pentanone [70], respectively. Fu and co-workers have presented the computational values of ionization potential for 160 organic molecules by the DFT-B3LYP calculations with 6-31+G(d) basis set and have reported that the computational value using the method and basis set has an error of the 6.5 kcal/mol as an average comparing with the experimental data [2]. In this study, the differences between theoretical values and experimental measurements are 2.1 kcal/mol for the acetone and 3.0 kcal/mol for the 3-pentanone, showing that these computational values are in good agreement with the experimental data. The results also indicate that the proper DFT

calculations are conducted in this study.

2.3 Force Field Parameters of Intermolecular Interaction

The potential energy function for the intermolecular interaction, V^{inter} , for the van der Waals (vdW) and coulomb interaction are represented by the following equation;

$$V^{inter} = \sum_{i \in I} \sum_{j \in J}^{atoms \ atoms} \varepsilon_{ij} \left[\left(\frac{R_{ij}^e}{r_{ij}} \right)^{12} - 2 \left(\frac{R_{ij}^e}{r_{ij}} \right)^6 \right] + \sum_{i \in I} \sum_{j \in J}^{atoms \ atoms} \frac{q_i q_j}{\varepsilon r_{ij}}, \quad (2.1)$$

where $i \in I$ and $j \in J$ are the i -th atom in the molecule I and j -th atom in the molecule J , ε_{ij} is the Lennard-Jones (L-J) potential parameter between atom i and atom j , R_{ij}^e is the equilibrium internuclear distance, which presents the minimum of potential energy as a function of atom distance, r_{ij} , q_i and q_j are the effective point charges of atom i and atom j , and ε is the relative permittivity, respectively. The L-J parameters between different atoms are assigned as an arithmetic average for R_{ij}^e , and geometric mean for ε_{ij} by the rule of Lorentz-Berthelot. In the molecular dynamics (MD) simulations in this study, all parameters of $R_{ij}^e/2$ and ε_{ij} are taken from the parm99 force field parameters. The RESP charges of the molecules are determined by the Merz-Singh-Kollman method [69] with DFT-B3LYP/6-31+G(d,p) calculations. In the Merz-Singh-Kollman method, the RESP charge is evaluated by fitting each points of put on the sphere around each atoms by the electrostatic potential. The following

subsection presents the results of calculation of RESP charge.

2.3.1 Partial charge

The evaluated RESP charges of the molecules, acetone and 3-pentanone, in the neutral and radical cationic states is listed in Table 2.2. The estimated partial charges of the O, C in carbonyl group and the methyl group of the acetone in the neutral state are the -0.535 a.u., +0.621 a.u. and the -0.044 a.u., respectively. The partial charges of that in the radical cationic state are the -0.015 a.u., +0.506 a.u. and the +0.253 a.u., respectively. While the partial charges of the O and C in carbonyl group, methylene group and methyl group of the 3-pentanone in the neutral state are the -0.517 a.u. and +0.530 a.u., -0.013 a.u. and +0.008 a.u., respectively. The partial charges of that in the radical cationic state are the -0.082 a.u. and +0.391 a.u., +0.183 a.u. and +0.163 a.u., respectively. These data show the localization of the charge distribution of the both of molecules in the radical cationic state to hydrophobic group. To assess the validity of these partial charges, the total dipole moments of both molecules are compared with the experimental data. The calculated total dipole moments of the acetone and 3-pentanone are 3.19 debye and 2.89 debye, respectively, showing close to the experimental data, 2.88 ± 0.03 debye and 2.82 debye, respectively. While those in the radical cationic state are 2.12 debye and 2.30 debye, showing that the polarization in the radical cationic state is small than that in the neutral state in both molecules.

Table 2.2: RESP charges of the acetone and 3-pentanone in the neutral (N) and radical cationic ($N + 1$) states by DFT-B3LYP-6-31+G(d,p) calculations. Units are elementary charge.

	N	$N+1$		N	$N+1$
<u>Acetone</u>					
C1	0.621	0.506	H6	0.069	0.175
O2	-0.535	-0.015	C7	-0.251	-0.272
C3	-0.251	-0.272	H8	0.069	0.175
H4	0.069	0.175	H9	0.069	0.175
H5	0.069	0.175	H10	0.069	0.175
<u>3-pentanone</u>					
C1	0.530	0.391	C9	-0.052	-0.098
O2	-0.517	-0.082	H10	0.020	0.087
C3	-0.023	-0.035	H11	0.020	0.087
H4	0.005	0.109	H12	0.020	0.087
H5	0.005	0.109	C13	-0.052	-0.098
C6	-0.023	-0.035	H14	0.020	0.087
H7	0.005	0.109	H15	0.020	0.087
H8	0.005	0.109	H16	0.020	0.087

2.4 Force Field Parameters of Intramolecular Interaction

The potential energy function for the intramolecular interaction, V^{intra} , of the molecule is represented as sum of the bond stretching, angle bending, and tor-

sional energy as the following equation,

$$\begin{aligned}
 V^{intra} = & \sum_{bonds} K_r (r - r_{eq})^2 \\
 & + \sum_{angles} K_\theta (\theta - \theta_{eq})^2 \\
 & + \sum_{dihedrals} \frac{V_{ijkl}^n}{2} [1 + \cos(n\phi_{ijkl} - \gamma_{ijkl})], \quad (2.2)
 \end{aligned}$$

where K_r and K_θ are spring constants of the stretching vibration and angle bending, r_{eq} and θ_{eq} are equilibrium bond length and angle, V^n is the spring constant of torsional energy constructed by atoms $ijkl$, n is the phase $ijkl$ period, and γ_{ijkl} is equilibrium torsion angle of $ijkl$, respectively. As mentioned in section 2.1, the force constants of the bond stretching vibration and angle bending, K_r and K_θ , of the molecules in radical cationic state are not prepared in AMBER force field. Therefore, these parameters are estimated in the following subsection. While, the force field parameters of torsion angle, V_{ijkl}^n , ϕ_{ijkl} and γ_{ijkl} , of the molecules in each state adopt the AMBER force field (parm99) with constraints by the harmonic potentials, as mentioned in CHAPTER 3.

2.4.1 Computational details

In order to estimate the spring constants of the intramolecular stretching vibration for the acetone and 3-pentanone in the neutral and radical cationic states, the potential energy surface of the molecules is investigated with different bond distance. With sweeping the potential energy surface, a certain range in the potential energy curve can be investigated in detail. The total energy of the structure each bond distance with the step of the bond distance for 0.01 Å is obtained by the DFT-B3LYP calculations with 6-31+G(d,p) basis set, which is

similar calculation method and basis set with the optimization, in order to sweep the potential energy surface. Then, the obtained potential energy surface is fitted by the harmonic potential function with the total 5 sample data around the most stable total energy, which is obtained by the optimization.

In similar way of the evaluation of the spring constant of the stretching vibration, the force constant of intramolecular angle bending for the molecules both of states is estimated from the dependence of the total energy of the molecule on the angle in the structure of molecule by the DFT-B3LYP/6-31+G(d,p) calculations. The steps of the angle bending are 0.5 degree; total 7 sampling data around the most stable total energy are used to estimate these force constant parameters. In this study, the angles around the atom C_{sp2} of the acetone and 3-pentanone are defined to lie in the same plane. Then, in order to estimate the force constants of two angle of O=C_{sp2}-C_{sp3} and an angle C_{sp3}-C_{sp2}-C_{sp3}, fitting function is defined by the following equation;

$$E^{gas}(\delta) = (K_i + K_j) \delta^2 \quad (2.3)$$

where E^{gas} is the total energy along with the displacement of the interest angles, δ , K_i and K_j are the force constants of interest of angles i and j , respectively. The force constants of the 3 angles around the atom C_{sp2} of the molecules are independently determined from the obtained 3 equations.

2.4.2 Bond stretching

The estimated force constants of intramolecular bond stretching for the acetone and 3-pentanone in the neutral and radical cationic states are listed in Table

2.3 and Table 2.4 with the AMBER force field parameter (parm99) [63, 51].

The force constants of $O=C_{sp^2}$ and $C_{sp^2}-C_{sp^3}$ for acetone in the neutral state are $932.3 \text{ kcal/mol/\AA}^2$ and $295.8 \text{ kcal/mol/\AA}^2$, respectively. The $O=C_{sp^2}$ by computation is too much larger than that by the parm99 ($570.0 \text{ kcal/mol/\AA}^2$), indicating considerably stronger binding in the former, because the computational values in this study are estimated by considering the interaction of carbonyl group from the methyl group. The $C_{sp^2}-C_{sp^3}$ is smaller than that of the parm99 (295.8

Table 2.3: The spring constants, K_r , and equilibrium lengths, r_{eq} , for the intramolecular bond stretching of acetone in the neutral (N) and radical cationic ($N + 1$) states with parm99 force field parameter. Units of K_r and r_{eq} are kcal/mol/\AA^2 and \AA .

Bond	PARM99 ^a		N		$N+1$	
	K_r	r_{eq}	K_r	r_{eq}	K_r	r_{eq}
O2 = C1	570.0	1.229	932.3	1.219	806.8	1.214
C3 – C1	317.0	1.522	295.8	1.518	251.0	1.524
H4 – C3	340.0	1.090	394.4	1.091	394.4	1.089
H5 – C3	340.0	1.090	376.5	1.096	376.5	1.095
H6 – C3	340.0	1.090	376.5	1.097	376.5	1.098
C7 – C1	317.0	1.522	295.8	1.518	251.0	1.524
H8 – C7	340.0	1.090	376.5	1.096	376.5	1.096
H9 – C7	340.0	1.090	376.5	1.097	376.5	1.098
H10 – C7	340.0	1.090	394.4	1.091	394.4	1.089

^a The parm99 force field parameters from Ref. [***] and [***].

Table 2.4: The force constants, K_r , and equilibrium lengths, r_{eq} , for the intramolecular bond stretching of 3-pentanone in the neutral (N) and radical cationic (N+1) states with parm99 force field parameter. Units of K_r and r_{eq} are kcal/mol/Å² and Å.

Bond	PARM99 ^a		N		N+1	
	K_r	r_{eq}	K_r	r_{eq}	K_r	r_{eq}
O2 = C1	570.0	1.229	927.8	1.219	950.2	1.192
C3 – C1	317.0	1.522	286.9	1.525	179.3	1.573
H4 – C3	340.0	1.090	358.6	1.100	376.5	1.095
H5 – C3	340.0	1.090	358.6	1.100	358.6	1.101
C6 – C1	317.0	1.522	286.9	1.525	179.3	1.573
H7 – C6	340.0	1.090	358.6	1.100	358.6	1.101
H8 – C6	340.0	1.090	358.6	1.100	376.5	1.095
C9 – C6	310.0	1.526	322.7	1.528	322.7	1.518
H10 – C9	340.0	1.090	385.5	1.094	394.4	1.092
H11 – C9	340.0	1.090	376.5	1.095	376.5	1.097
H12 – C9	340.0	1.090	385.5	1.094	394.4	1.093
C13 – C3	310.0	1.526	322.7	1.528	317.5	1.518
H14 – C13	340.0	1.090	385.5	1.094	394.4	1.092
H15 – C13	340.0	1.090	376.5	1.095	376.5	1.097
H16 – C13	340.0	1.090	385.5	1.094	394.4	1.093

^a The parm99 force field parameters from Ref. [***] and [***].

kcal/mol/Å²), indicating weaker bonding. While, for the 3-pentanone in the neutral state, the force constants of O=C_{sp2}, C_{sp2}-C_{sp3} and the average of C_{sp3}-C_{sp3} are 927.8 kcal/mol/Å², 286.9 kcal/mol/Å² and 322.7 kcal/mol/Å², showing that the value of O=C_{sp2} is also too much larger than that of the parm99 and the values of C_{sp2}-C_{sp3} and C_{sp3}-C_{sp3} are smaller and larger than the parm99 (63.0 kcal/mol/Å² and 310.0 kcal/mol/Å²), respectively.

On the other hand, the difference of force constants of O=C_{sp2} and C_{sp2}-C_{sp3} in the radical cationic state from that in the neutral are -127.5 kcal/mol/Å² and -44.8 kcal/mol/Å², indicating weaker than the neutral state, respectively. While, for the 3-pentanone in the radical cationic state, the O=C_{sp2} is 950.2 kcal/mol/Å², which is larger than that in the neutral state (927.8 kcal/mol/Å²). These results of 3-pentanone have different propensity to the acetone. While, the C-C for 3-pentanone has similar trend to that for acetone.

2.4.3 Angle bending

The estimated force constants of intramolecular angle bending for the acetone and 3-pentanone in the neutral and radical cationic states are listed in Table 2.5 and Table 2.6 with the AMBER force field parameter (parm99) [63, 51]. The force constants of C_{sp2}=O-C_{sp2} for the acetone and 3-pentanone in neutral state are the 80.0 kcal/mol/deg² and 84.0 kcal/mol/deg², respectively, showing that the value of acetone equal to the parm99 (80.0 kcal/mol/deg²) and that of 3-pentanone larger than the parm99. The C_{sp3}-C_{sp2}-C_{sp3} of both of molecules are smaller than the parm99 with the difference of 5.3 kcal/mol/deg² for acetone and 1.5 kcal/mol/deg² for 3-pentanone, respectively. The C_{sp2}-C_{sp3}-C_{sp3} of the

3-pentanone is 106.9 kcal/mol/deg², showing that the result is considerably larger than the parm99 (63.0 kcal/mol/deg²).

In the radical cationic state, the force constants of 3 angles around the C_{sp2} for both of molecules and C_{sp3}-C_{sp3}-C_{sp2} of the 3-pentanone are considerably smaller than that in the neutral state with the difference of 46.2 kcal/mol/deg² at most, showing that the conformation of these molecules in the radical cationic state diffusive in the direction of carbon chain.

Table 2.5: The spring constants, K_θ , and equilibrium angles, θ_{eq} , for the intramolecular angle bending of acetone in the neutral and radical cationic states with parm99 force field parameter. Units of K_θ and θ_{eq} are kcal/mol/deg² and deg.

Angle	PARM99 ^a		<i>N</i>		<i>N</i> +1	
	K_θ	θ_{eq}	K_θ	θ_{eq}	K_θ	θ_{eq}
C3 – C1 = O2	80.0	120.4	80.0	121.6	33.8	119.0
H4 – C3 – C1	50.0	109.5	65.7	110.1	68.8	111.4
H5 – C3 – C1	50.0	109.5	63.6	110.7	63.2	107.1
H6 – C3 – C1	50.0	109.5	62.2	109.8	60.3	106.0
C7 – C1 = O2	80.0	120.4	80.0	121.6	33.8	119.0
C7 – C1 – C3	63.0	117.0	57.7	116.8	48.0	122.0
H8 – C7 – C1	50.0	109.5	63.6	110.7	63.2	107.1
H9 – C7 – C1	50.0	109.5	62.2	109.8	60.3	106.0
H10 – C7 – C1	50.0	109.5	65.7	110.1	68.8	111.4

^a The parm99 force field parameters from Ref. [***] and [***].

Table 2.6: The spring constants, K_θ , and equilibrium angles, θ_{eq} , for the intramolecular angle bending of 3-pentanone in the neutral and radical cationic states with parm99 force field parameter. Units of K_θ and θ_{eq} are kcal/mol/deg² and deg.

Angle	PARM99 ^a		<i>N</i>		<i>N</i> +1	
	K_θ	θ_{eq}	K_θ	θ_{eq}	K_θ	θ_{eq}
C3 – C1 = O2	80.0	120.4	84.0	121.8	41.5	122.0
H4 – C3 – C1	50.0	109.5	67.7	107.6	67.7	104.6
H5 – C3 – C1	50.0	109.5	67.7	107.6	62.8	101.2
C6 – C1 = O2	80.0	120.4	84.0	121.8	41.5	122.0
C6 – C1 – C3	63.0	117.0	61.5	116.4	47.0	115.9
H7 – C6 – C1	50.0	109.5	67.7	107.6	62.8	101.2
H8 – C6 – C1	50.0	109.5	67.7	107.6	62.8	104.6
C9 – C6 – C1	63.0	111.1	106.9	114.2	87.3	114.8
H10 – C9 – C6	50.0	109.5	72.6	111.0	72.6	112.3
H11 – C9 – C6	50.0	109.5	67.7	110.5	62.8	106.9
H12 – C9 – C6	50.0	109.5	72.6	111.0	72.6	112.2
C13 – C3 – C1	63.0	111.1	106.9	114.2	87.3	114.8
H14 – C13 – C3	50.0	109.5	72.6	111.0	72.6	112.3
H15 – C13 – C3	50.0	109.5	67.7	110.5	62.8	106.9
H16 – C13 – C3	50.0	109.5	72.6	111.0	72.6	112.2

^a The parm99 force field parameters from Ref. [***] and [***].

2.5 Concluding Remarks

This chapter have presented the optimized structures and the developed force field parameters of bond stretching, angle bending, partial charge for the acetone and 3-pentanone in the neutral and radical cationic states. The optimized structure and the force field parameter are estimated by the density functional theory (DFT) calculations with the B3LYP method and the 6-31+G(d,p) basis set, which are higher level than that used at AMBER force field parameters (parm99). The optimized structure of acetone in the neutral state are comparative with the experimental measurement. The ionization potentials obtained by the estimation of the total energies of the optimized structures between the neutral and radical cationic states are good agreement with the experimental data. The determined partial charges of these molecules reproduce the dipole, which is in agreement with the experimental data.

CHAPTER 3

Structure and Hydration

Properties of Organic

Compounds in Neutral and

Radical Cationic States

3.1 Introduction

In the previous chapter, the optimized structure and the force field parameters for the organic molecules, acetone and 3-pentanone, in the neutral and radical cationic states were estimated originally by the density functional theory (DFT) calculations with high-level basis set. The purposes of this chapter are to perform the molecular dynamics (MD) simulations of these organic molecules using the force field parameters developed in chapter 2 and to investigate the structure and hydration properties of these organic compounds in the neutral and radical

cationic states, including the meaning of test of the developed force field parameters. For the analysis of these properties, the conformation and fluctuation in the thermal equilibrium state in solution obtained by carrying out the MD simulations are compared with in the liquid and gas phases and with the neutral and radical cationic states. The excess chemical potentials of these molecules are also compared in the neutral and radical cationic states with comparison of theoretical and experimental values in the neutral state. From these results, the ionization effect of these organic compounds on the excess chemical potential is discussed before computation of redox potential of these molecules in this chapter.

3.2 Computational Procedure

This section presents the theoretical background to estimate the excess chemical potential of solute molecule in bulk water and the simulation method of the excess chemical potential by the energy representation (ER) method.

3.2.1 Chemical potential

A weak solution system composed of $N + 1$ molecules is considered in this study. The first N molecules constitute the solvent system and the $(N + 1)$ -th molecule is an solute molecule. Chemical potential of the solute molecule in solution, μ , can be explicitly expressed by statistical-mechanical description. Hamiltonian of the whole molecular system, H_{N+1} , is written as

$$H_{N+1}(\mathbf{p}^{N+1}, \mathbf{r}^{N+1}) = H_{N+1}(\mathbf{p}^N, \mathbf{r}^N, \mathbf{p}_{N+1}, \mathbf{r}_{N+1}) \quad (3.1)$$

$$= \frac{1}{2m} \sum_i^N \mathbf{p}_i^2 + \frac{\mathbf{p}_{N+1}^2}{2m_{N+1}} + V_{N+1}(\mathbf{r}^N, \mathbf{r}_{N+1}), \quad (3.2)$$

where \mathbf{p}^{N+1} and the \mathbf{p}_{N+1} are momentum of first "N" and the $(N + 1)$ -th molecules, \mathbf{r}^{N+1} and the \mathbf{r}_{N+1} are coordinate of first "N" and the $(N + 1)$ -th molecules, m and the m_{N+1} are mass of first N and the $(N + 1)$ -th molecules, respectively. V_{N+1} is potential energy of the whole molecular system written by the following equation;

$$V_{N+1}(\mathbf{r}^N, \mathbf{r}_{N+1}) = V_N(\mathbf{r}^N) + V_{N+1}^{intra} + V(\mathbf{r}^N, \mathbf{r}_{N+1}), \quad (3.3)$$

where V_N , V_{N+1}^{intra} , and V represent the sum of intramolecular and intermolecular interactions over first N molecules, intramolecular interaction of the $(N + 1)$ -th molecule, and the intermolecular interaction between the $(N + 1)$ -th and the rest of first N molecules, respectively. For simplicity, if the intramolecular interaction in the whole system does not be considered, then the V_{N+1}^{intra} can be ignored as following equation;

$$V_{N+1}(\mathbf{r}^N, \mathbf{r}_{N+1}) = V_N(\mathbf{r}^N) + V(\mathbf{r}^N, \mathbf{r}_{N+1}). \quad (3.4)$$

Partition function of $N + 1$ molecular system, Q_{N+1} , is written as

$$Q_{N+1}(\mathbf{r}^N, \mathbf{r}_{N+1}) = \frac{1}{N!1!} \frac{1}{h^{3(N+1)}} \iint \exp \left\{ -\frac{H_{N+1}(\mathbf{p}^{N+1}, \mathbf{r}^{N+1})}{k_B T} \right\} d\mathbf{p}^{N+1} d\mathbf{r}^{N+1} \quad (3.5)$$

$$= \frac{1}{N!1!\Lambda^{3N}\Lambda_{N+1}^3} \iint \exp \left\{ -\frac{V_{N+1}(\mathbf{r}^N, \mathbf{r}_{N+1})}{k_B T} \right\} d\mathbf{r}^N d\mathbf{r}_{N+1} \quad (3.6)$$

where h is the Planck's constant, k_B is the Boltzmann constant, T is the system temperature, Λ^{3N} and Λ_{N+1}^3 are the thermal de Broglie wave length of the first N and the $(N + 1)$ -th molecules, written as $(2m\pi k_B T)^{3N/2}$ and $(2m_{N+1}\pi k_B T)^{3/2}$,

respectively. Partition function of first N molecules, Q_N , is also written as

$$Q_N(\mathbf{r}^N) = \frac{1}{N! \Lambda^{3N}} \int \exp \left\{ -\frac{V_N(\mathbf{r}^N)}{k_B T} \right\} d\mathbf{r}^N. \quad (3.7)$$

Chemical potential of the solute molecule in solution, μ , is the difference of free energy between the pure solvent and solution systems. The μ is statistical mechanically described with (3.6) and (3.7) as the following equation,

$$\mu = -k_B T \log \left\{ \frac{Q_{N+1}}{Q_N} \right\} \quad (3.8)$$

$$= -k_B T \log \left\{ \frac{1}{1! \Lambda_{N+1}^3} \frac{\iint \exp \left\{ -\frac{V_{N+1}(\mathbf{r}^N, \mathbf{r}_{N+1})}{k_B T} \right\} d\mathbf{r}^N d\mathbf{r}_{N+1}}{\int \exp \left\{ -\frac{V_N(\mathbf{r}^N)}{k_B T} \right\} d\mathbf{r}^N} \right\} \quad (3.9)$$

$$= k_B T \log(\rho \Lambda_{N+1}^3) - k_B T \log \left\{ \frac{\iint \exp \left\{ -\frac{V_{N+1}(\mathbf{r}^N, \mathbf{r}_{N+1})}{k_B T} \right\} d\mathbf{r}^N d\mathbf{r}_{N+1}}{\iint \exp \left\{ -\frac{V_N(\mathbf{r}^N)}{k_B T} \right\} d\mathbf{r}^N d\mathbf{r}_{N+1}} \right\} \quad (3.10)$$

where ρ is defined as solute concentration, written as $\rho = 1!/V$, however V is the volume of the pure solvent system. If the solute molecule is put on the origin of coordinate space (i.e. $\mathbf{r}'_i = \mathbf{r}_i - \mathbf{r}_{N+1}$), the μ is written as

$$\mu = k_B T \log(\rho \Lambda_{N+1}^3) - k_B T \log \left\{ \frac{\int \exp \left\{ -\frac{V_{N+1}(\mathbf{r}'^N)}{k_B T} \right\} d\mathbf{r}'^N}{\int \exp \left\{ -\frac{V_N(\mathbf{r}'^N)}{k_B T} \right\} d\mathbf{r}'^N} \right\} \quad (3.11)$$

$$= k_B T \log(\rho \Lambda_{N+1}^3) - k_B T \log \left\langle \exp \left\{ -\frac{V(\mathbf{r}'^N)}{k_B T} \right\} \right\rangle, \quad (3.12)$$

where $\langle \rangle$ is the ensemble average on the pure solvent system. In equation (3.12), the first term is chemical potential of the solute molecule in ideal gas. The second

term is excess chemical potential (also called solvation free energy) of the solute molecule,

$$\mu^{ex} = -k_B T \log \left\langle \exp \left\{ -\frac{V(\mathbf{r}^N)}{k_B T} \right\} \right\rangle. \quad (3.13)$$

However, the μ^{ex} can not be calculated on its own. The next subsection presents briefly the computational method for the calculation of the excess chemical potential by the ER method.

3.2.2 Energy representation method

The Energy Representation (ER) method developed by Matubayasi's group is adopted for the estimation of excess chemical potential of solute molecule in solution, μ^{ex} , with MD simulation in this study. In the ER method, the excess chemical potential of solute molecule can be presented as a function of the energy distribution functions, $\rho^e(\varepsilon)$ and $\rho_0^e(\varepsilon)$, and the correlation function $\chi_0(\varepsilon, \eta)$. These energy distribution and the correlation are functions of energy coordinate ε , which is a pair intermolecular energy between the solute molecule and surrounding solvent molecules, that are the $(N+1)$ -th molecule and first N molecules defined in previous section. For the calculations of the energy distribution functions, $\rho^e(\varepsilon)$ and the $\rho_0^e(\varepsilon)$, the intermolecular energy between the solute molecule and surrounding solvent molecules is calculated in the solution system and the pure solvent system.

The energy distribution function $\rho^e(\varepsilon)$ is expressed as follow by following description of Matubayasi;

$$\rho^e(\varepsilon) = \left\langle \sum_i \delta(\nu(\psi, \mathbf{x}_i) - \varepsilon) \right\rangle, \quad (3.14)$$

where ψ is the coordinate of solute molecule, ν is the potential function for the solute and solvent pair interaction, \mathbf{x}_i denotes the coordinate (the set of position and orientation) of i -th solvent molecule, respectively. The summation is taken over all the solvent molecules, and the energy distribution is obtained by the calculation of ensemble average. The solution system is the system of interest in which the solute molecule interacts with surrounding solvent molecules under the solute and solvent interaction, ν , of interest at full coupling. The pure solvent system denotes the system in which no interaction physically present between the solute molecule and solvent molecules. The energy distribution function, $\rho_0^e(\varepsilon)$, and the correlation function $\chi_0(\varepsilon, \eta)$ are constructed by placing the solute molecule in the pure solvent system as a test particle. The actual form of the excess chemical potential using these distribution functions and the correlation function and the detail of computational methodology are presented in Refs. [29, 30, 31]. The practical computational details of the thermal equilibrium MD simulations and the excess chemical potential with ER method are presented in the following section.

3.3 Computational Details

3.3.1 Molecular dynamics simulation

The MD simulation of the organic compounds, acetone and 3-pentanone, in the neutral and radical cationic states in water solvent is performed with the AMBER 11 program packages. For the MD simulations of these molecules in the neutral and radical cationic states, the force field parameter of the stretching vibration

and angle bending of intramolecular potential, and partial charge of intermolecular potential originally developed in chapter 2. However the stretching vibration and angle bending potential parameters including hydrogen atom of these molecules assign AMBER force field 03 (parm99) [63, 64]. The intramolecular torsion angle including the hydrogen atom of the methyl and methylene groups, which is the H-C_{sp3}-C_{sp2}=O in the structure of the acetone, H-C_{sp3}-C_{sp3}-C_{sp2} in the structure of 3-pentanone, and improper torsion C_{sp3}-C_{sp2}=O-C_{sp3} in the structure of both molecules, is constrained with harmonic potential, $V_{\phi}^{constraint}$, as follow;

$$V_{\phi}^{constraint}(\phi) = \sum_{dihedrals \in M_{N+1}} K_{\phi}(\phi - \phi_{eq}) \quad (3.15)$$

where $dihedrals \in M_{N+1}$ is the torsion angles in the $(N + 1)$ -th molecule, K_{ϕ} is the spring constant of the torsion angle, ϕ is the torsion angle of interest in the molecule, ϕ_{eq} is the equilibrium torsion angle, respectively. The ϕ_{eq} of these molecules in the neutral and radical cationic states is obtained from the optimized structures determined in chapter 2. The spring constant, K_{ϕ} , for the constraint of torsion angle is estimated from the dependence of the total energy of the molecule on the torsion angle in the structure of molecule by the density functional theory (DFT) calculations with B3LYP/6-31+G(d,p) by the Gaussian 03 program package [68]. The threshold used to the convergence of self consistent field (SCF) calculation is ten digits. The fitting to the dependence of the total energy is carried out from $\phi_{eq} - 45$ to $\phi_{eq} + 45$ to be composed the torsion angle of periodic function. The fitting steps are 0.5 degree, therefore total energy of 180 data is prepared for the estimation of K_{ϕ} . The equilibrium torsion angle and the spring constant of the acetone and 3-pentanone in the neutral and radical cationic

states are listed in the Table 3.1 and Table 3.2. The force field parameters for the other intramolecular torsion angle of 3-pentanone, the Lennard-Jones (L-J) potential parameter used to compute the intermolecular interaction in the whole system, and the stretching vibration and angle bending of solvent molecule assigns the AMBER force field 03 (parm99).

For the MD simulation, Langevin thermostat and barostat are used to control system temperature ($T = 300$ K) and the pressure ($P = 1$ atm). The acetone and 3-pentanone are solvated by 1,425 water molecules in a cubic box with $39.8 \text{ \AA} \times 37.4 \text{ \AA} \times 38.0 \text{ \AA}$, and 1,790 water molecules in a cubic box with 44.5 \AA

Table 3.1: Spring constant and equilibrium torsion angle for the harmonic potential, K_ϕ and ϕ_{eq} used to the MD simulation of acetone. The number behind the atomic symbol is compatible with the number showed in Figure 2.1. Units of K_ϕ and ϕ_{eq} are kcal/mol/deg.² and deg..

Torsion angle	Neutral state		Radical cationic state	
	K_ϕ	ϕ_{eq}	K_ϕ	ϕ_{eq}
H4 - C3 - C1 = O2	54.2	5.5	51.7	8.0
H5 - C3 - C1 = O2	50.8	127.1	48.9	130.4
H6 - C3 - C1 = O2	50.7	-114.8	48.8	-112.5
C7 - C1 = O2 - C3	35.7	180.0	32.3	180.0
H8 - C7 - C1 = O2	50.7	127.0	48.9	130.3
H9 - C7 - C1 = O2	50.7	-115.0	48.8	-112.6
H10 - C7 - C1 = O2	54.2	5.4	51.7	7.9

Table 3.2: Spring constant and equilibrium torsion angle for the harmonic potential, K_ϕ and ϕ_{eq} used to the MD simulation of 3-pentanone. The number behind the atomic symbol is compatible with the number showed in Figure 2.1. Units of K_ϕ and ϕ_{eq} are kcal/mol/deg.² and deg..

Torsion angle	Neutral state		Radical cationic state	
	K_ϕ	ϕ_{eq}	K_ϕ	ϕ_{eq}
C6 - C1 = O2 - C3	37.8	180.0	25.8	180.1
H10 - C9 - C6 - C1	53.3	59.6	50.5	61.6
H11 - C9 - C6 - C1	54.0	180.0	50.6	180.3
H12 - C9 - C6 - C1	53.3	-59.6	51.1	-62.1
H14 - C13 - C3 - C1	53.3	59.6	50.5	61.6
H15 - C13 - C3 - C1	54.0	-180.0	50.6	-179.7
H16 - C13 - C3 - C1	53.3	-59.6	51.1	-62.1

$\times 39.3 \text{ \AA} \times 39.5 \text{ \AA}$, as shown in Figure 3.1 and Figure 3.2, respectively. The TIP3P (transferable intermolecular potential 3 point) model [65] is adopted for the solvent molecule (water molecule). Particle Mesh Ewald (PME) method [66] is used for the calculation of coulomb interaction. For the MD simulations of the radical cationic acetone and 3-pentanone under the periodic boundary conditions, the operation for neutralization of the system is conducted by adding counter-ion, Cl^- . Cut off length for the coulomb and vdW interactions are 12 \AA . A time step for the MD simulation is 2 fs. The bond length including the hydrogen atom are constrained by SHAKE method [56].

Energy minimization is performed by the steepest descent method with fixing

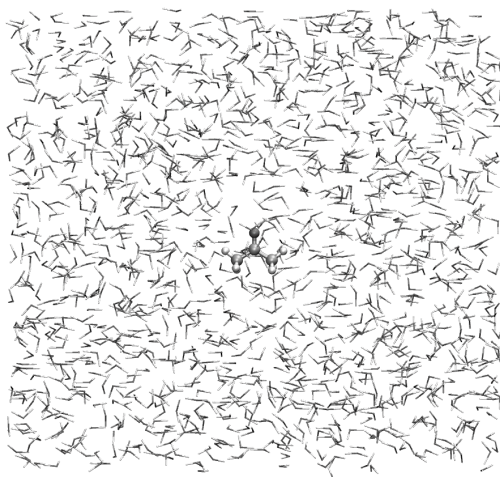


Figure 3.1: Initial solution system for acetone in neutral state.

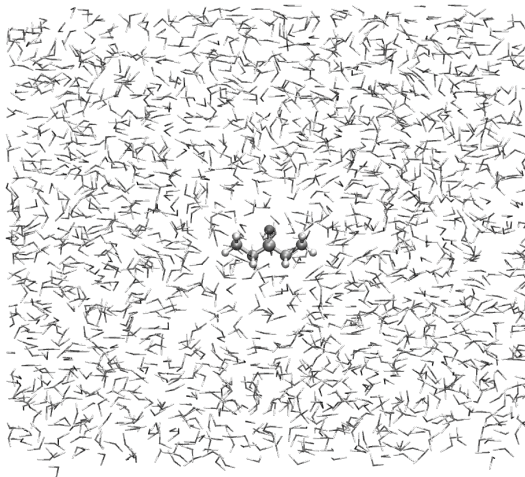


Figure 3.2: Initial solution system for 3-pentanone in neutral state.

the heavy atoms of solute molecule. The MD simulations are carried out in the constant NPT condition with constraints of solute molecule with $50 \text{ kcal/mol}/\text{\AA}^2$ spring constant, and then system temperature is gradually increased in increments of 50 K from 100 K to 300 K for 100 ps. After that, the NPT -MD simulations are performed in which the constraints of solute are gradually reduced in increments of $12.5 \text{ kcal/mol}/\text{\AA}^2$ to zero for 100 ps. Finally, the equilibrium NPT -MD simulations are carried out for 10 ns.

3.3.2 Root mean square deviation

In this study, the thermal equilibration of solute molecule is accessed by analysis of the Root Mean Square Deviation (RMSD) for the heavy atoms, oxygen and carbon atoms of the acetone and 3-pentanone, as a function of MD time steps. the RMSD of solute molecule, $(N + 1)$ -th molecule, is expressed by following

equation;

$$RMSD = \left[\left(\frac{1}{N_{N+1}^{atom}} \right) \sum_{i \in M_{N+1}}^{N_{N+1}^{atom}} |\mathbf{r}_i - \mathbf{r}_i^{\circ}| \right]^{1/2} \quad (3.16)$$

where N_{N+1}^{atom} is the number of atoms in the $(N + 1)$ -th molecule, $i \in M_{N+1}$ is the i -th atom in the $(N + 1)$ -th molecule, \mathbf{r}_i is the coordinate of i -th atom, \mathbf{r}_i° is the reference coordinate of i -th atom, respectively. The reference coordinate is defined to the optimized structure. The translation and rotation of solute molecule are removed on the calculation of RMSD. The whole conformational change of solute molecule from optimized structure can be found by the analysis of RMSD of solute molecule.

3.3.3 Radial distribution function

The Radial Distribution Function (RDF), $g(r)$, is suitable in order to analyze the structure of solvent system surrounding solute molecule. The $g(r)$ is defined as the ratio of the number density in the whole system and the average of number density of the other atomic species present at spherical shell of thickness Δr , which is located in distance, r , away from one of the atomic species of interest. In this study, the RDF between the atom C_{sp2} of the acetone and 3-pentanone and the oxygen atom of water molecules is analyzed, then the $g(r)$ is expressed as the following equation;

$$g(r) = \frac{1}{4\pi r^2 \Delta r} \frac{V}{N_{O_{water}}} \left\langle \Delta N^{O_{water}}(r) \right\rangle \quad (3.17)$$

where V is the system volume, $N_{O_{water}}$ is the number of oxygen atoms of the water molecule in the whole system, $\Delta N^{C_{sp2}-O_{water}}$ is the number of the oxygen atoms present at the spherical shell. The number of oxygen atoms of the water molecule

present at inside of distance r from the atom C_{sp2} of these molecules is derived from the equation (3.17) as follow;

$$N(r) = \rho_{O_{\text{water}}} \int_0^r 4\pi r^2 g(r) dr \quad (3.18)$$

where $\rho_{O_{\text{water}}}$ is the number density of oxygen atom of water molecule in the whole system.

3.3.4 Energy distribution function

The excess chemical potential of solute molecule, which is the sampled configuration in the equilibrium MD simulation, in solution is calculated by using the Energy Representation Module (ERMOD) program packages [67]. In order to estimate the excess chemical potential, energy distribution functions for the solution and pure solvent systems and correlation function are prepared according to the ER method introduced in section 3.2.2 using two MD simulations for these systems.

For the solution system, the sampled structure of solute molecule obtained from the equilibrium MD simulation is put in the center of MD cell, and the water molecules (TIP3P) are arranged around the solute molecule. The MD cell length for the acetone and 3-pentanone systems is same as that using the equilibrium MD simulation. The *NPT*-MD simulation of the solution system is performed for 300 ps under the same conditions as the equilibrium MD simulation. The configuration of solute molecule is fixed in this simulation. The coordinates of the solution system are stored every 10 fs after the system energy is sufficiently equilibrated, therefore total 30,000 snapshots are prepared for the estimation of the energy distribution function, ρ^e .

On the other hand, for the pure solvent system, the pure water system, which has the same number of water molecules and the system size as the solution system, is prepared. The *NPT*-MD simulation of the pure solvent system is performed for 100 ps. The coordinates of the pure solvent system are stored every 1 ps, and 100 snapshots are prepared. After that, the sampled structure, which is the same configuration as the solution system, is randomly inserted 1,000 times into the pure solvent system of each snapshot: total 100,000 sampling data are prepared for the estimation of the energy distribution function, ρ_0^e and the correlation function χ_0 .

These procedures are done for all the sampled structures obtained from the equilibrium MD simulation, to estimate the excess chemical potential, μ^{ex} , with the fluctuation of solute conformation in the solution.

3.4 Results and Discussion

The conformation and fluctuation of the organic molecules, acetone and 3-pentanone, between the neutral and radical cationic states in solution are investigated in the following subsection, and hydration properties of these molecules are discussed with the computation of excess chemical potential in the neutral and radical cationic states.

3.4.1 Conformation and fluctuation in solution

The RMSDs of acetone and 3-pentanone in the neutral and radical cationic states are shown in Figure A.2 and Figure 3.4. As shown in these Figure, the RMSD of

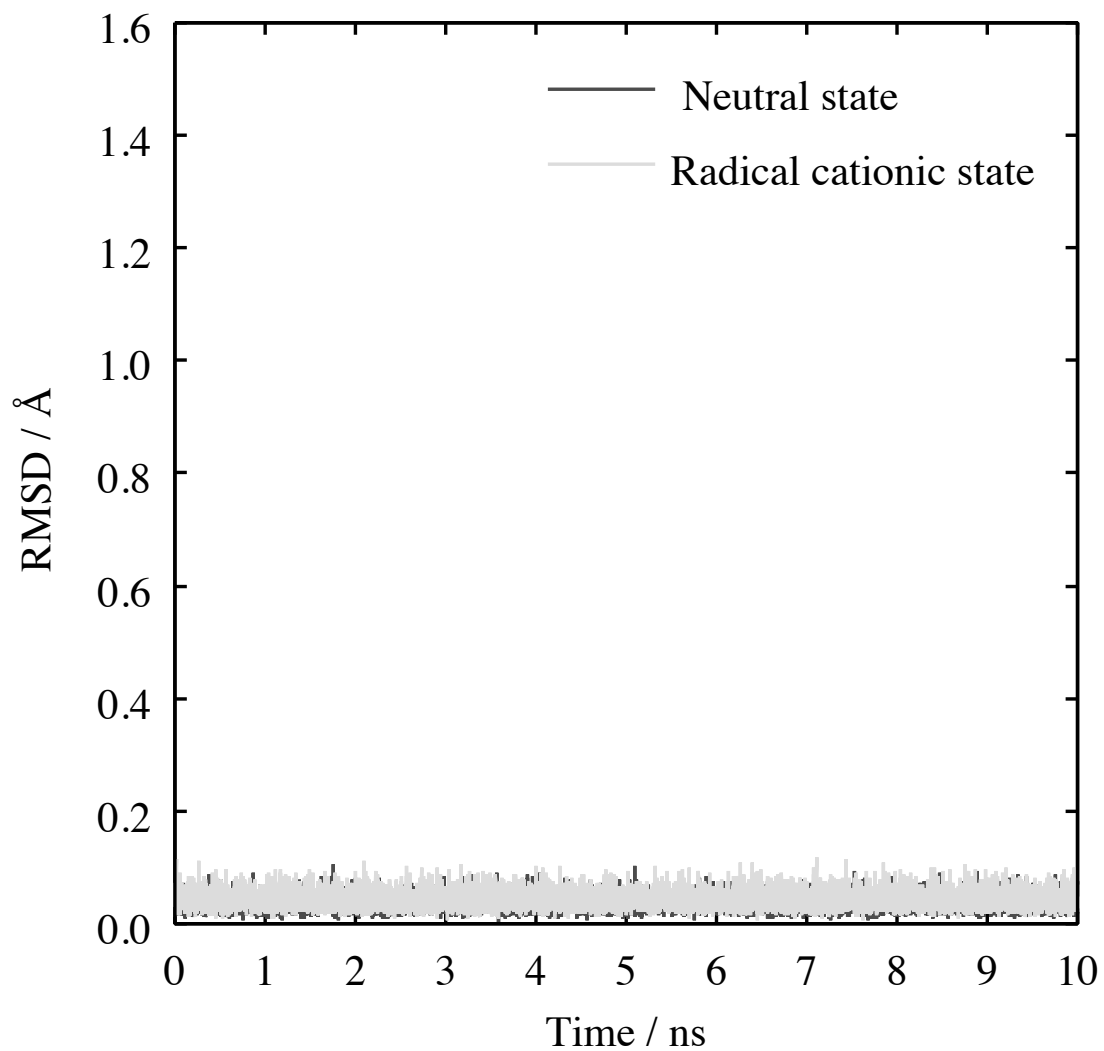


Figure 3.3: The RMSD of acetone in the neutral and radical cationic states as a function of MD time steps.

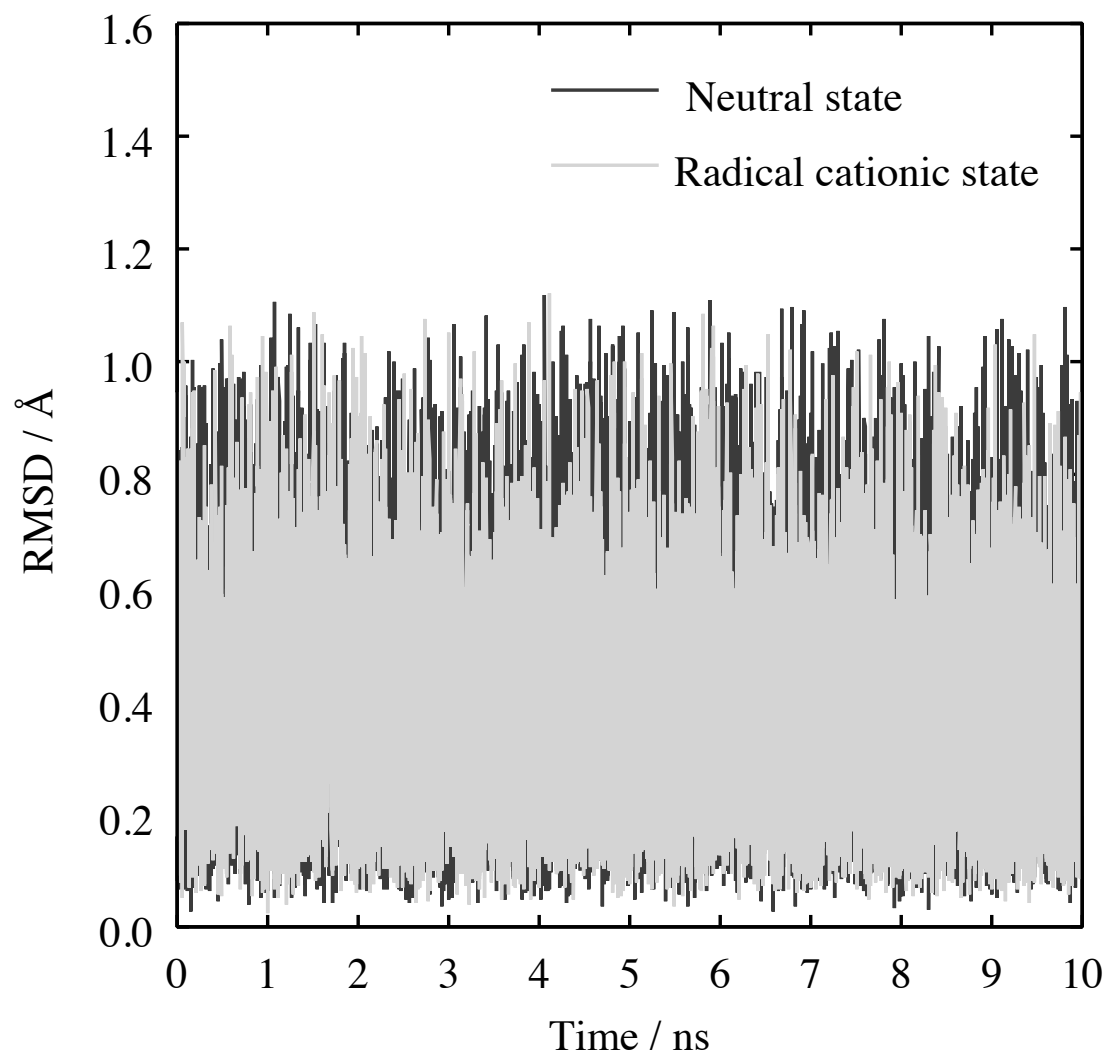


Figure 3.4: The RMSD of 3-pentanone in the neutral and radical cationic states as a function of MD time steps.

the acetone and 3-pentanone in the neutral and radical cationic states is confirmed sufficiently equilibrated in a short time. In equilibrium state, the average of RMSD of acetone in the neutral and radical cationic states is the 0.036 Å and 0.043 Å. The average of RMSD of the 3-pentanone in both of states is the 0.395 Å and 0.467 Å. The RMSD of 3-pentanone in both of states is larger than that of acetone due to the fluctuation of the dihedral of X-C_{sp3}-C_{sp2}-O in structure of 3-pentanone. While, the instantaneous values of the RMSD of acetone and 3-pentanone in the neutral and radical cationic states are in about 1.0 Å compared with the reference structure (Optimized structure). These results indicate that the acetone and 3-pentanone in both of states exists as adamant molecule in solution.

Solution structure of the acetone and 3-pentanone in the neutral and radical cationic states is shown in Table 3.3. In the Table 3.3, the average value of intramolecular bond length, the O=C_{sp2} and C_{sp2}-C_{sp3} for acetone, the C_{sp3}-C_{sp3} for 3-pentanone, added to those bond length of acetone, and the average value of intramolecular angle, the O=C_{sp2}-C_{sp3} for acetone, C_{sp3}-C_{sp3}-C_{sp2} for 3-pentanone, added to that angle of acetone, are shown. Then C_{sp2}-C_{sp3}, C_{sp3}-C_{sp3}, O=C_{sp2}-C_{sp3}, and C_{sp3}-C_{sp3}-C_{sp2} use the average value considered for intramolecular symmetry. The changes of intramolecular bond lengths, O=C_{sp2} and C_{sp2}-C_{sp2}, and angle, O=C_{sp2}-C_{sp3}, in solution from that in gas phase are +0.002 Å, -0.004 Å, and -0.4 deg. for acetone in neutral state. The changes of intramolecular bond lengths, O=C_{sp2}, C_{sp2}-C_{sp2}, C_{sp3}-C_{sp3}, and angle, O=C_{sp2}-C_{sp3}, C_{sp3}-C_{sp3}-C_{sp2} in solution from that in gas phase for 3-pentanone are +0.004 Å, +0.012 Å, +0.006 Å, and -0.4 deg., +0.6 deg.. The standard deviations of intramolecular bond

Table 3.3: The average value and standard deviation of intramolecular bond length and angle for the acetone and 3-pentanone in the neutral and radical cationic states (showed by using valence of molecule, N and $N + 1$) in solution. These intramolecular conformation of optimized structure are shown to compare in liquid phase with in gas phase. Units of bond length and angle are Å and deg..

	$O = C^{sp2}$		$C^{sp2} - C^{sp3}$		$C^{sp3} - C^{sp3}$		$O = C^{sp2} - C^{sp3}$		$C^{sp3} - C^{sp3} - C^{sp2}$	
	N	$N+1$	N	$N+1$	N	$N+1$	N	$N+1$	N	$N+1$
	<u>Acetone</u>									
Optimized structure ^a	1.219	1.214	1.518	1.524	121.6	119.0
MD simulation										
Average value	1.221	1.215	1.514	1.523	121.2	119.0
Standard deviation	0.019	0.020	0.045	0.049	4.1	5.6
	<u>3-pentanone</u>									
Optimized structure ^a	1.219	1.192	1.525	1.573	1.528	1.518	121.8	122.0	114.2	114.8
MD simulation										
Average value	1.223	1.193	1.537	1.589	1.534	1.527	121.4	121.3	114.8	115.7
Standard deviation	0.019	0.019	0.045	0.057	0.044	0.044	3.9	5.2	3.9	4.2

^a Conformation obtained by the optimization in gas phase by the DFT calculations presented in CHAPTER 2.

length and angle of the acetone and 3-pentanone are 0.045 Å and 4.1 deg. at a maximum, showing that the average value of the intramolecular bond length and angle of both molecules are obtained from a good convergence with the analysis of the standard errors, 0.045×10^{-2} Å, 4.1×10^{-2} deg..

On the other hand, the difference of conformation in the neutral and radical cationic states of the acetone and 3-pentanone in solution is shown in Table 3.3. The bond lengths, $O=C_{sp2}$ and $C_{sp2}-C_{sp3}$, and the angle, $O=C_{sp2}-C_{sp3}$, are the -0.006 Å and +0.009 Å, -2.2 deg. for acetone. The bond lengths, $O=C_{sp2}$, $C_{sp2}-C_{sp3}$, $C_{sp3}-C_{sp3}$, and the angles, $O=C_{sp2}-C_{sp3}$, $C_{sp3}-C_{sp3}-C_{sp2}$, are the -0.030 Å, +0.052 Å, -0.007 Å, and the -0.1 deg., +0.9 deg. for 3-pentanone. The difference of standard deviations of the bond length and angle of both of molecules are 0.073 Å and 6.9 deg. at a maximum, showing a good convergence to the difference value of the bond length and angle in the neutral and radical cationic states. These results shows that $O=C_{sp2}$ and $C_{sp2}-C_{sp3}$ in the conformation of the acetone and 3-pentanone in the radical cationic state is diminished and increased from that in the neutral state. The detailed analysis of these results on the conformational change in the neutral and radical cationic states of both of molecules, for instance, drawing the radial distribution function between the O, C_{sp2} , C_{sp3} in these molecules, and the oxygen and hydrogen atoms in water molecule, should be done with the discussion of hydration properties of both of molecules in the neutral and radical cationic states; this would be a future work.

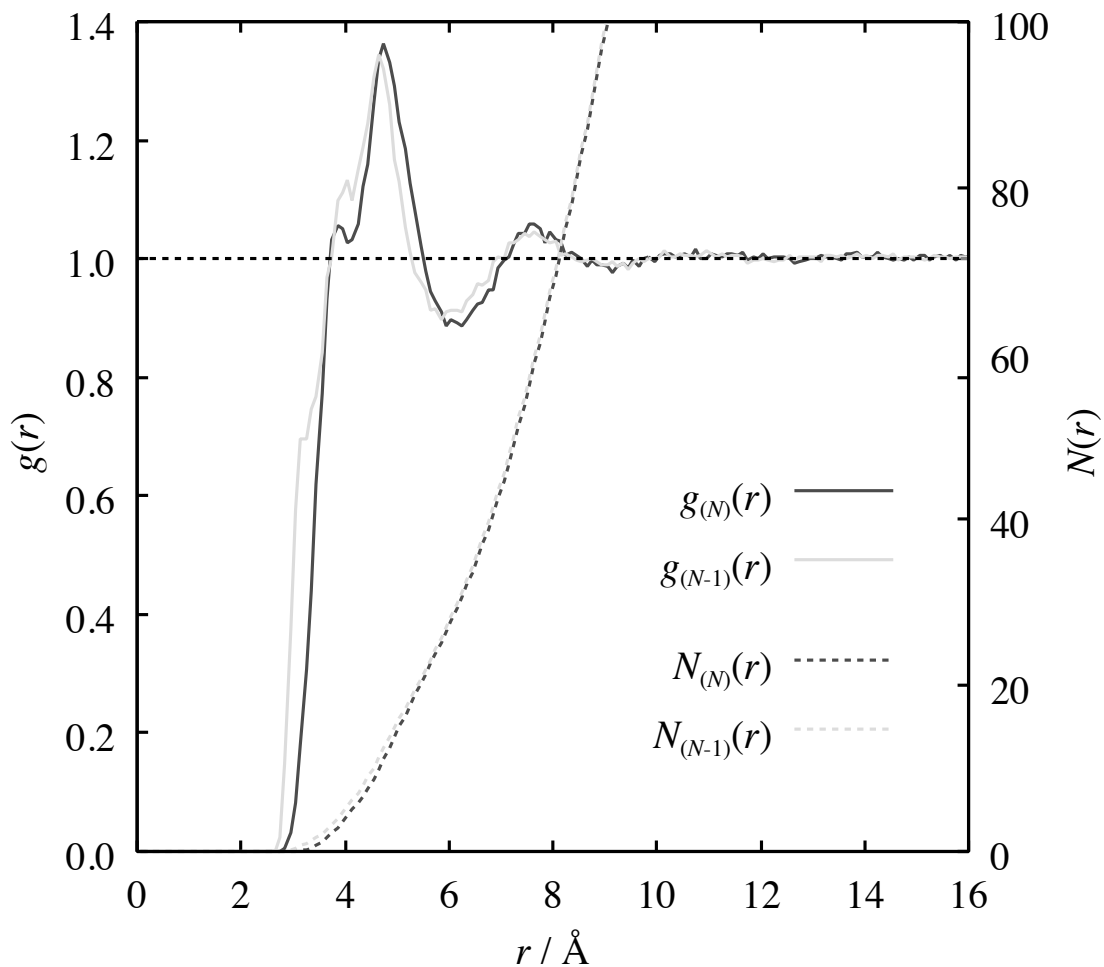


Figure 3.5: RDF between the COM of acetone and the oxygen atom of the water molecules is shown in the neutral and radical cationic states, the $g_{(N)}(r)$ and $g_{(N-1)}(r)$. The number of oxygen atoms of the water molecule are shown as a function of distance from the COM of acetone in the neutral and radical cationic states, the $N_{(N)}(r)$ and $N_{(N-1)}(r)$

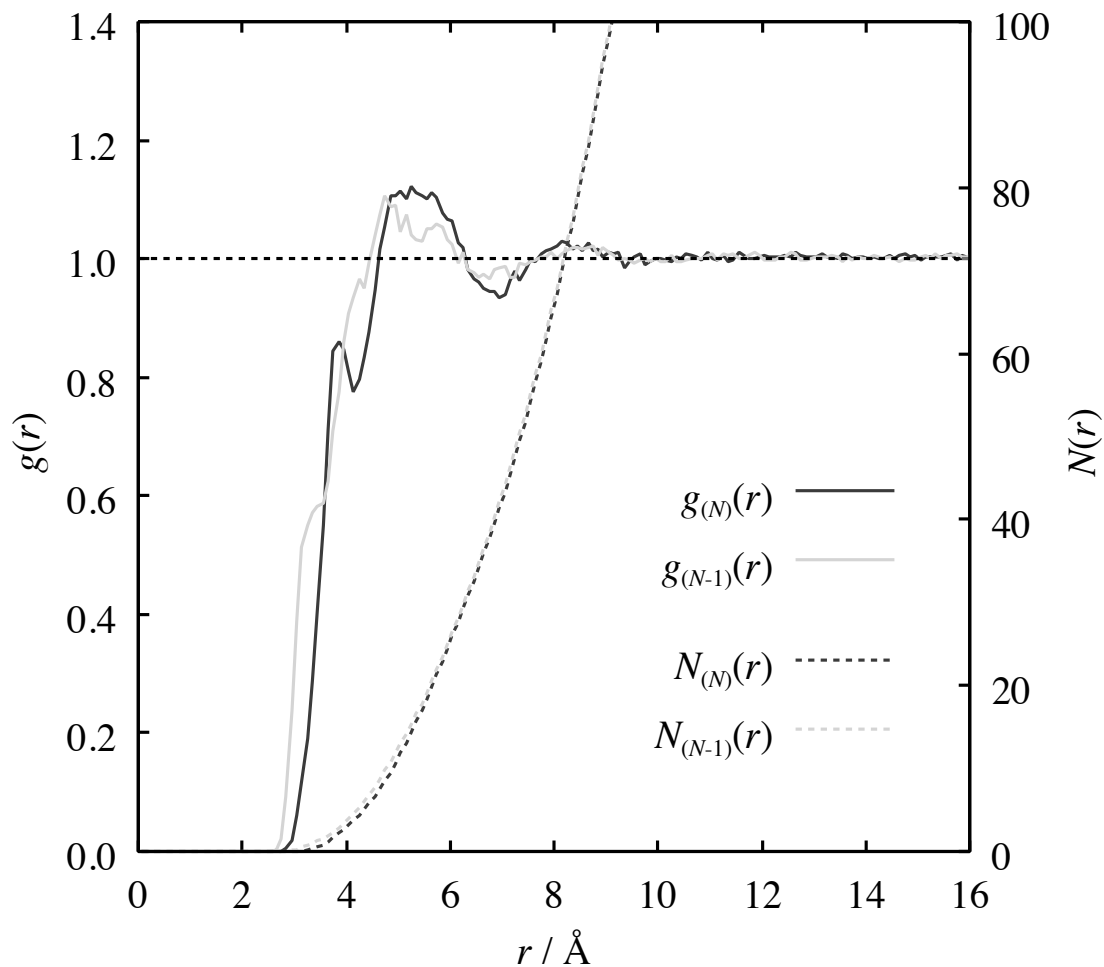


Figure 3.6: RDF between the COM of 3-pentanone and the oxygen atom of the water molecules is shown in the neutral and radical cationic states, the $g_{(N)}(r)$ and $g_{(N-1)}(r)$. The number of oxygen atoms of the water molecule are shown as a function of distance from the COM of 3-pentanone in the neutral and radical cationic states, the $N_{(N)}(r)$ and $N_{(N-1)}(r)$

3.4.2 Solvent structure

Radial distribution function (RDF) between the center of mass (COM) of the solute molecules and the oxygen of the water molecules is investigated for analysis of solvent structure around the solute molecules, acetone and 3-pentanone, in the neutral and radical cationic states, as shown in the Figure 3.5 and Figure 3.6. Comparing the RDF of the acetone and 3-pentanone systems, the first peak of 3-pentanone system is lower than that of acetone because of the difference of excluded volume in the acetone and 3-pentanone. The Figure 3.5 and Figure 3.6 shows that the oxygen atoms of the water molecules are located more close to around the solute molecule in neutral state than that in radical cationic state both of acetone and 3-pentanone. This is because the attractive interactions between the positively charged solute molecule and surrounding water molecules in the solution of molecule in the radical cationic state become more strong than that in the neutral state.

3.4.3 Excess chemical potential

The different 400 configurations are evenly taken from 0 ns to 10 ns to calculate the average of the excess chemical potential of the acetone and 3-pentanone in the neutral and radical cationic states. The excess chemical potentials of acetone and 3-pentanone in the neutral and radical cationic states are estimated by the energy distribution functions ρ^e and ρ_0^e in the solution and pure solvent systems, which are shown in the Figure 3.7 and Figure 3.8. The convergences of the average of excess chemical potential of acetone and 3-pentanone are accessed by plotting those as a function of the number of configurations in the neutral and

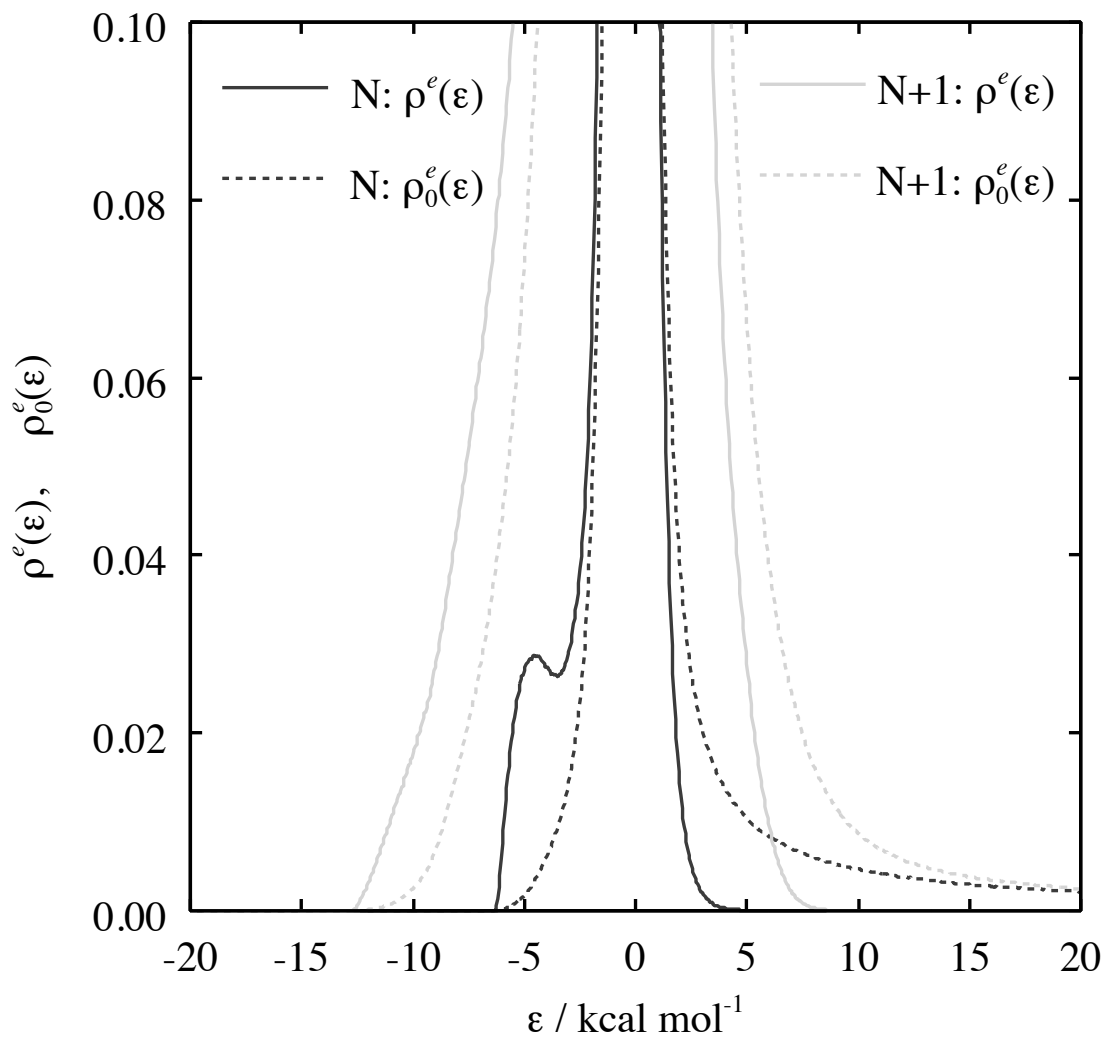


Figure 3.7: The energy distribution function $\rho^e(\varepsilon)$ and $\rho_0^e(\varepsilon)$, which are averaged on the 400 configurations, for acetone in the neutral (N) and radical cationic ($N + 1$) states.

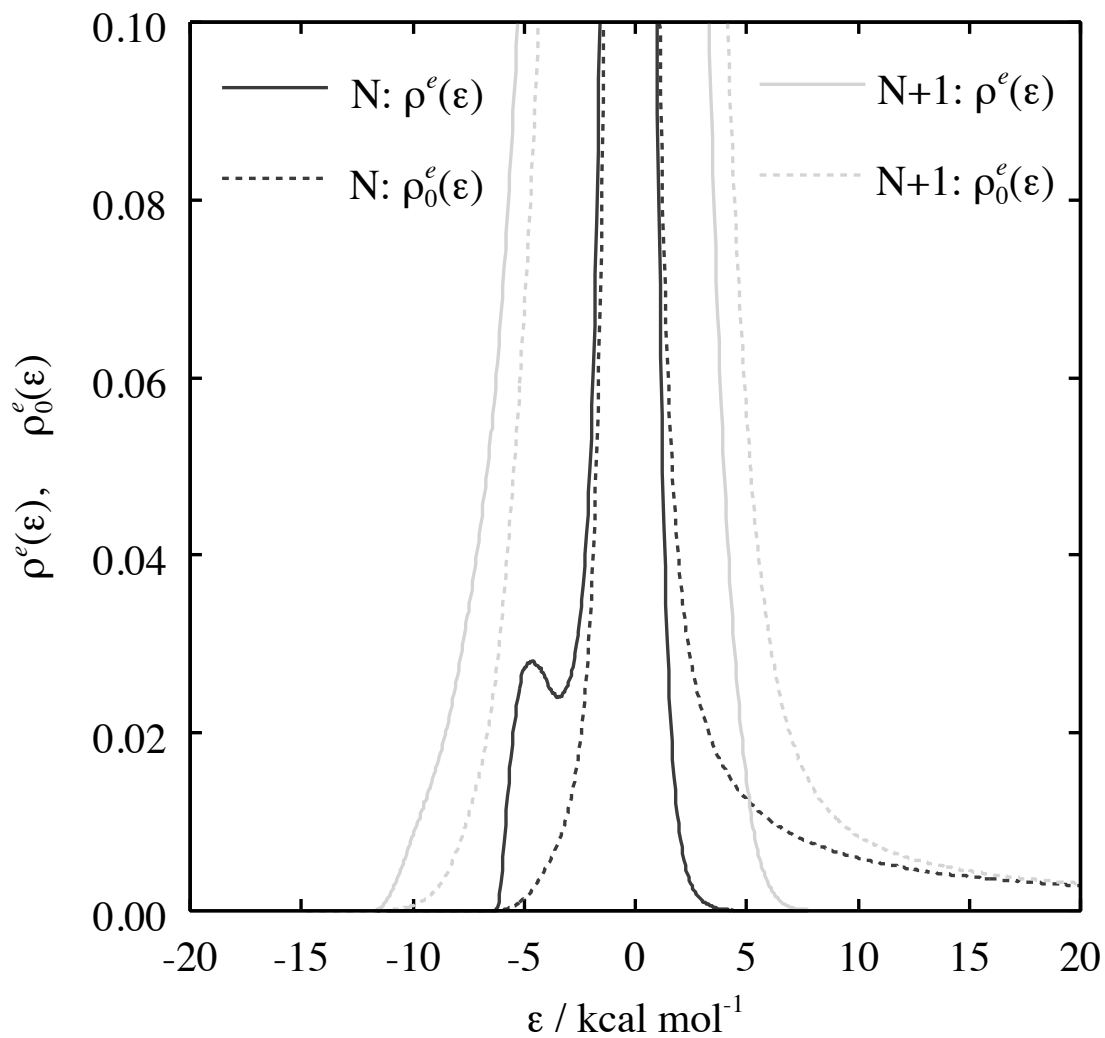


Figure 3.8: The energy distribution function $\rho^\epsilon(\epsilon)$ and $\rho_0^\epsilon(\epsilon)$, which are averaged on the 400 configurations, for 3-pentanone in the neutral (N) and radical cationic ($N + 1$) states.

radical cationic states (see Figure 3.9 and Figure 3.10). The average values of excess chemical potential of both molecules are shown to be sufficiently converged with 400 snapshots in the neutral and radical cationic states. The results of excess chemical potential of these molecules are listed in Table 3.4. The average

Table 3.4: Excess chemical potentials, $\Delta\mu^{ex}$, of acetone and 3-pentanone in the neutral and radical cationic states. The units are in kcal/mol. The values in parentheses show the standard deviation.

Molecule	State	Calculated $\Delta\mu^{ex}$	Experimental data ^a
Acetone	Neutral	-2.30 (0.16)	-3.80
	Radical cation	-34.79 (2.62)	...
3-pentanone	Neutral	-0.43 (0.16)	-3.41
	Radical cation	-27.89 (2.95)	...

^a Experimental data of the solvation free energies for acetone and 3-pentanone in water at 25 °C from Ref. [***]

values of the excess chemical potential of the acetone and 3-pentanone in the neutral state are the -2.30 kcal/mol and -0.43 kcal/mol, respectively. The values of the standard deviation of these molecules are 0.16 kcal/mol and 0.16 kcal/mol, showing a good convergence of the calculations of excess chemical potential of these molecules. The present of the average of $\Delta\mu_{(N)}$ of acetone is reasonably agreement with the experimental data, -3.80 kcal/mol [71]. The excess chemical potential of 3-pentanone in the neutral state is larger than that of acetone, showing larger hydrophobicity of the 3-pentanone. This should be due to the addition of the hydrocarbons at the end of acetone molecule. The similar hydration char-

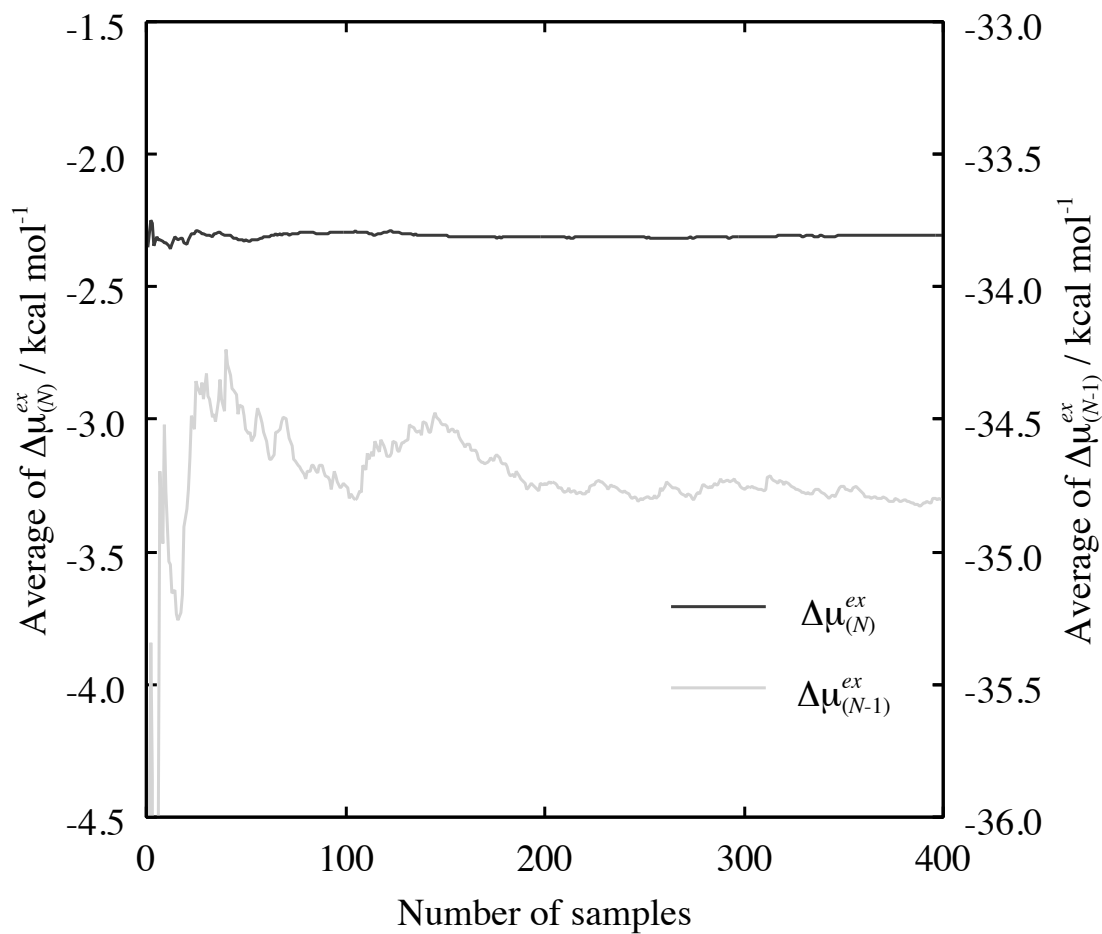


Figure 3.9: The average value of the excess chemical potential for acetone in the neutral and radical cationic states, the $\Delta\mu_{(N)}^{ex}$ and $\Delta\mu_{(N-1)}^{ex}$, as a function of the number of configurations.

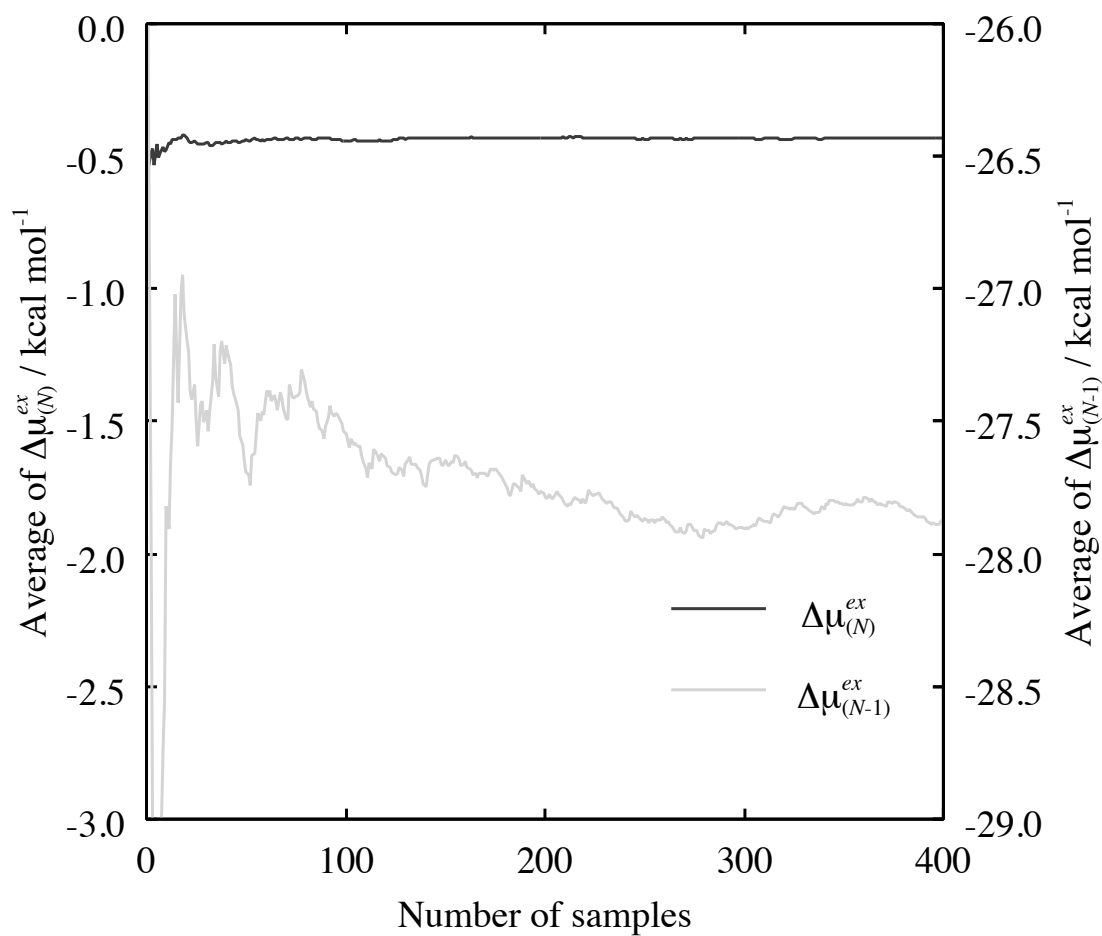


Figure 3.10: The average value of the excess chemical potential for 3-pentanone in the neutral and radical cationic states, the $\Delta\mu_{(N)}^{ex}$ and $\Delta\mu_{(N-1)}^{ex}$, as a function of the number of configurations.

acter can be shown in the experimental data (see Table 3.4). The difference of excess chemical potential of 3-pentanone between computation and experiment is 2.98 kcal/mol, showing that the computation of excess chemical potential of 3-pentanone is larger than that of experimental data. This could be due to the constraints of torsion angle in the 3-pentanone; because of the constraints of the torsion angle, the molecular conformations, which have better affinity with conformations of surrounding water molecules, could not be sampled in the MD simulation, resulting in the larger excess chemical potential of the 3-pentanone. However, if the revolution of methyl group is free, the sampling efficiency from MD simulation is considered to be down. The constraints of the torsion angle is considered to be not really matter due to subtract of the excess chemical potential in the neutral and the radical cationic states when the ionized effect of excess chemical potential of these molecules. There could be other possibility that the hydrophobicity of the added methyl group to acetone is overestimated due to the improper L-J parameters, which is transferred from AMBER force field 03 (parm99). The improvement of the simulation condition and the force field parameters should be done for more accurate estimation; this would be a future work.

The average values of the excess chemical potential of the acetone and 3-pentanone in the radical cationic state are the -34.79 kcal/mol and -27.89 kcal/mol, respectively. The values of the standard deviation of these molecules are 2.62 kcal/mol and 2.95 kcal/mol, respectively. Comparing the excess chemical potential of acetone and that of 3-pentanone in the radical cationic state, the excess chemical potential of 3-pentanone is larger than that of acetone. The standard

deviation of excess chemical potential of 3-pentanone is smaller than that of acetone. These values show the similar results with the comparison of the excess chemical potential of the acetone and 3-pentanone in the neutral state. The resultant excess chemical potential of the acetone and 3-pentanone in the cationic state are shown to be much lower on average, about 30 kcal/mol, than those in the neutral state. From the results, both of acetone and 3-pentanone in the radical cationic state are stable in solution whether the standard deviation of excess chemical potential of both molecules in the radical cationic state is larger than that in the neutral state. Thus, the ionization effect on the computation of excess chemical potential is significant in both of molecules.

3.5 Concluding Remarks

This chapter studies the structure and hydration properties of the acetone and 3-pentanone in the neutral and radical cationic states by using the molecular dynamics (MD) simulation in solution and the free energy calculation, including the meaning of test of the force field parameters developed in chapter 2. The excess chemical potential of each molecule in the neutral and radical cationic states are estimated by energy representation (ER) method. The computation of excess chemical potential of acetone in neutral state is close to the experimental data, while that of the 3-pentanone is larger than the experimental data. This difference of computation of 3-pentanone might be caused by the constraints of the torsion angle of intramolecule and the improper L-J potential parameter of methyl group assigned by AMBER force field 03 (parm99). However, the estimated excess chemical potential of 3-pentanone is larger than that of acetone in both

of states, showing similar tendency with the experimental data. The evaluated excess chemical potentials of the acetone and 3-pentanone in the cationic state are shown to be much lower (30 kcal/mol on average) than those in the neutral state, showing that the ionization effect of acetone and 3-pentanone on the estimation of excess chemical potentials should be significant in both of molecules.

CHAPTER 4

A Hybrid Type Approach With MD and DFT Calculations: Evaluation of Redox Potential of Organic Compounds

4.1 Introduction

The purposes of this chapter is to present a simple procedure to calculate the redox potentials of the small organic molecules, acetone and 3-pentanone, by using a hybrid type calculation with the molecular dynamics (MD) simulation and the density functional theory (DFT) calculation and to estimate the redox potential of the simple small molecules, acetone and 3-pentanone, by our conventional approach. In this hybrid method, the thermodynamics cycle model of the redox reaction is used to estimate the value of redox potential. The ionization free

energy of the molecules in gas phase is calculated by the DFT method for the sampling configurations taken from the MD simulation. The excess chemical potential according to the thermodynamic cycle model is calculated by the energy representation (ER) method, as shown in chapter 3. The redox potential of the molecules is discussed in relation to the difference of the redox potentials between the molecules with the experimental data.

4.2 Computational Procedure

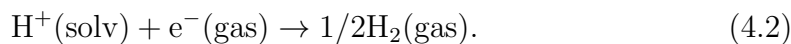
The computational procedure to evaluate the redox potential of organic molecule is based upon the popular methods [22, 23, 24, 26, 36] with calculation of standard Gibbs free energy of redox reaction using the thermodynamics cycle model.

4.2.1 Redox potential

The standard redox potential, E° , can be expressed by the Nernst equation with the free energy change in oxidation reaction, ΔG , as following equation;

$$E^\circ = \Delta G/nF + E^{\text{NHE}}, \quad (4.1)$$

where F is the Faraday constant (96,485.3365 C/mol) and n is the number of electrons related to the oxidation reaction, respectively. In the equation (4.1), the standard state is commonly associated with the reference normal hydrogen electrode (NHE),



The NHE potential has known to be -4.44 V in theoretical study and has used to estimate the standard redox potential of several molecules [58].

4.2.2 Gibbs free energy of redox reaction

In this study, the free energy of solute molecule in solution, G , is defined using the chemical potential of solute molecule in solution is expressed by the equation (3.12) and (3.13) introduced in chapter 3 and the average of total energy of solute molecule in solution, E . Then the G is given as following equation;

$$G = k_B T \log(\rho \Lambda_{N+1}^3) + \mu^{ex} + E \quad (4.3)$$

The free energy change in oxidation reaction, ΔG , is difference of the free energy between the reduced and oxidized states in solution. The $k_B T \log(\rho \Lambda_{N+1}^3)$ of the first term in equation (4.3) is neglected in the case of same density of solute molecule in the reduced and oxidized states. Therefore, the ΔG is given by the following equation according to the thermodynamic cycle model as shown in Figure 4.1,

$$\Delta G = \Delta E + \{ \Delta \mu_{(N-1)}^{ex} - \Delta \mu_{(N)}^{ex} \} \quad (4.4)$$

$$\Delta E = E_{(N-1)} - E_{(N)}, \quad (4.5)$$

where ΔE means the ionization free energy in gas phase, and $E_{(N)}$ and $E_{(N-1)}$ are the total energy of the reduced and the oxidized molecules, respectively. N denotes the valence of the molecule. $\Delta \mu_{(N)}^{ex}$ and $\Delta \mu_{(N-1)}^{ex}$ are the excess chemical potential of the reduced and the oxidized molecules, respectively. In this study, the reduced and oxidized states denote the neutral and radical cationic states.

In order to estimate the ionization free energy, the average of total energy in gas phase by sampled configurations obtained from the MD simulation of the molecules in water solvation are calculated. The average of the ionization free

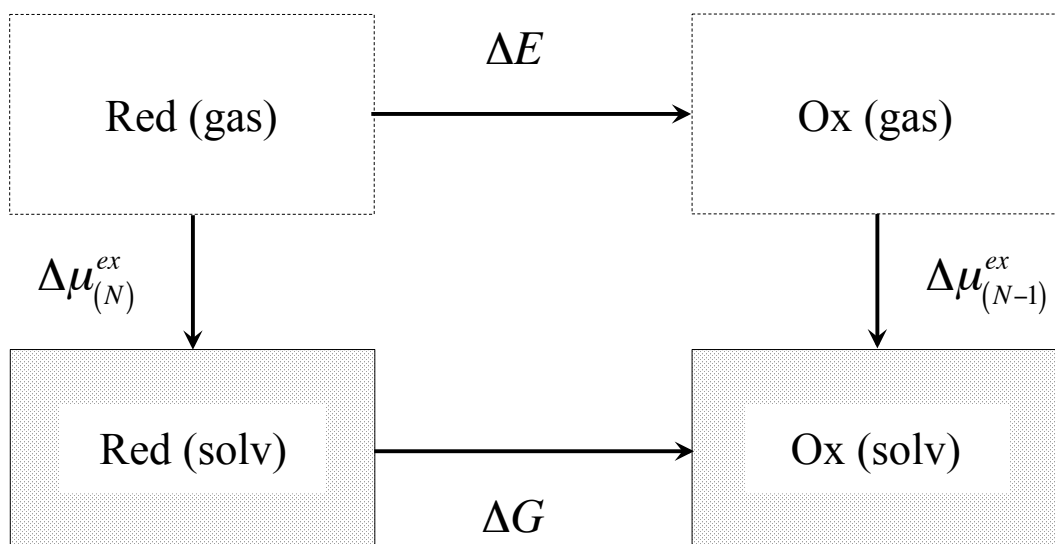


Figure 4.1: Thermodynamic cycle model used in calculation of free energy change in oxidation reaction. "Red (gas)" and "Ox (gas)" indicates the reduced and the oxidized molecules in gas phase, and "Red (solv)" and "Ox (solv)" indicates the reduced and the oxidized molecules in salvation. The free energy change is evaluated without computing excess chemical potential of an excess electron.

energy is calculated by the DFT calculation with the B3LYP method [59, 60] and 6-31+G(d,p) basis set [61, 62]. The excess chemical potential of molecules is estimated by using the energy representation (ER) method with MD simulation, which is evaluated and discussed in chapter 3.

4.3 Results and Discussion

The ionization free energy of process shown in Figure 4.1 is discussed in the following subsection, and the redox potential of the molecules are also discussed in

relation to the difference of the redox potential for the two molecules as mentioned in the introduction.

4.3.1 Ionization free energy

The different 400 configurations are evenly taken from each equilibrium system obtained by the MD simulations to calculate the average of the ionization free energy. Figure 4.2 and Figure 4.2 shows the average values of total energy of each molecule as a function of number of configurations, showing that the total energy $E_{(N)}$ and $E_{(N-1)}$ for the acetone and 3-pentanone in the neutral and radical cationic states are sufficiently converged in a kcal/mol. The values of the total energy $E_{(N)}$ and $E_{(N-1)}$ are -121,217.2 kcal/mol and -120,996.4 kcal/mol, respectively. On the other hand, the values of the $E_{(N)}$ and $E_{(N-1)}$ for 3-pentanone are -170,559.2 kcal/mol and -170,348.0 kcal/mol, respectively. The values of standard deviation of the $E_{(N)}$ and $E_{(N-1)}$ are 1.0 kcal/mol and 0.9 kcal/mol for acetone, and 1.4 kcal/mol and 1.3 kcal/mol for 3-pentanone, respectively. The standard deviation of the total energies is arising out of the configurations sampled from the MD simulation. The average of the ionization free energies, ΔE , of acetone and 3-pentanone are presented in Table 4.1. The value of the average of ΔE of each molecule becomes 220.8 kcal/mol and 211.2 kcal/mol with the standard deviations, 1.4 kcal/mol and 1.9 kcal/mol, respectively. The present of the average of ΔE of the acetone and 3-pentanone are not so different from the previous results of the ionization potentials obtained by the optimization in gas phase by the DFT calculations in chapter 2, which are the 220.9 kcal/mol and 212.0 kcal/mol, and from the first adiabatic ionization energies in gas phase [70], which are the 223 kcal/mol and 215 kcal/mol.

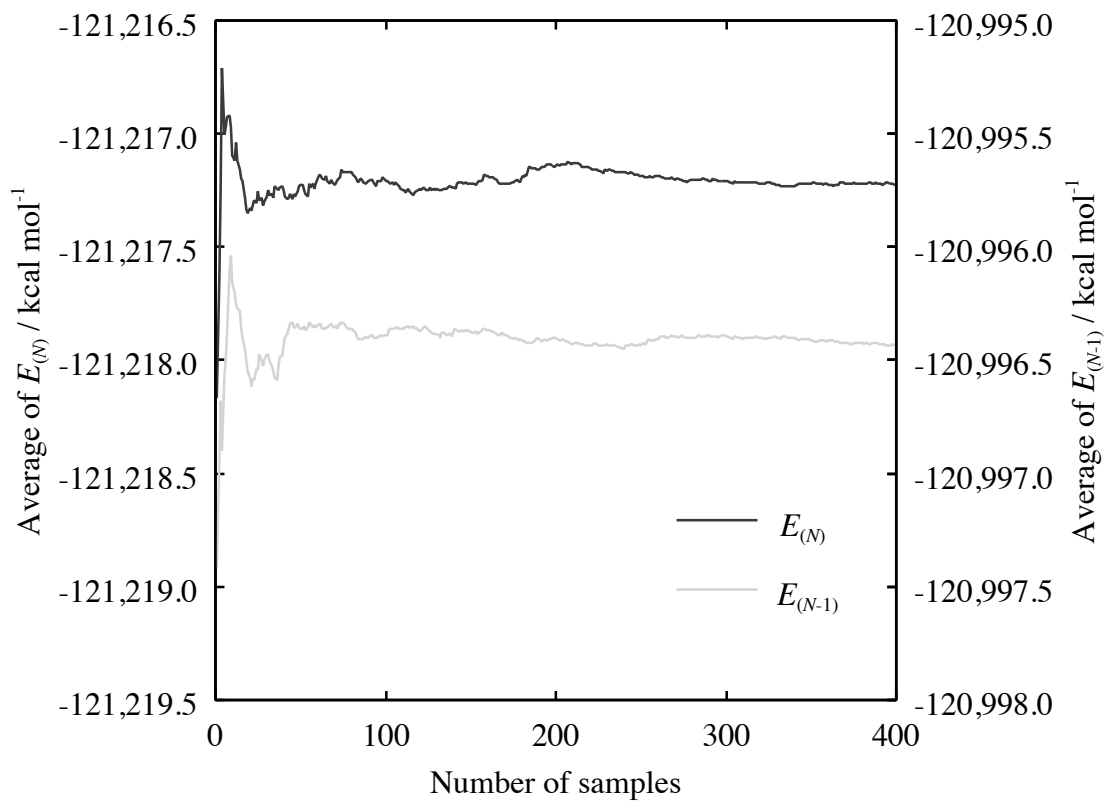


Figure 4.2: The average of the total energies for acetone in the neutral and radical cationic states, $E_{(N)}$ and $E_{(N-1)}$, as a function of the number of configurations.

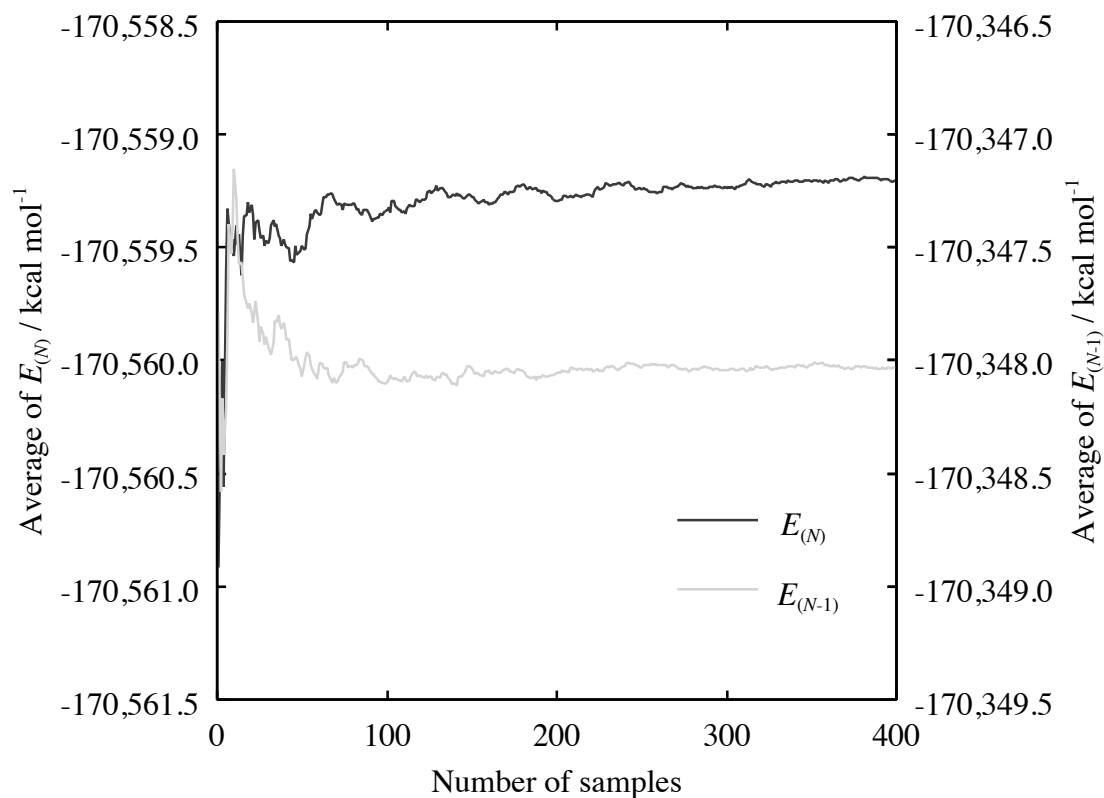


Figure 4.3: The average of the total energies for 3-pentanone in the neutral and radical cationic states, $E_{(N)}$ and $E_{(N-1)}$, as a function of the number of configurations.

4.3.2 Standard redox potential

From the results of the ionization free energy and the excess chemical potential of each state, the standard Gibbs free energy, ΔG , and the standard redox potential, E° , of each molecule are estimated according to equation (4.4) and (4.1). The values of ΔG for acetone and 3-pentanone become 188.3 kcal/mol and 183.7 kcal/mol shown in Table 4.1, respectively. The values of standard deviation of ΔG for each molecule are 3.0 kcal/mol and 3.5 kcal/mol, respectively. The standard redox potential E° of each molecule becomes 3.7 V for acetone and 3.5 V for 3-pentanone with the standard deviations, 0.1 V and 0.2 V, respectively. The E° of each molecule is different from the experimental values, which is 0.16 V and 0.14 V for acetone and 3-pentanone, respectively [72]. According to our conventional approach, the discrepancies of the values of standard redox potential of the each molecule between the computation and experiment might arise from the effect of the excess chemical potential on the oxidized state of the molecule

Table 4.1: The average of ionization free energies, ΔE , the average of excess chemical potentials of molecule in the neutral and the radical cationic states, $\Delta\mu_{(N)}^{ex}$ and $\Delta\mu_{(N-1)}^{ex}$, and the standard Gibbs free energies ΔG of redox reaction, for the acetone and 3-pentanone. The units are in kcal/mol. The values in parentheses show the standard deviation.

Molecule	ΔE	$\Delta\mu_{(N)}^{ex}$	$\Delta\mu_{(N-1)}^{ex}$	ΔG
Acetone	220.8 (1.4)	-2.3 (0.2)	-34.8 (2.6)	188.3 (3.0)
3-pentanone	211.2 (1.9)	-0.4 (0.2)	-27.9 (3.0)	183.7 (3.5)

in solvation in computational procedure. The detailed discussions of the effect of the number of water molecules in the simulation cell and the counter-ion on the calculation of the excess chemical potential of the radical cationic molecule are given in appendix B. To agree the computations of the standard redox potential of molecules with the experiments, the effect of the counter-ion in solvation should be sufficiently investigated in the future.

4.3.3 Relative value of redox potentials

In order to counter the effect of the number of water molecules and the counter-ion on the calculation of the excess chemical potential of the radical cationic state, the difference of the redox potentials, ΔE° , of each molecule is focused on the computations of the standard redox potential of the molecules, acetone and 3-pentanone. The ΔE° is calculated by the following equation,

$$\Delta E^\circ = E_{\text{acetone}}^\circ - E_{\text{3-pentanone}}^\circ \quad (4.6)$$

$$= \Delta(\Delta G) / F. \quad (4.7)$$

where $\Delta(\Delta G)$ is the difference of standard Gibbs free energies between acetone and 3-pentanone. From the result of the ΔG of each molecule, the values of $\Delta(\Delta G)$ and ΔE° become the 4.6 kcal/mol and 0.2 V by the equation (4.6) with the standard deviations, the 4.6 kcal/mol and 0.2 V, respectively. The results of $\Delta(\Delta G)$ and ΔE° are in agreement with the experimental data, which is 0.4 kcal/mol and 0.02 V [72], within the standard deviations, respectively. It is considered that the effect of the counter-ion in the system of the radical cationic state is countered by calculating the difference of the standard Gibbs free energy between each molecule. These results suggest that the redox reaction with electron

transfer between molecules might be discussed by using the present computational procedure from the viewpoint of the difference of the redox potential.

4.4 Concluding Remarks

In this chapter, a simple procedure to evaluate the redox potential of molecules have been presented by using a hybrid type calculation with molecular dynamics (MD) and density functional theory (DFT) calculations. The redox potential of the molecules, acetone and 3-pentanone, is calculated by our conventional approach. The free energy change in redox reaction is estimated from the ionization free energy in gas phase and the excess chemical potential according to the thermodynamic cycle model. The average of the ionization free energy and the excess chemical potential have been calculated by the sampled configurations obtained from the MD simulation of the molecules in the neutral and radical cationic states.

The redox potential of the molecules calculated by the present procedure have been discussed in relation to the difference of the redox potentials. The difference of the redox potentials between acetone and 3-pentanone obtained by the results of these calculations is in agreement with the experimental data within the standard deviation. These results suggest that the redox reaction with electron transfer between molecules by using the present computational procedure might be discussed from the viewpoint of the difference of the redox potential.

CHAPTER 5

General Conclusion

This thesis has presented a simple calculation method to estimate the redox potential of molecules by using a thermodynamic cycle model with a hybrid type method with molecular dynamics (MD) and density functional theory (DFT) calculations, as shown in chapter 4. In this method, the redox potential of molecules are calculated by estimation of ionization free energy and excess chemical potentials of molecules in the neutral and radical cationic states in solution. In order to obtain the solute structures in solution, the all atom MD simulation of the molecules in neutral and radical cationic states using explicit water model have performed in chapter 3 with the force field parameters developed in chapter 2.

In this thesis, the redox potential of the simple small molecules, acetone and 3-pentanone, evaluated by the conventional approach. Firstly, the optimized structures and the force field parameters in the reduced and oxidized state, which are considered as the neutral and radical cationic states for the organic molecules, have been presented. The optimized structure and the force field parameter are estimated by the DFT-B3LYP/6-31+G(d,p) calculations, which are higher

level than that used at AMBER force field parameters (parm99). The optimized structure of acetone in the neutral state are comparative with the experimental measurement. The ionization potentials obtained by the estimation of the total energies of the optimized structures between the neutral and radical cationic states are good agreement with the experimental data. The determined partial charges of these molecules reproduce the dipole, which is in agreement with the experimental data.

Using developed these force field parameters, the MD simulation of these molecules have been performed for 10 ns in the neutral and radical cationic states. From the results of the MD simulations, the structure and hydration properties of the acetone and 3-pentanone in the neutral and radical cationic states are investigated to calculate the redox potential of these molecules. For the estimation of the excess chemical potential of the molecules, the energy representation (ER) method is used. The computation of excess chemical potential of acetone in neutral state is close to the experimental data, while that of the 3-pentanone is larger than the experimental data. This difference of computation of 3-pentanone might be caused by the constraints of the torsion angle of intramolecule and the improper L-J potential parameter of methyl group assigned by AMBER force field 03 (parm99). However, the estimated excess chemical potential of 3-pentanone is larger than that of acetone in both of states, showing similar tendency with the experimental data. The excess chemical potentials of these molecules in the cationic state are shown to be much lower (30 kcal/mol on average) than those in the neutral state, showing that the ionization effect of acetone and 3-pentanone on the estimation of excess chemical potentials should be significant in both of

molecules.

Taking the excess chemical potentials of acetone and 3-pentanone in the neutral and radical cationic states, and adding the estimation of ionization free energies of these molecules using the sampling configurations taken from the MD simulations in solution, the redox potential of acetone and 3-pentanone are estimated with the presented conventional approach. The values of the redox potential is 3.7 V for acetone and 3.5 V for 3-pentanone, showing the discrepancies of the experimental data, 0.16 V and 0.14 V, respectively. The values of standard deviation is 0.1 V for acetone and 0.2 V for 3-pentanone, respectively. The discrepancies of redox potential of these molecules between the computation and the experiment is might be occurred to the effect of the number of water molecules in the simulation cell and the counter-ion on the calculation of the excess chemical potential of the radical cationic molecule. The detailed discussions of the effect of those are given in appendix B. In order to counter these effects, the redox potential of the molecules calculated by the present procedure have been discussed in relation to the difference of the redox potentials. The difference of the redox potentials between acetone and 3-pentanone obtained by the results of these calculations is 0.2 V with the standard deviation, 0.2V, showing agreement with the experimental data within the standard deviation. From the result, the redox reaction with electron transfer between molecules by using the present computational procedure might be discussed from the viewpoint of the difference of the redox potential.

On the other hand, the presented computational method to estimate the redox potential is investigated whether it is possible to apply to the proteins. In ap-

pendix A, the redox potential of metalloprotein, azurin, has been estimated with the similar computational method in the case of organic molecules. However, the ionization free energy of the protein in solution according to the thermodynamic cycle model is calculated by the quantum mechanics/molecular mechanics (QM/MM) calculations. The evaluated redox potential of the protein have been also compared with the experimental data and discussed the redox potential of the protein with computation of the difference of redox potential between the protein and the organic molecules, acetone and 3-pentanone, evaluated in chapter 4.

While, the development of the computational method to remove the errors of the computation of redox potential of these molecules with the experimental value are interested. Appendix C has presented development of computational method to estimate the redox potential of the molecules using the spherical boundary MD simulation, as a incoming valuable introduction.

APPENDIX A

A Hybrid Type Approach With MD and QM/MM Calculations: Evaluation of Redox Potential of Metalloprotein

A.1 Introduction

This thesis has presented mainly a hybrid type approach with molecular dynamics (MD) and density functional theory (DFT) calculations for evaluation of redox potential of the organic molecules. The results of redox potential of the molecules estimated by the hybrid type method in chapter 4 have shown the possibility to discuss from the viewpoint of the difference of the redox potential. However, the presented computational method should be investigated whether it is apply to the proteins, indeed.

The purpose of this appendix is to calculate the redox potential of metalloprotein, azurin, by a hybrid type approach with MD and quantum mechanics/molecular mechanics (QM/MM) calculations. Basic computational procedure and method are similar with the hybrid type approach with MD and DFT calculations, however, ionization free energy in solution is estimated by the QM/MM calculations. From these results, the evaluated redox potentials of the protein are compared with the experimental data and between the protein and the organic molecules, acetone and 3-pentanone, evaluated in chapter 4.

A.2 Materials

The X-ray structure of azurin is obtained from the protein data bank (PDB), 4AZU in the reduced state [73, 74] and 1E5Y in the oxidized state [75, 76]. The structure of azurin, which is blue copper protein of 128 amino acids, consist of eight β -strands forming two β -sheets. The active site of azurin is coordinated by three ligands: N^δ of His 46, N^δ of His 117 and S^γ of Cys112, forming an equatorial plane around the copper. Moreover, two weaker ligands are present: S of Met121 and the carbonyl group of Gly45. Structure of azurin in reduced state are shown in Figure A.1.

A.3 Computational Procedure

Computational procedure is similar with chapter 4. However, the ionization free energy of the protein in water solvent are estimated by the QM/MM calculations. The computational method show the following subsection.



Figure A.1: The X-ray structure of Azurin in the reduced and oxidized states. This Figure is done RMS fit between the reduced and oxidized states.

A.4 Computational Details

A.4.1 Molecular dynamic simulation

The MD simulation of the blue copper protein, azurin, in the reduced and oxidized states in water solvent is performed with the AMBER 11 program packages. For the MD simulations of the protein in the reduced and oxidized states, the force field parameter of the stretching vibration, angle bending of active site are originally developed from the dependence of the total energy of the molecule on the bond and angle in the structure of protein by the DFT-B3LYP/6-31G(d,p) calculations. The partial charge of the active site of protein is determined by the Merz-Singh-Kollman method, which is RESP charge. Others force field parameters are adopted by the Amber force field (parm99).

For the MD simulation, Langevin thermostat and barostat are used to control system temperature ($T = 300$ K) and the pressure ($P = 1$ atm). The azurin are solvated by 15,065 water molecules in a cubic box with $80.3 \text{ \AA} \times 74.2 \text{ \AA} \times 80.3 \text{ \AA}$. The TIP3P (transferable intermolecular potential 3 point) model [65] is adopted for the solvent molecule (water molecule). Particle Mesh Ewald (PME) method [66] is used for the calculation of coulomb interaction. For the MD simulations of the reduced and oxidized azurin under the periodic boundary conditions, the operation for neutralization of the system is conducted by adding counter-ion, 3 Na^+ for reduced azurin and 2 Na^+ for oxidized azurin. Cut off length for the coulomb and vdW interactions are 12 \AA . A time step for the MD simulation is 2 fs. The bond length including the hydrogen atom are constrained by SHAKE method [56].

Energy minimization is performed by the steepest descent method with fixing the heavy atoms of solute molecule. The MD simulations are carried out in the constant NPT condition with constraints of solute molecule with 50 kcal/mol/Å² spring constant, and then system temperature is gradually increased in increments of 10 K from 0 K to 300 K for 300 ps. After that, the NPT -MD simulations are performed in which the constraints of solute are gradually reduced in increments of 1.0 kcal/mol/Å² to zero for 500 ps. Finally, the equilibrium NPT -MD simulations are carried out for 20 ns.

A.4.2 Hybrid QM/MM calculation

The ionization free energy is calculated by using the quantum mechanics/molecular mechanics (QM/MM) calculations. In this study, The QM region is defined by the active site of the protein. The MM region is defined by the non-active site of the protein and the solvent molecule. Then, the MM is the point charge. The total energy E of solute molecule is defined by the following equation;

$$E = \left\langle \Phi_{\text{QM/MM}} | \hat{H}_{\text{QM/QM}} | \Phi_{\text{QM/MM}} \right\rangle, \quad (\text{A.1})$$

where $\hat{H}_{\text{QM/QM}}$ is total hamiltonian for the QM region. $\Phi_{\text{QM/MM}}$ is calculated with the following equation;

$$\left\langle \Phi_{\text{QM/MM}} | \hat{H}_{\text{QM/MM}}^{\text{total}} | \Phi_{\text{QM/MM}} \right\rangle = E_{\text{QM/MM}}^{\text{total}}. \quad (\text{A.2})$$

Then, the total hamiltonian, $\hat{H}_{\text{QM/MM}}^{\text{total}}$ is expressed by the follow;

$$\hat{H}_{\text{QM/MM}}^{\text{total}} = \hat{H}_{\text{QM/QM}} + \hat{H}_{\text{QM/MM}} + H_{\text{MM/MM}}, \quad (\text{A.3})$$

where $\hat{H}_{\text{QM/MM}}$, $H_{\text{MM/MM}}$ are the hamiltonian of the interaction of wave function and MM point charges, the interaction energy between the point charges, re-

spectively. It is significant to consider the QM/MM boundary condition. In this study, link atoms method is adopted to the QM/MM boundary condition.

A.4.3 Energy distribution function

The *NPT*-MD simulation of the solution system is performed for 1 ns under the same conditions as the equilibrium MD simulation. The configuration of solute molecule is fixed in this simulation. The coordinates of the solution system are stored every 10 fs after the system energy is sufficiently equilibrated, therefore total 100,000 snapshots are prepared for the estimation of the energy distribution function, ρ^e . The *NPT*-MD simulation of the pure solvent system is performed for 1ns. The coordinates of the pure solvent system are stored every 1 ps, and 1,000 snapshots are prepared. After that, the sampled structure, which is the same configuration as the solution system, is randomly inserted 1,000 times into the pure solvent system of each snapshot: total 1,000,000 sampling data are prepared for the estimation of the energy distribution function, ρ_0^e and the correlation function χ_0 .

A.5 Results and Discussion

The root mean square deviation (RMSD) of the backbone atoms (C_α) of azurin in the reduced and oxidized states. The RMSD showed that both system of azurin is sufficiently equilibrated after 14 ns, both of states.

The averaged total energy of reduced and oxidized states, $E_{(N)}$ and $E_{(N+1)}$, are -2,614,628.4 kcal/mol and -2.614,538.6 kcal/mol, respectively. The standard

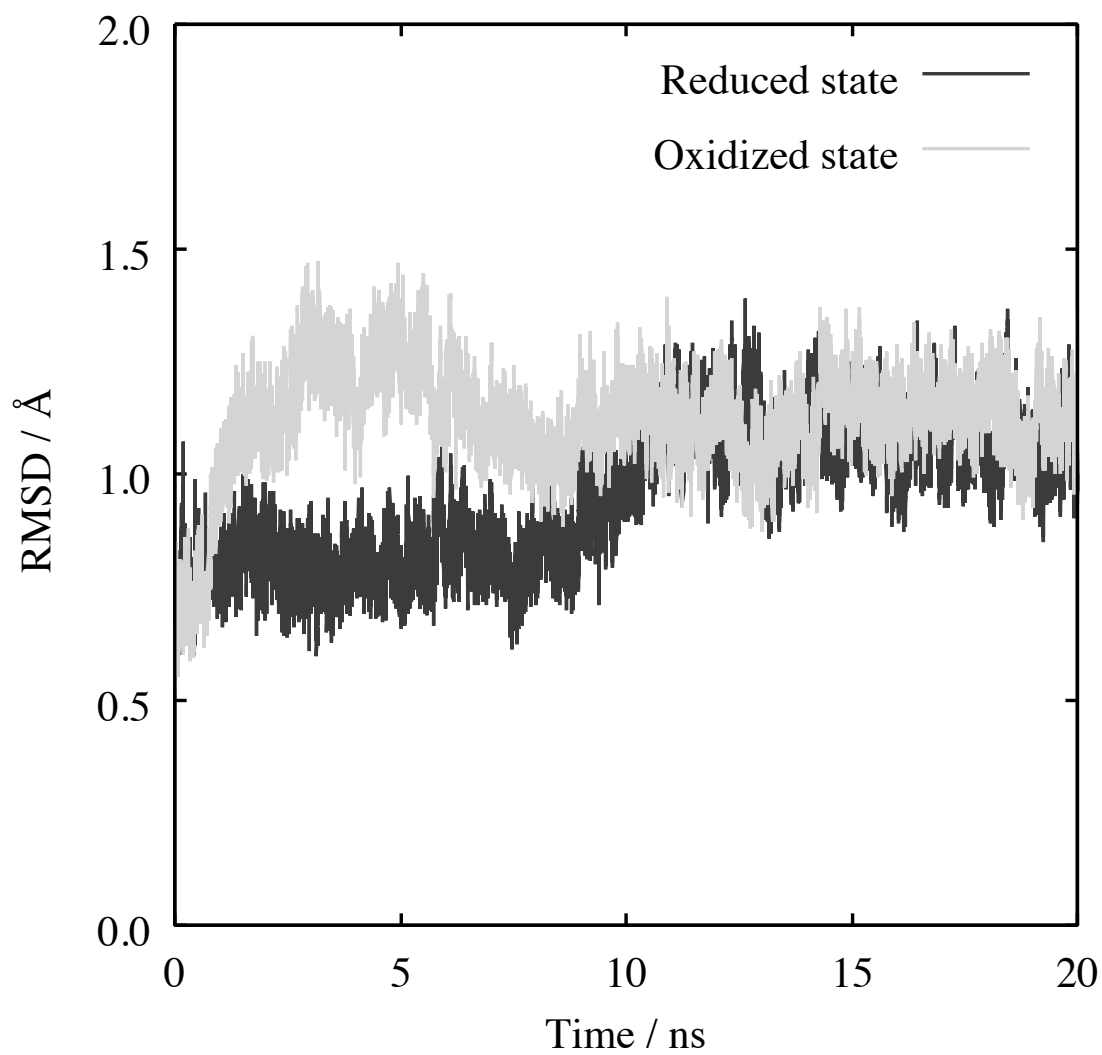


Figure A.2: The RMSD of azurin in the reduced and oxidized states as a function of MD time steps.

deviation of $E_{(N)}$ and $E_{(N+1)}$ are 5.2 kcal/mol and 5.9 kcal/mol, respectively. The averaged ionization free energy, ΔE , is 90.0 kcal/mol with standard deviation, 7.9 kcal/mol. On the other hand, the excess chemical potentials in the reduced and oxidized states are -985.2 kcal/mol and -884.3 kcal/mol, with the standard deviation, 16.6 kcal/mol and 14.7 kcal/mol respectively.

From these results, the free energy change in oxidation reaction, ΔG , and the redox potential, E° , is 190.9 kcal/mol and 3.8 V, respectively. The standard deviations of each value are 23.5 kcal/mol and 1.0V, respectively. The result of redox potential is much larger than the experimental data, 0.32 V.

The differences of ΔG and E° between the azurin and acetone is 2.6 kcal/mol and 0.14 V with the standard deviation, 23.7 kcal/mol and 1.0 V, respectively. The differences of those between the azurin and 3-pentanone is 7.2 kcal/mol and 0.34 V with the standard deviation, 23.8 kcal/mol and 1.0 V, respectively. While, the differences of that between the azurin and acetone in the experimental data are 3.5 kcal/mol and 0.15 V, respectively. The differences of those between the azurin and 3-pentanone in the experimental data are 4.0 kcal/mol and 0.17 V, respectively. These computational values of average ΔG and E° show an agreement with the experimental data more than the difference of ΔG and E° between the acetone and 3-pentanone. This result show that the presented computational approach to estimate the redox potential of molecules is possible to apply to the proteins. However, the standard deviations of the difference of ΔG and E° between the azurin and acetone and between the azurin and 3-pentanone are too much larger than that between the acetone and 3-pentanone. The source of this large standard deviation is due to the excess chemical potentials of the

molecules. The development of computational approach including the method for the calculation of excess chemical potential is future work.

A.6 Summary

This appendix estimates the redox potential of metalloprotein, azurin, by using the hybrid type method with molecular dynamics (MD) and quantum mechanics/molecular mechanics (QM/MM) calculations. The value of the redox potential of metalloprotein, azurin, is different from the experimental data. However, the difference of the redox potential between the azurin and the other organic molecules is an agreement with the experimental data. This result show that the presented computational approach to estimate the redox potential of molecules is possible to apply to the proteins.

APPENDIX B

Effect of Counter-ion on Evaluation of Redox Potential

B.1 Introduction

In chapter 4, the evaluated redox potentials of the organic molecules, acetone and 3-pentanone, by the conventional approach in this study have the discrepancies of the values between the computations and experiments. These results should be analyzed the details, even though the relative value of the redox potentials of these molecules is even better.

The purpose of this appendix is to investigate the source of the disagreements of the redox potentials of the organic molecules with those of experimental values. One of the possibilities of the disagreements is the treatment of the long range interaction of the radical cationic state of the solutes with water molecules. The number of water molecules in the simulation cell might be insufficient to consider the long range interactions. In this study, for the decision of the number of water

molecules, the radial distribution function (RDF) of the center of mass (COM) of solute molecule and oxygen of water molecule pairs is analyzed in the systems of the acetone and 3-pentanone in the neutral and radical cationic states. These results of RDF show that the second peak is located at about 7.6 Å and 8.2 Å 8.5 Å in the acetone and 3-pentanone system, respectively, and the structuring of water make no nearly appearance to the more region, as shown in Figure 3.5 and Figure 3.6. In this study, cell size more than twice the cell-box of the size of structuring region of water in each system. Takahashi and co-workers has presented the standard reduction free energy of flavin ring in the condition of 676 water molecules by using the quantum mechanics/molecular mechanics molecular dynamics (QM/MM-MD) simulations and has obtained the reasonable result of 9.6 kcal/mol in the comparison with the experimental data [36]. This report would be helpful for understanding use of the number of water molecules in this study. However, the dependence of the excess chemical potential is not only the structure of solute and solvent molecules, but also energy between the solute and solvent molecules. Therefore, the estimation of the excess chemical potential requires the investigation of the effect of the number of water molecules.

Another possibilities is the effect of the counter-ion in the system of radical cationic state of the solute molecule on the calculation of excess chemical potential by the energy representation (ER) method. In this study, along the scheme of ER method, the radical cationic solute molecule and the trajectory of pure water system in neutral state are used to estimate the energy distribution function in the pure solvent system ρ_0^e . However, in the calculation of that in the solution system ρ^e , the trajectory of neutralized system by using the counter-ion is adopted. Thus,

these energy distribution function are estimated from the systems not agreement the charge of system.

From these consideration, this appendix computes the excess chemical potential of molecule, acetone, increasing the number of water molecules and the sampling data to estimate the energy distribution functions, ρ^e and ρ_0^e .

B.2 Computational Details

Computational details of the excess chemical potential are similar with that shown in chapter 3. In this appendix B, the dependence of the excess chemical potential from the number of water molecules are investigated in the case of 1,425 (used in chapter 3 and chapter 4), 2,850, 4,275 as the number of water molecules, called 1,425 solvent system, 2,850 solvent system, 4,275 solvent system, including the case of solution system in this appendix. The system sizes of 1,425, 2,850, and 4,275 solvent system is $36.5 \text{ \AA} \times 34.3 \text{ \AA} \times 34.6 \text{ \AA}$, $45.7 \text{ \AA} \times 43.4 \text{ \AA} \times 43.9 \text{ \AA}$, and $52.3 \text{ \AA} \times 50.0 \text{ \AA} \times 50.0 \text{ \AA}$. The *NPT*-MD simulation of the solution system is performed for 1 ns: total 100,000 snapshots are prepared for the estimation of the energy distribution function, ρ^e . While, the *NPT*-MD simulation of the pure solvent system is performed for 300 ps: total 100,000 sampling data are prepared for the estimation of the energy distribution function, ρ_0^e , which sampling is similar with that shown in chapter 3. The result of the investigation of the dependence of the excess chemical potential from the number of sampling for the estimation of ρ_0^e is confirmed.

B.3 Results and Discussion

B.3.1 Dependence of redox potential from the number of water molecules

Table B.1 show the dependence of the excess chemical potential of acetone in the neutral and radical cationic states, $\mu_{(N)}^{ex}$ and $\mu_{(N+1)}^{ex}$, the free energy change in oxidation reaction, ΔG , redox potential, E° from the number of water molecules. As shown in Table B.1, there is no dependence of the $\mu_{(N)}^{ex}$ from the number of water molecules, showing similar values with computational value in chapter 3, -2.3 kcal/mol. However, the $\mu_{(N+1)}^{ex}$ in the 1,425, 2,850 and 4,275 solvent system are the -36.43 kcal/mol, -35.55 kcal/mol and -34.57 kcal/mol with the standard deviations, 1.51 kcal/mol, 1.40 kcal/mol and 2.39 kcal/mol, respectively. In proportion of the value of $\mu_{(N+1)}^{ex}$, the E° in the 1,425, 2,850 and 4,275 solvent system are the 3.65 V, 3.69 V and 3.73 V with the standard deviations, 0.09 V,

Table B.1: Dependence of the excess chemical potential in the neutral and radical cationic states, $\mu_{(N)}^{ex}$ and $\mu_{(N+1)}^{ex}$, the free energy change in oxidation reaction, ΔG , redox potential, E° from the number of water molecules. Units of the $\mu_{(N)}^{ex}$, $\mu_{(N+1)}^{ex}$, ΔG and the E° are the kcal/mol and the V.

N^{water}	$\Delta\mu_{(N)}^{ex}$	$\Delta\mu_{(N-1)}^{ex}$	ΔG	E°
1,425	-2.29 (0.23)	-36.43 (1.51)	186.67 (2.05)	3.65 (0.09)
2,850	-2.32 (0.22)	-35.55 (1.40)	187.58 (1.97)	3.69 (0.09)
4,275	-2.27 (0.24)	-34.57 (2.39)	188.51 (2.77)	3.73 (0.12)

0.09 V and 0.12 V, respectively. These results show unstable of excess chemical potential by increasing the number of water molecules.

In order to investigate that reason, the average of excess chemical potential of acetone in the radical cationic state, $\mu_{(N-1)}^{ex}$, using a configuration of 10 ns is plotted in Figure B.1. With the Figure B.1, change of distance between the center of mass (COM) of acetone and the counter-ion is plotted in Figure B.2. These Figures compares the excess chemical potential and the distance between the COM of acetone and the counter-ion of acetone with the number of water molecules. As shown in Figure B.1 and Figure B.2, it is found that behavior of the counter-ion effects to the excess chemical potential of the molecule. This result show that the effect of the number of sampling for solution system to the excess chemical potential is the effect of the state probability of the counter-ion in simulation cell. Therefore, increasing the number of sampling or the number of water molecules (it is mean the system size), the effect of the counter-ion might be small because it is considered that the number of sampling for solution system, which means the distribution of counter-ion in the simulation cell, is insufficient.

Then, the number of sampling for the solution system is increased to 1,000,000 in order to investigate the effect of the number of sampling for the solution system. Firstly, Figure B.3 show the state probability distribution of distance between the COM of acetone and the counter-ion. The Figure B.3 show that the more the number of water molecules increase, the more snapshot existed the counter-ion remote from the solute molecule can be sampled from the MD simulation for the solution system. The average of the difference of excess chemical potential, $\Delta(\Delta\mu_{(N-1)}^{ex})$, of acetone between the 1,425 and 2,850 solvent systems and between

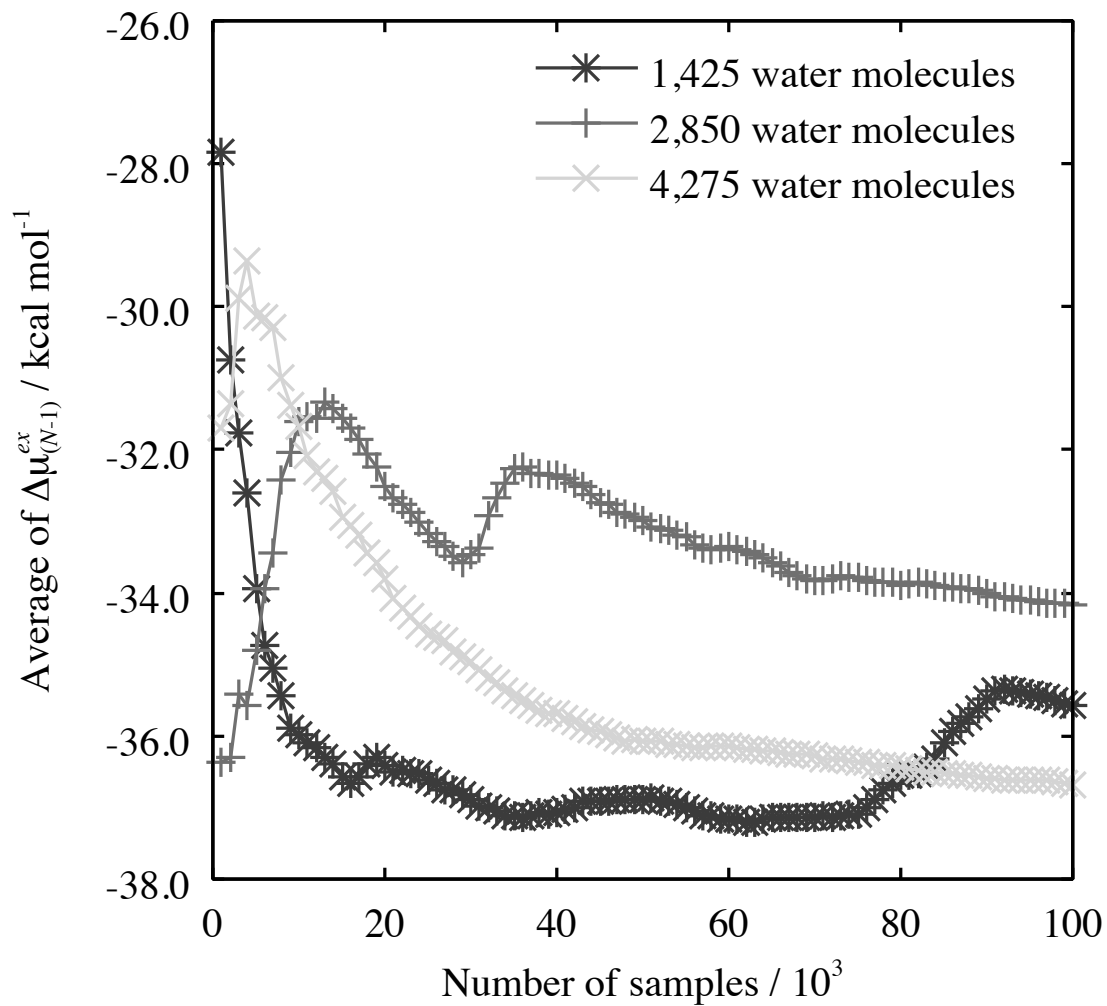


Figure B.1: The average of excess chemical potential of acetone in the radical cationic state, $\mu_{(N-1)}^{ex}$, using a configuration of 10 ns as a function of the number of samples for solution system.

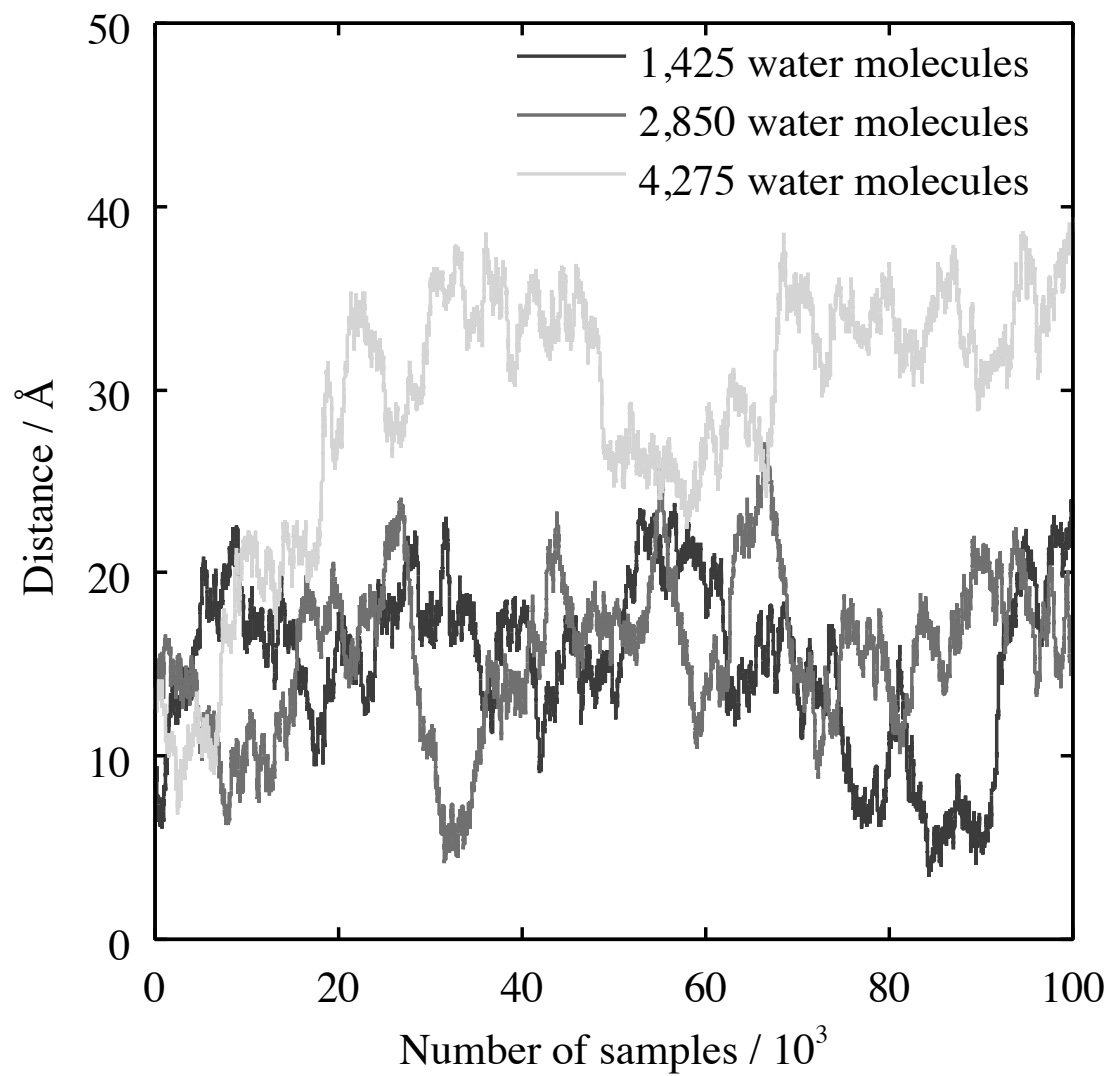


Figure B.2: Change of distance between the COM of acetone and the counter-ion as a function of the number of samples for solution system.

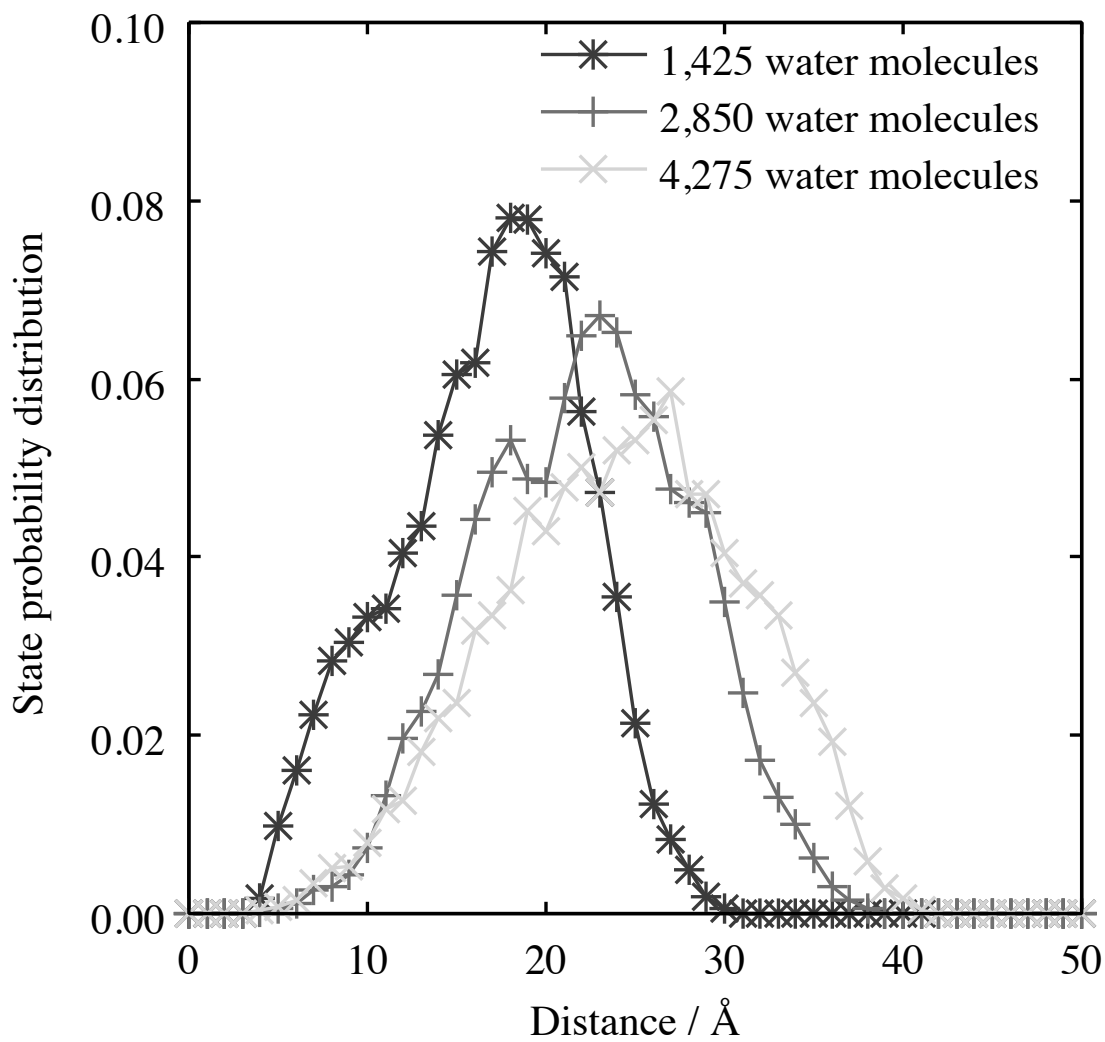


Figure B.3: State probability distribution of distance between the COM of acetone and the counter-ion.

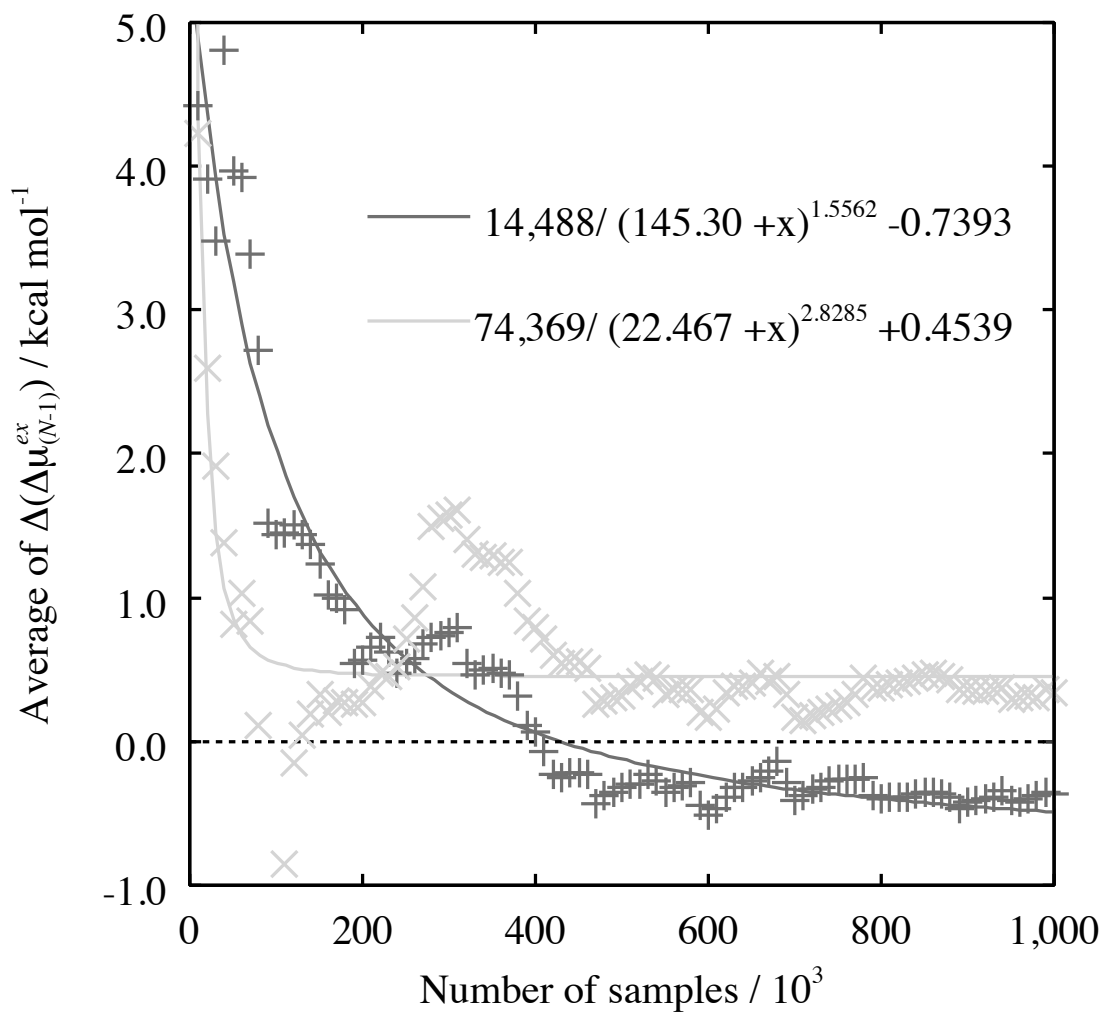


Figure B.4: The average of the difference of excess chemical potential, $\Delta(\Delta\mu_{(N-1)}^{ex})$, of acetone between the 1,425 and 2,850 solvent systems (dark) and between the 1,425 and 4,250 solvent systems (thin). Points indicate the each value. Curve lines indicate the fitting curves each point.

the 1,425 and 4,250 solvent systems, as shown in Figure B.4. The average of the $\Delta(\Delta\mu_{(N-1)}^{ex})$ between the 1,425 and 2,850 solvent systems is gradually reduced and has negative value in 1,000,000 -th sampling. While, The average of the $\Delta(\Delta\mu_{(N-1)}^{ex})$ between the 1,425 and 4,250 solvent systems is converged with positive value. From a viewpoint of the state probability distribution of distance between the COM of acetone and the counter-ion, the average of the $\Delta(\Delta\mu_{(N-1)}^{ex})$ between the 1,425 and 4,250 solvent systems is considered to be more negative charge than that between the 1,425 and 4,250 solvent systems. From these results, remarkably stable region might exist around the solute molecule in the solution system containing the counter-ion. These results should be more investigated with the free energy profile on the distance between the COM of acetone and the counter-ion and so on: this would be a future work.

B.4 Summary

This appendix investigates the source of the disagreements of the redox potential of the organic molecules with those experimental data, shown in chapter 4. In order to investigate this source, the effects of the number of water molecules and the counter-ion on the computation of excess chemical potential in the radical cationic state of acetone are investigated with re-calculation of the excess chemical potential in solution system by the energy representation (ER) method increasing the number of water molecules and sampling in solution system to estimate the energy distribution function for solution system. The results of these calculations show that the one of the source of the disagreements of the redox potential with the experiment is the effect of counter-ion on the calculation of excess chemical

potential of radical cationic molecule and the redox potential of molecule.

APPENDIX C

Computation of Redox Potential of Molecules by MD simulation of Water Droplet

C.1 Introduction

Appendix B have investigated the effect of the counter-ion on the estimation of excess chemical potential of the organic molecule, acetone, in radical cationic state by the energy representation (ER) method. The investigation shows that it is not easy to estimate the redox potential or the free energy change in redox reaction of the molecule using the neutralized system inserted of counter-ion. In order to calculate the excess chemical potential by using the ER method, preparation of sufficiently large cell size enough to be ignored the effect of the counter-ion is not realistic due to computational cost. The computational method without using the counter-ion by molecular dynamics (MD) simulation is required to estimate

the redox potential.

The purpose of this Appendix presents the computational method to estimate the redox potential of the molecule by using the MD simulation on droplet model and estimates the redox potential of organic molecules, acetone and 3-pentanone. In this Appendix, the redox potential of the molecules is estimated from the ionization potential in gas phase and the solvation free energy of the molecule in the neutral and radical cationic states by using the free energy perturbation (FEP) method. The computational value of redox potential of the molecules is compared with the experimental value with discussions of the difference of the redox potentials of the molecules.

C.2 Computational Procedure

In this Appendix, the solvation free energy of the molecule is calculated by using the free energy perturbation (FEP) method differently from the Chapter 3 (the energy representation method). Firstly, the following subsection presents the methodology of the estimation of solvation free energy by using the FEP method.

C.2.1 Solvation free energy

The solvation free energy of solute molecule is derived using similar English notation of Chapter 3. The potential energy of the whole molecular system, V_{N+1} , is written by the following equation [77];

$$V_{N+1}(\mathbf{r}^{N+1}; \boldsymbol{\lambda}) = V_N(\mathbf{r}^N) + V(\mathbf{r}_{N+1}, \mathbf{r}^N; \boldsymbol{\lambda}) + V_{N+1}^{intra}, \quad (\text{C.1})$$

where $\boldsymbol{\lambda}$ is any coupling parameter. The intermolecular interaction in the whole system, V , is expressed by two-body interactions. Zacharias and co-workers have presented the V using two coupling parameter, $\boldsymbol{\lambda} = (\lambda_1, \lambda_2)$, as following equation [78, 79];

$$V(\mathbf{r}_{N+1}, \mathbf{r}^N; \lambda_1, \lambda_2) = \lambda_1 \sum_{i \in M^N} \sum_{j \in M_{N+1}} \frac{1}{4\pi\epsilon_0} \frac{q_i q_j}{r_{ij}} + \lambda_2 \sum_{i \in M^N} \sum_{j \in M_{N+1}} \epsilon_{ij} \left\{ \frac{A_{ij}^{12}}{[r_{ij}^2 + \delta(1 - \lambda_2)]^6} - \frac{B_{ij}^6}{[r_{ij}^2 + \delta(1 - \lambda_2)]^3} \right\} \quad (\text{C.2})$$

where $i \in M^N$ and $j \in M_{N+1}$ are i -th atom in one of the N molecules and the j -th atom in the $(N + 1)$ -th molecule, ϵ_0 is the dielectric constant of vacuum, r_{ij} is distance between atom i and atom j , A_{ij} and B_{ij} are the Lennard-Jones (LJ) potential parameters, δ is a adjustment parameter which prevents divergence of van der Waals interaction caused by the overlapping between the $(N + 1)$ -the molecule and the other molecules. According to equation (C.2), in the case of $\boldsymbol{\lambda} = (\lambda_1, \lambda_2) = (0, 0)$, it is equal to the existence in gas phase both of the first N molecules and the $N + 1$ -th molecule because there is no interaction between the first N molecules and the $N + 1$ -th molecule, on the other hand, $\boldsymbol{\lambda} = (\lambda_1, \lambda_2) = (1, 1)$ is equal to the solution state.

The difference of free energy between the two states of $\boldsymbol{\lambda} = 1$ and $\boldsymbol{\lambda} = 0$, which is the solvation free energy ΔG^{sol} , is given as the following equation;

$$\Delta G^{sol} = G(\boldsymbol{\lambda} = 1) - G(\boldsymbol{\lambda} = 0) \quad (\text{C.3})$$

$$= -k_B T \log \left\{ \frac{Q_{N+1}(\boldsymbol{\lambda} = 1)}{Q_{N+1}(\boldsymbol{\lambda} = 0)} \right\} \quad (\text{C.4})$$

$$= -k_B T \log \langle \exp [V_{N+1}(\boldsymbol{\lambda} = 1) - V_{N+1}(\boldsymbol{\lambda} = 0)/k_B T] \rangle_{\boldsymbol{\lambda}=0}. \quad (\text{C.5})$$

The equation (C.5) uses the equation (3.6). According to the equation (C.5), the ΔG^{sol} is calculated by the ensemble average of the term of the difference of the V_{N+1} between the state of $\boldsymbol{\lambda} = 1$ and $\boldsymbol{\lambda} = 0$ on the state of $\boldsymbol{\lambda} = 0$. However, the equation (C.5) is applied with the case of enough to the overlapping of the state probability of each state in relation to the nonbonding interactions between the $(N + 1)$ -th molecule and the first N molecules. If the overlapping is not enough, the ΔG^{sol} is given as following equation by considering the intermediate state,

$$\Delta G^{sol} = \sum_{\boldsymbol{\lambda}=0}^1 [-k_B T \log \langle -\Delta V'_{N+1}/k_B T \rangle_{\boldsymbol{\lambda}}] \quad (\text{C.6})$$

$$= \sum_{\boldsymbol{\lambda}=0}^1 \Delta G_{\boldsymbol{\lambda}}^{sol} \quad (\text{C.7})$$

where $\Delta V'_{N+1} = V_{N+1}(\boldsymbol{\lambda} + d\boldsymbol{\lambda}) - V_{N+1}(\boldsymbol{\lambda})$.

In the equation (C.7), the $\boldsymbol{\lambda} = (\lambda_1, \lambda_2)$ is changed by the following equation,

$$\lambda_1 = \begin{cases} 0 & \text{if } 0 \leq \lambda_2 \leq \alpha, \\ \frac{\lambda_2 - \alpha}{1 - \alpha} & \text{if } \alpha < \lambda_2 \leq 1 \end{cases} \quad (\text{C.8})$$

where α is adjustable parameter which prevents divergence of V_{N+1} by the coulomb interaction between the $(N + 1)$ molecule and the first N molecules. In this study, the value of δ is set to be 5 \AA^2 . In order to determine the value of α , the solvation free energy of the molecule, acetone, is calculated by the FEP method setting the following value of parameter; 0.1, 0.2, 0.3, 0.4 and 0.5. Then, in the cases of $\alpha = (0.1, 0.2 \text{ and } 0.3)$, the $\Delta G_{\boldsymbol{\lambda}}^{sol}$ is diverged, therefore, the value of α is set to be 0.4. According to the equation (C.8), the intermediate state of two straight lines is adopted. λ_2 changes its value from 0.0 to 0.4 at an interval of 0.025 with λ_1 fixed at 0. Then, the λ_2 is changed from 0.4 to 1.0 at intervals of 0.025 with the value of λ_1 according to the following equation; $\lambda_1 = 1/0.6\lambda_2 - 0.4/0.6$.

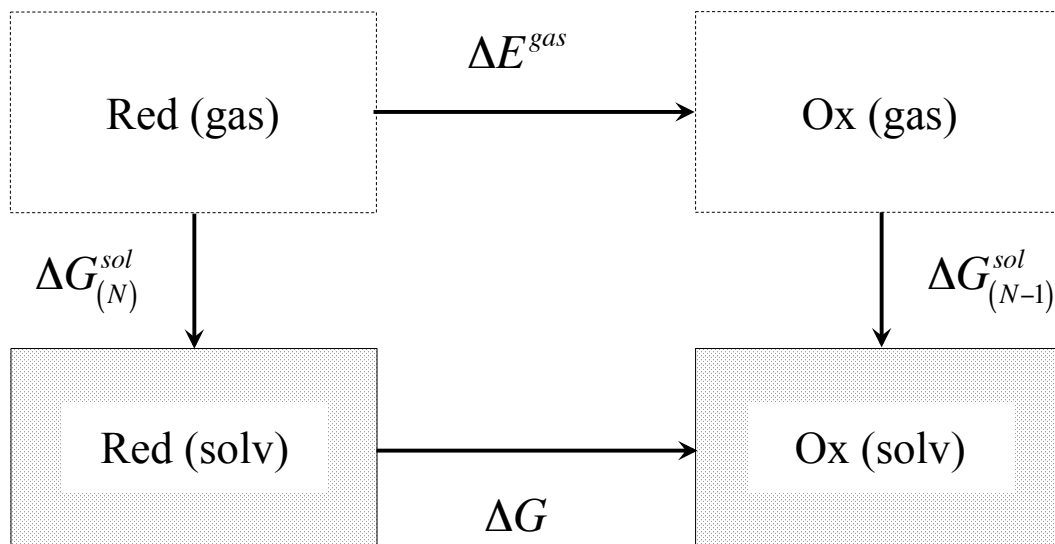


Figure C.1: Thermodynamic cycle model used in calculation of free energy change in oxidation reaction.

C.2.2 Gibbs free energy of redox reaction

The Gibbs free energy of redox reaction, ΔG , is given as the following equation, as shown in Figure C.1,

$$\Delta G = \Delta E^{gas} + \{ \Delta G_{(N-1)}^{sol} - \Delta G_{(N)}^{sol} \} \quad (C.9)$$

$$\Delta E^{gas} = E_{(N-1)}^{gas} - E_{(N)}^{gas}, \quad (C.10)$$

where ΔE^{gas} means the ionization potential in gas phase, and $E_{(N)}$ and $E_{(N-1)}$ are the total energy of the reduced and the oxidized molecules in gas phase, respectively. Then, N denotes the valence of the molecule. $\Delta G_{(N)}^{sol}$ and $\Delta G_{(N-1)}^{sol}$ are the solvation free energy of the reduced and the oxidized molecules, respectively. In this study, the ionization potential of the molecules is calculated in Chapter 2 by using the density functional theory (DFT) calculations with B3LYP method

and 6-31+G(d,p) basis set.

C.3 Computational Details

The MD simulations of the organic molecules, acetone and 3-pentanone, in the neutral and radical cationic states are performed using water droplet model in condition of spherical boundary condition as showing to the following subsection.

C.3.1 MD simulation of water droplet model

The MD simulation of the organic molecules, acetone and 3-pentanone, in the neutral and radical cationic states in water droplet is performed with the Namd 2.9 program packages. For the MD simulations of these molecules in the neutral and radical cationic states, the force field parameter of the stretching vibration and angle bending of intramolecular potential, and partial charge of intermolecular potential originally developed in chapter 2. However the stretching vibration and angle bending potential parameters including hydrogen atom of these molecules assign AMBER force field 03 (parm99) [63, 64]. The intramolecular torsion angle including the hydrogen atom of the methyl and methylene groups, which is the $\text{H-C}_{\text{sp}3}\text{-C}_{\text{sp}2}\text{=O}$ in the structure of the acetone, $\text{H-C}_{\text{sp}3}\text{-C}_{\text{sp}3}\text{-C}_{\text{sp}2}$ in the structure of 3-pentanone, and improper torsion $\text{C}_{\text{sp}3}\text{-C}_{\text{sp}2}\text{=O-C}_{\text{sp}3}$ in the structure of both molecules, is constrained with harmonic potential shown in Table 3.1 and Table 3.2. The force field parameters for the other intramolecular torsion angle of 3-pentanone, the Lennard-Jones (L-J) potential parameter used to compute the intermolecular interaction in the whole system, and the stretching vibration and angle bending of solvent molecule assigns the AMBER force field 03 (parm99).

For the MD simulation, Langevin thermostat is used to control system temperature ($T = 300$ K). The acetone and 3-pentanone in the neutral and radical cationic states are solvated by droplet consisted of 2,185 water molecules with radius of 25.0 Å, respectively. The TIP3P model [65] is adopted for the solvent molecule (water molecule). Full coulomb and van der Waals interactions are calculated in the MD simulation. The spherical boundary condition is adopted with harmonic potential with force constant, 10 kcal/mol/Å². The distance between the center of mass of solute molecule and the center of mass of pure droplet is constrained by spring constant 1.0 kcal/mol because the molecules, acetone and 3-pentanone including the hydrophobic group evaporate. A time step for the MD simulation is 2 fs. The bond length including the hydrogen atom are constrained by SHAKE method [56].

Energy minimization is performed by the steepest descent method with fixing the heavy atoms of solute molecule. The MD simulations are carried out in the constant NVT condition with constraints of solute molecule with 50 kcal/mol/Å² spring constant, and then system temperature is gradually increased in increments of 20 K from 0 K to 300 K for 150 ps. After that, the NVT -MD simulations are performed in which the constraints of solute are gradually reduced in increments of 5.0 kcal/mol/Å² to zero for 100 ps. Finally, the equilibrium NVT -MD simulations are carried out for 1 ns.

C.4 Results and Discussion

The values of ionization potential of acetone and 3-pentanone estimated in Chapter 2 is shown in Table C.1, which is 220.9 kcal/mol for acetone. The computa-

Table C.1: The ionization potentials in gas phase, ΔE^{gas} , the solvation free energies of molecule in the neutral and the radical cationic states, $\Delta G_{(N)}^{sol}$ and $\Delta G_{(N-1)}^{sol}$, and the standard Gibbs free energies ΔG of redox reaction, for the acetone and 3-pentanone. The units are in kcal/mol. The values for 3-pentanone are in estimation.

Molecule	ΔE^{gas}	$\Delta G_{(N)}^{sol}$	$\Delta G_{(N-1)}^{sol}$	ΔG
Acetone	220.9	-0.4	-43.8	177.6
3-pentanone

tional values of solvation free energy of the molecule, acetone, in the neutral and radical cationic states, $\Delta G_{(N)}^{sol}$ and $\Delta G_{(N+1)}^{sol}$, are also shown in Table C.1. The values of $\Delta G_{(N)}^{sol}$ and $\Delta G_{(N+1)}^{sol}$ are -0.4 kcal/mol and -43.8 kcal/mol for acetone, respectively. In this study, the computational value of $\Delta G_{(N)}^{sol}$ is different from the experimental data, -3.80 kcal/mol, than the comparing of the previous computational result estimated in Chapter 3, -2.3 kcal/mol, with the experimental data. In order to analyze the result, the solvation free energy of acetone in neutral state is calculated by using the FEP method introduced in this Chapter in the periodic boundary condition. Then, the estimated value of $\Delta G_{(N)}^{sol}$ in periodic boundary condition is -3.0 kcal/mol, showing good agreement with the experimental data than the computation of average of excess chemical potential of solute molecule by the energy representation (ER) method shown in Chapter 3. It is considered that the discrepancy of the value of $\Delta G_{(N)}^{sol}$ between the droplet model and the cubic model is caused by the constraint by harmonic potential between the center of mass (COM) of solute molecule and COM of pure droplet. Therefore, the

result in this study shows the unstable in solution comparing the previous result, however, the effect of the constraint of solute molecule on the estimation of solvation free energy might be countered by subtracting the solvation free energy between the neutral and radical cationic states. .

According to equation (C.9) and equation (4.1), the free energy change in oxidation reaction, ΔG , and the standard redox potential, E° , are 177.6 kcal/mol and 3.26 V for acetone, respectively as shown in Table C.1. The differences of the ΔG and E° between the previous study shown in Chapter 4 and this study are -10.7 kcal/mol and -0.4 V, respectively, showing that the values of ΔG and E° are improved in this study. However, the E° for acetone is different from the experimental data, 0.16 V [72]. From the result, the computational model including the solvation effect of the excess electron might be considered to estimate the standard redox potential of the molecule.

REFERENCES

- [1] R. A. Marcus, N. Sutin, "Electron transfers in chemistry and biology", *Biochimica et Biophysica Acta*, **811**, 265-322 (1985).
- [2] Y. Fu, L. Liu, H. Z. Yu, Y. M. Wang, Q. X. Guo, "Quantum-Chemical Predictions of Absolute Standard Redox Potentials of Diverse Organic Molecules and Free Radicals in Acetonitrile", *J. Am. Chem. Soc.*, **127**, 7227-7234 (2005).
- [3] R. A. Marcus, "Electron transfer reactions in chemistry. Theory and experiment.", *Rev. Mod. Phys.*, **65**, 599-610 (1993).
- [4] H. B. Gray, J. R. Winkler, "ELECTRON TRANSFER IN PROTEINS", *Annu. Rev. Biochem.*, **65**, 537-561 (1996).
- [5] D. Voet, J. G. Voet, *Biochemistry, 3rd ed*, (New York: John Wiley and Sons; 2004).
- [6] V. Adler, Z. Yin, K. D. Tew, Z. Ronai, "Role of redox potential and reactive oxygen species in stress signaling", *Oncogene*, **18**, 6104-6111 (1999).

- [7] H. Lodish, A. Berk, C. A. Kaiser, M. Krieger, M. P. Scott, A. Bretscher, H. Ploegh, P. Matsudaira, "Molecular Cell Biology, 6th ed, (W.H. Freeman and Co Ltd; 2007).
- [8] V. K. Yachandra, V. J. DeRose, M. J. Latimer, I. Mukerji, K. Sauer, M. P. Klein, "Where Plants Make Oxygen: A Structural Model for the Photosynthetic Oxygen-Evolving Manganese Cluster", *Science*, **260**, 675-679 (1993).
- [9] H. B. Gray, J. R. Winkler, "Electron flow through metalloproteins", *Biochim. Biophys. Acta.*, **1797**, 1563-1572 (2010).
- [10] P. Atanassov, C. Apblett, S. Banta, S. Brozik, S. C. Barton, M. Cooney, B. Y. Liaw, S. Mukerjee, S. D. Minter, "Enzymatic Biofuel Cells", *The Electrochemical Society Interface*, **Summer**, 28-31 (2007).
- [11] E. B. Goh, E. E. K. Baidoo, J. D. Keasling, H. R. Beller, "Engineering of Bacterial Methyl Ketone Synthesis for Biofuels", *Appl. Environ. Microbiol.*, **78**, 70-80 (2012).
- [12] T. Ikeda, K. Kano, "An Electrochemical Approach to the Studies of Biological Redox Reactions and Their Applications to Biosensors, Bioreactors, and Biofuel Cells", *J. Biosci. Bioeng.*, **92**, 9-18 (2001).
- [13] H. Dau, C. Limberg, T. Reier, M. Risch, S. Roggan, P. Strasser, "The Mechanism of Water Oxidation: From Electrolysis via Homogeneous to Biological Catalysis", *Chem. Cat. Chem.*, **2**, 724-761 (2010).

- [14] A. Zouni, H. T. Witt, J. Kern, P. Fromme, N. Krauss, W. Saenger, P. Orth, "Crystal structure of photosystem II from *Synechococcus elongates* at 3.8 Å resolution", *Nature*, **409**, 739-743 (2001).
- [15] Y. Umena, K. Kawakami, J. R. Shen, N. Kamiya, "Crystal structure of oxygen-evolving photosystem II at a resolution of 1.9 Å", *Nature*, **473**, 55-61 (2011).
- [16] B. Kok, B. Forbush, M. McGloin, "COOPERATION OF CHARGES IN PHOTOSYNTHETIC O₂ EVOLUTION-I. A LINEAR FOUR STEP MECHANISM", *Photochem. Photobiol.*, **11**, 457-475 (1990).
- [17] P. Kollman, "Free Energy Calculations: Applications to Chemical and Biochemical Phenomena", *Chem. Rev.*, **93**, 2395-2417 (1993).
- [18] S. Miertus, E. Scrocco, J. Tomasi, "ELECTROSTATIC INTERACTION OF A SOLUTE WITH A CONTINUUM. A DIRECT UTILIZATION OF AB INITIO MOLECULAR POTENTIALS FOR THE PREVISION OF SOLVENT EFFECTS", *Chem. Phys.*, **55**, 117-129 (1981).
- [19] H. M. Senn, W. Thiel, "QM/MM Methods for Biomolecular Systems", *Angew. Chem. Int. Ed.*, **48**, 1198-1229 (2009).
- [20] T. Matsui, Y. Kitagawa, M. Okumura, Y. Shigeta, S. Sakaki, "Consistent Scheme for Computing Standard Hydrogen Electrode and Redox Potentials", *J. Comput. Chem.*, **34**, 21-26 (2013).

- [21] L. Haya, F. J. Sayago, A. M. Mainar, C. Cativiela, J. S. Urieta, "Quantum-chemical predictions of redox potentials of carbamates in methanol", *Phys. Chem. Chem. Phys.*, **13**, 17696-17703 (2011).
- [22] L. E. Roy, E. Jakubikova, M. G. Guthrie, E. R. Batista, "Calculation of One-Electron Redox Potentials Revisited. Is It Possible to Calculate Accurate Potentials with Density Functional Methods?", *J. Phys. Chem. A*, **113**, 6745-6750 (2009).
- [23] Y. Fu, L. Liu, H. Z. Yu, Y. M. Wang, Q. X. Guo, "Quantum-Chemical Predictions of Absolute Standard Redox Potentials of Diverse Organic Molecules and Free Radicals in Acetonitrile", *J. Am. Chem. Soc.*, **127**, 7227-7234 (2005).
- [24] P. Winget, C. J. Cramer, D. G. Truhlar, "Computation of equilibrium oxidation and reduction potentials for reversible and dissociative electron-transfer reactions in solution", *Theor. Chem. Acc.*, **112**, 217-227 (2004).
- [25] M. H. Baik, R. A. Friesner, "Computing Redox Potentials in Solution: Density Functional Theory as A Tool for Rational Design of Redox Agents", *J. Phys. Chem. A*, **106**, 7407-7412 (2002).
- [26] P. Winget, E. J. Weber, C. J. Cramer, D. G. Truhlar, "Computational electrochemistry: aqueous one-electron oxidation potentials for substituted anilines", *Phys. Chem. Chem. Phys.*, **2**, 1231-1239 (2000).
- [27] J. G. Kirkwood, "Statistical Mechanics of Fluid Mixtures", *J. Chem. Phys.*, **3**, 300-313 (1935).

- [28] M. P. Allen, D. J. Tildesley, *Computer Simulation of Liquids*, (Oxford University Press: Oxford; 1987).
- [29] N. Matubayasi, M. Nakahara, "Theory of solutions in the energetic representation. I. Formulation", *J. Chem. Phys.*, **113**, 6070-6081 (2000).
- [30] N. Matubayasi, M. Nakahara, "Theory of solutions in the energy representation. II. Functional for the chemical potential", *J. Chem. Phys.*, **117**, 3605-3616 (2002).
- [31] N. Matubayasi, M. Nakahara, "Theory of solutions in the energy representation. III. Treatment of the molecular flexibility", *J. Chem. Phys.*, **119**, 9686-9702 (2003).
- [32] Y. Karino, M. V. Fedorov, N. Matubayasi, "End-point calculation of solvation free energy of amino-acid analogs by molecular theories of solution", *Chem. Phys. Lett.*, **496**, 351-355 (2010).
- [33] H. Hu, W. Yang, "Free Energies of Chemical Reactions in Solution and in Enzymes with Ab Initio Quantum Mechanics/Molecular Mechanics Methods", *Annu. Rev. Phys. Chem.*, **59**, 573-601 (2008).
- [34] T. Hori, H. Takahashi, S. Furukawa, M. Nakano, W. Yang, "Computational Study on the Relative Acidity of Acid by the QM/MM Method Combined with the Theory of Energy Representation", *J. Phys. Chem. B.*, **111**, 581-588 (2007).

- [35] Z. Zeng, H. Hu, X. Fu, W. Yang, "Calculating solution redox free energies with ab initio quantum mechanical/molecular mechanical minimum free energy path method", *J. Chem. Phys.*, **130**, 164111 1-8 (2009).
- [36] H. Takahashi, H. Ohno, R. Kishi, M. Nakano, M. Matubayasi, "Computation of the free energy change associated with one-electron reduction of coenzyme immersed in water: A novel approach within the framework of the quantum mechanical/molecular mechanical method combined with the theory of energy representation", *J. Chem. Phys.*, **129**, 205103 1-14 (2008).
- [37] M. Sulpizi, S. Raugei, J. V. Vondele, P. Carloni, M. Sprik, "Calculation of Redox Properties: Understanding Short- and Long-Range Effects in Rubredoxin", *J. Phys. Chem. B*, **111**, 3969-3976 (2007).
- [38] M. Cascella, A. Magistrato, I. Tavernelli, P. Carloni, U. Rothlisberger, "Role of protein frame and solvent for the redox properties of azurin from *Pseudomonas aeruginosa*", *Proc. Natl. Acad. Sci.*, **103**, 19641-19646 (2006).
- [39] P. A. Loach, *Handbook of Biochemistry and Molecular Biology*, 3rd ed., (CRC Press; 1976).
- [40] T. Pascher, B. G. Karlsson, M. Nordling, B. G. Malmstrom, T. Vanngard, "Reduction potentials and their pH dependence in site-directed-mutant forms of azurin from *Pseudomonas aeruginosa*", *Eur. J. Biochem.*, **212**, 289-296 (1993).
- [41] B. Alberts, A. Johnson, J. Lewis, M. Raff, K. Roberts, P. Walter, *Molecular Biology of the Cell*, 4th ed., (Garland Science; 2002).

- [42] Q. Shao, S. Jiang, "Effect of Carbon Spacer Length on Zwitterionic Carboxybetaines", *J. Phys. Chem. B*, **117**, 1357-1366 (2013).
- [43] A. D. MacKerell, Jr., D. Bashford, M. Bellott, R. L. Dunbrack, Jr., J. D. Evanseck, M. J. Field, S. Fischer, J. Gao, H. Guo, S. Ha, D. Joseph-McCarthy, L. Kuchnir, K. Kuczera, F. T. K. Lau, C. Mattos, S. Michnick, T. Ngo, D. T. Nguyen, B. Prodhom, W. E. Reiher, III, B. Roux, M. Schlenkrich, J. C. Smith, R. Stote, J. Staub, M. Watanabe, J. Wiorkiewicz-Kuczera, D. Yin, M. Karplus, "All-Atom Empirical Potential for Molecular Modeling and Dynamics Studies of Proteins", *J. Phys. Chem. B*, **102**, 3586-3616 (1998).
- [44] J. Wang, R. M. Wolf, J. W. Caldwell, P. A. Kollman, D. A. Case, "Development and Testing of a General Amber Force Field", *J. Comp. Chem.*, **25**, 1157-1174 (2004).
- [45] S. J. Weiner, P. A. Kollman, D. A. Case, U. C. Singh, C. Ghio, G. Alagona, S. Profeta, Jr., P. Weiner, "A New Force Field for Molecular Mechanical Simulation of Nucleic Acids and Proteins", *J. Am. Chem. Soc.*, **106**, 765-784 (1984).
- [46] W. D. Cornell, P. Cieplak, C. I. Bayly, I. R. Gould, K. M. Merz, Jr., D. M. Ferguson, D. C. Spellmeyer, T. Fox, J. W. Caldwell, P. A. Kollman, "A Second Generation Force Field for the Simulation of Proteins", *J. Am. Chem. Soc.*, **117**, 5179-5197 (1995).

- [47] S. L. Mayo, B. D. Olafson, W. A. Goddard III, "DREIDING: A Generic Force Field for Molecular Simulations", *J. Phys. Chem.*, **94**, 8897-8909 (1990).
- [48] A. T. Hagler, E. Huler, S. Lifson, "Energy Functions for Peptides and Proteins. I. Derivation of a Consistent Force Field Including the Hydrogen Bond from Amide Crystals", *J. Am. Chem. Soc.*, **96**, 5319-5327 (1974).
- [49] S. Lifson, A. T. Hagler, P. Dauber, "Consistent Force Field Studies of Intermolecular Forces in Hydrogen-Bonded Crystals. 1. Carboxylic Acids, Amides, and the C=O...H- Hydrogen Bonds", *J. Am. Chem. Soc.*, **101**, 5111-5121 (1974).
- [50] W. L. Jorgensen, D. S. Maxwell, J. Tirado-Rives, "Development and Testing of the OPLS All-Atom Force Field on Conformational Energetics and Properties of Organic Liquids", *J. Am. Chem. Soc.*, **118**, 11225-11236 (1996).
- [51] J. Wang, P. Cieplak, P. A. Kollman, "How Well Does a Restrained Electrostatic Potential (RESP) Model Perform in Calculating Conformational Energies of Organic and Biological Molecules?", *J. Comp. Chem.*, **21**, 1049-1074 (2000).
- [52] A. Jakalian, B. L. Bush, D. B. Jack, C. I. Bayly, "Fast, Efficient Generation of High-Quality Atomic Charges. AM1-BCC Model: I. Method", *J. Comp. Chem.*, **21**, 132-146 (2000).
- [53] A. Jakalian, D. B. Jack, C. I. Bayly, "Fast, Efficient Generation of High-Quality Atomic Charges. AM1-BCC Model: II. Parameterization and Validation", *J. Comp. Chem.*, **23**, 1623-1641 (2002).

- [54] P. C. Hariharan, J. A. Pople, "The Influence of Polarization Functions on Molecular Orbital Hydrogenation Energies", *Theor. Chim. Acta. (Berl.)*, **28**, 213-222 (1973).
- [55] G. W. Spitznagel, T. Clark, J. Chandrasekhar, P. V. R. Schleyer, "Stabilization of methyl anions by first-row substituents. The superiority of diffuse function-augmented basis sets for anion calculations", *J. Comp. Chem.*, **3**, 363-371 (1982).
- [56] G. J. Martyna, "Constant pressure molecular dynamics algorithms", *J. Chem. Phys.*, **101**, 4177-4189 (1994).
- [57] T. Iijima, "Zero-point average Structure of a Molecular Containing Two Symmetric Internal Rotors. Acetone", *Bull. Chem. Soc. Jpn.*, **45**, 3526-3530 (1972).
- [58] S. Trasatti, "THE ABSOLUTE ELECTRODE POTENTIAL: AN EXPLANATORY NOTE", *Pure and Appl. Chem.*, **58**, 955-966 (1986).
- [59] A. D. Becke, "Density-functional thermochemistry. III. The role of exact exchange", *J. Chem. Phys.*, **98**, 5648-5652 (1993).
- [60] C. Lee, W. Yang, R. G. Parr, "Development of the Colle-Salvetti correlation-energy formula into a functional of the electron density", *Phys. Rev. B*, **37**, 785-789 (1988).
- [61] J. D. Dill, J. A. Pople, "Self-consistent molecular orbital methods. XV. Extended Gaussian-type basis sets for lithium, beryllium, and boron", *J. Chem. Phys.*, **62**, 2921-2923 (1975).

- [62] T. Clark, J. Chandrasekhar, G. W. Spitznagel, P. V. R. Schleyer, "Efficient diffuse function-augmented basis sets for anion calculations. III. The 3-21+G basis set for first-row elements, Li-F", *J. Comp. Chem.*, **4**, 294-301 (1983).
- [63] S. J. Weiner, P. A. Kollman, "An All Atom Force Field for Simulations of Proteins and Nucleic Acids", *J. Comp. Chem.*, **24**, 1999-2012 (2003).
- [64] Y. Duan, C. Wu, S. Chowdhury, M. C. Lee, G. Xiong, W. Xiong, R. Yang, P. Cieplak, R. Luo, T. Lee, J. Caldwell, J. Wang, P. Kollman, "A Point-Charge Force Field for Molecular Mechanics Simulations of Proteins Based on Condensed-Phase Quantum Mechanical Calculations", *J. Comp. Chem.*, **24**, 1999-2012 (2003).
- [65] W. L. Jorgensen, J. Chandrasekhar, J. D. Madura, R. W. Impey, M. L. Klein, "Comparison of simple potential functions for simulating liquid water", *J. Chem. Phys.*, **79**, 926-935 (1983).
- [66] T. Darden, D. York, L. Pedersen, "Particle mesh Ewald: An $N \bullet \log(N)$ method for Ewald sums in large systems", *J. Chem. Phys.*, **98**, 10089-10092 (1993).
- [67] Energy Representation module (ERmod). Available from: <http://sourceforge.net/projects/ermod/>.
- [68] M. J. Frisch, G. W. Trucks, H. B. Schlegel, G. E. Scuseria, M. A. Robb, J. R. Cheeseman, J. A. Montgomery, Jr., T. Vreven, K. N. Kudin, J. C. Burant, J. M. Millam, S. S. Iyengar, J. Tomasi, V. Barone, B. Mennucci, M. Cossi, G. Scalmani, N. Rega, G. A. Petersson, H. Nakatsuji, M. Hada, M. Ehara,

- K. Toyota, R. Fukuda, J. Hasegawa, M. Ishida, T. Nakajima, Y. Honda, O. Kitao, H. Nakai, M. Klene, X. Li, J. E. Knox, H. P. Hratchian, J. B. Cross, V. Bakken, C. Adamo, J. Jaramillo, R. Gomperts, R. E. Stratmann, O. Yazyev, A. J. Austin, R. Cammi, C. Pomelli, J. W. Ochterski, P. Y. Ayala, K. Morokuma, G. A. Voth, P. Salvador, J. J. Dannenberg, V. G. Zakrzewski, S. Dapprich, A. D. Daniels, M. C. Strain, O. Farkas, D. K. Malick, A. D. Rabuck, K. Raghavachari, J. B. Foresman, J. V. Ortiz, Q. Cui, A. G. Baboul, S. Clifford, J. Cioslowski, B. B. Stefanov, G. Liu, A. Liashenko, P. Piskorz, I. Komaromi, R. L. Martin, D. J. Fox, T. Keith, M. A. Al-Laham, C. Y. Peng, A. Nanayakkara, M. Challacombe, P. M. W. Gill, B. Johnson, W. Chen, M. W. Wong, C. Gonzalez, and J. A. Pople, Gaussian 03, Revision D.02, Gaussian, Inc., Wallingford CT, 2004.
- [69] B. H. Besler, K. M. Merz, P. A. Kollman, "Atomic charges derived from semiempirical methods", *J. Comp. Chem.*, **11**, 431-439 (1990).
- [70] D. R. Lide, *CRC Handbook of Chemistry and Physics*, (CRC Press; 2004).
- [71] J. Wang, W. Wang, S. Huo, M. Lee, P. A. Kollman, "Solvation Model Based on Weighted Solvent Accessible Surface Area", *J. Phys. Chem. B*, **105**, 5055-5067 (2001).
- [72] R. H. Baker, H. Adkins, "Oxidation Potential of Ketones and Aldehyde", *J. Am. Chem. Soc.*, **62**, 3305-3314 (1940).
- [73] H. Nar, A. Messerschmidt, R. Huber, "Crystal Structure Analysis of Oxidized *Pseudomonas aeruginosa* Azurin at pH 5.5 and pH 9.0", *J. Mol. Biol.*, **221**, 765-772 (1991).

- [74] H. Nar, A. Messerschmidt, R. Huber, "X-ray Crystal Structure of the Two Site-specific Mutants His35Gln and His35Leu of Azurin from *Pseudomonas aeruginosa*", *J. Mol. Biol.*, **218**, 427-447 (1991).
- [75] J. M. Guss, H. D. Bartunik, H. C. Freeman, "Accuracy and Precision in Protein Structure Analysis: Restrained Least-Squares Refinement of the Structure of Poplar Plastocyanin at 1.33 Å Resolution", *Acta Cryst.*, **B48**, 790-811 (1992).
- [76] J. M. Guss, P. R. Harrowell, M. Murata, V. A. Norris, H. C. Freeman, "Crystal Structure Analyses of Reduced (Cu^1) Poplar Plastocyanin at Six pH Values", *J. Mol. Biol.*, **192**, 361-387 (1986).
- [77] K. Fujimoto, N. Yoshii, S. Okazaki, "Molecular dynamics study of solubilization of immiscible solutes by a micelle: Free energy of transfer of alkanes from water to the micelle core by thermodynamic integration method", *J. Chem. Phys.*, **133**, 074511-1-6 (2010).
- [78] T. C. Beutler, A. E. Mark, R. C. van Schaik, P. R. Gerber, W. F. van Gunsteren, "Avoiding singularities and numerical instabilities in free energy calculations based on molecular simulations", *Chem. Phys. Lett.*, **222**, 529-539 (1994).
- [79] M. Zacharias, T. P. Straatsma, J. A. McCammon, "Separation-shifted scaling, a new scaling method for Lennard-Jones interactions in thermodynamic integration", *J. Chem. Phys.*, **100**, 9025-9031 (1994).